ADDIS ABABA UNIVERSITY
SCHOOL OF GRADUATE STUDIES
SCHOOL OF EARTH SCIENCES

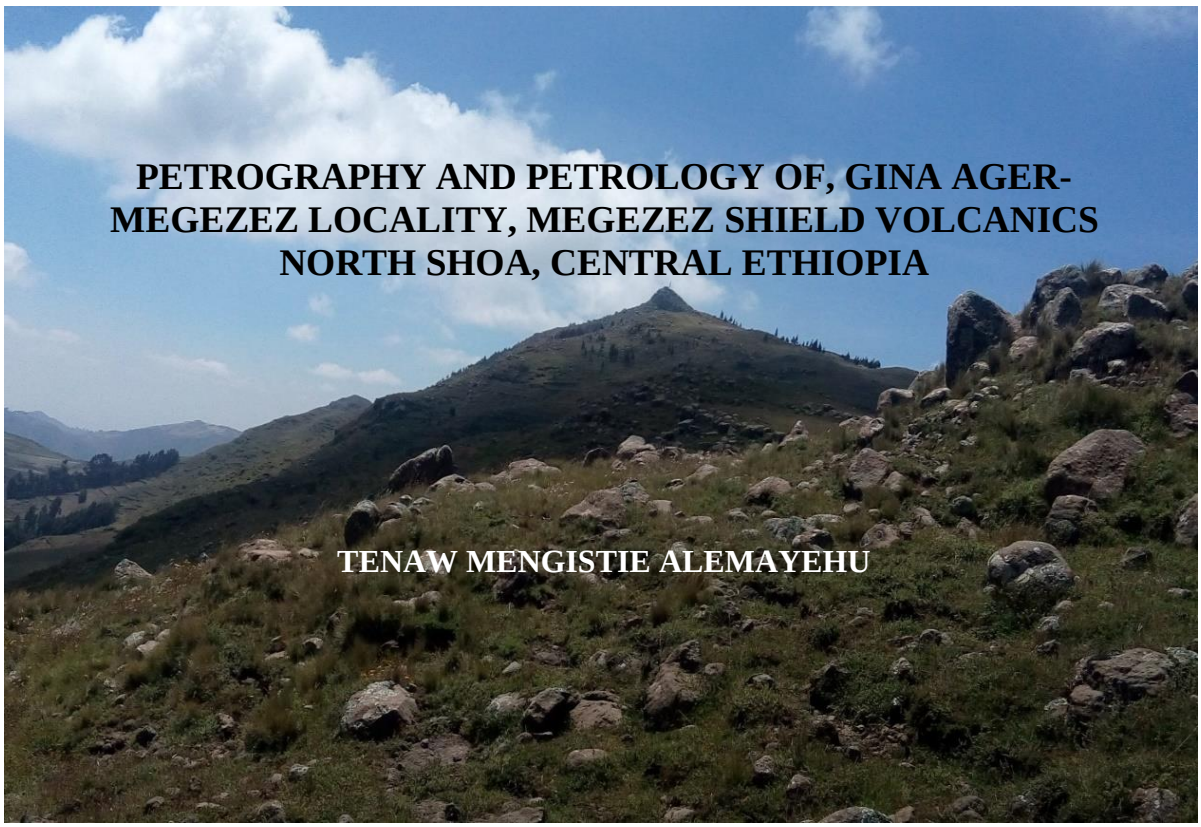

PETROGRAPHY AND PETROLOGY OF, GINA AGER-MEGEZEZ LOCALITY, MEGEZEZ SHIELD VOLCANICS NORTH SHOA, CENTRAL ETHIOPIA

TENAW MENGISTIE ALEMAYEHU

A thesis submitted to the School of Earth Sciences, graduate program, Addis Ababa University in partial fulfillment of the requirements for the degree of Master of Sciences in Geological Sciences (Petrology)

June 2018
Addis Ababa, Ethiopia

ADDIS ABABA UNIVERSITY
SCHOOL OF GRADUATE STUDIES
SCHOOL OF EARTH SCIENCES

PETROGRAPHY AND PETROLOGY OF GINA AGER-MEGEZEZ LOCALITY, MEGEZEZ SHIELD VOLCANICS NORTH SHOA, CENTRAL ETHIOPIA

BY

TENAW MENGISTIE ALEMAYEHU

ADVISOR: DEREJE AYALEW (Prof.)

A thesis submitted to the School of Graduate Studies of Addis Ababa University in partial fulfillment of the requirements for the degree of Master of Science in Geological Sciences (Petrology)

June 2018
Addis Ababa, Ethiopia

ADDIS ABABA UNIVERSITY
SCHOOL OF GRADUATE STUDIES
SCHOOL OF EARTH SCIENCES

PETROGRAPHY AND PETROLOGY OF, GINA AGER-MEGEZEZ LOCALITY, MEGEZEZ SHIELD VOLCANICS NORTH SHOA, CENTRAL ETHIOPIA

BY

TENAW MENGISTIE ALEMAYEHU

Approved by the Examining Committee:

Dr. Balemwal Atnafu	_____	_____
(Head, School of Earth Sciences)	Signature	Date
Prof. Dereje Ayalew	_____	_____
(Advisor)	Signature	Date
Prof. Gezahegn Yirgu	_____	_____
(Examiner)	Signature	Date
Dr. Mulugeta Alene	_____	_____
(Examiner)	Signature	Date

Declaration for Originality

I declare that this thesis is my original work for the requirement of master's degree accomplished under the supervision of Prof. Dereje Ayalew, School of Earth Sciences, Addis Ababa University, during the year 2017/18. My further declaration is that this work has not been presented and/ or submitted to any other college, institution, or university for the award of any degree or diploma. All secondary data, sources and materials used in the thesis work have duly cited and acknowledged.

Tenaw Mengistie Alemayehu (MSc candidate)

Signature _____ Date _____

This is to certify that the above declaration made by the candidate is correct to the best of my knowledge.

Prof. Dereje Ayalew (Advisor)

Signature _____ Date _____

Abstract

Megezez shield volcanics is a mountain area with elevation ~3593 meter above mean sea level forming gentle slope of (~5^0); situated on the north western margin of main Ethiopian rift, central Ethiopia. The area is located 125 kms northeast of Addis Ababa. It is characterized by fissural volcanics with the pre-rift phase of eruption of mid-Miocene age (10.5 Ma). The main objective of this thesis work is to understand the petrography and geochemical compositions of Megezez shield volcanic products and finally to assess their petrogenesis. The present study is aimed to address geological data on Megezez shield volcanics via: 1) detailed geological map; 2) composite stratigraphic section; and 3) detailed petrographic and geochemical data. Twenty samples for petrographic analysis; nine samples for geochemical analysis and structural analysis has been utilized to achieve objectives of the research. Basalt, rhyolite, trachydacite, trachybasalt, and trachyandesite are major volcanic units of Megezez shield volcanics. The studied volcanic products are affected by tectonics of crustal extension. Major geological structures include joints, NE-SW strike and SE dipping normal faults imitating the general orientation of border faults of the Main Ethiopian Rift. Megezez volcanic products show wide variation in chemical composition (45.5-72.2 wt% SiO2) as mafic and intermediate-felsic suite. Basalt and intermediate rocks are transitional type; whereas, the rhyolite rock unite is peralkaline. Selected variation and spider diagrams of major and trace elements show parallel trends indicating the volcanic rocks are co-genetic with the major role of fractional crystallization. Assimilation fractional crystallization has some role to form evolved (intermediate) rocks observed from Rb Vs Rb/Nb discriminating diagram.

Key words: *Megezez shield volcanics, petrography, Fractional crystallization, Assimilation Fractional Crystallization, Crustal Contamination*

Acknowledgement

'Almighty God' is the first to be acknowledged to successfully achieve my objective, and always made everything possible from the beginning up to now.

I am glad to give my gratitude acknowledgement to Debre Berhan University giving the chance to attend my MSc program with no load while paying full salary for two years. The same gratitude is given to Addis Ababa University for accepting my request and delivering the required knowledge for the requirement of degree of masters in Geosciences/ Petrology.

There is no descriptive and adequate word to express my feeling of gratitude to my advisor prof. Dereje Ayalew for his constructive comments, follow-up and encouragement throughout this thesis work. He has always helped me from the beginning to present and made me strong enough to face difficulties with confidence in every movement. I would like to give thank for Dr. Balemwal Atinafu and Dr. Mulugeta Alene, school head and school graduate program coordinator respectively, school of earth sciences, Addis Ababa University, for their academic, administrative and financial support to successfully finish my thesis in a given time line.

Australian Laboratory Services (ALS) private limited company also given acknowledgement for geochemical analysis with significant discount in analysis cost and short time line of data receive. My acknowledgement goes to Asagirt Woreda administrative offices, local people of Megezez area and Gina Ager town for their hospitality, willingness, honesty, and openness to give necessary information during mapping and data collection.

From the beginning to the end of this research work I got lots of support from my friends, colleagues. Specially Mr. Mengistu Kassa (Debre Berhan university), prof. Gezahegn Yirgu, Mr. Amdemichael Zafu, Mr. Bahiru Zinaye, Mr. Million Alemayehu, Mr. Samuel Getachew, Mr. Biniam Fentie, Mr. Ermias Filfilu and Mr. Abate Asen (Addis Ababa university) for their continuous encouragement, comments and multi-dimensional support to reach here. I have gratitude feeling to thank my family and friends especially w/ro Firehiwot Asega, w/ro Amelework Dessie, Mr. Tewodros Tilahun, Mr. Mitiku Kebede, my brothers, sisters and other persons not mentioned here for their unlimited support to complete my thesis work.

Table of content

List of Figures

List of Tables

Acronyms

DEM	Digital Elevation Model
SRTM	Shuttle Radar Topography Mission
ERDAS	Earth Resources Data Analysis System
GIS	Geographical Information Systems
UTM	Universal Transverse Mercator
CSA	Central Statistical Agency
GSE	Geological Survey of Ethiopia
PS	Planation Surface
EARS	East African Rift System
MER	Main Ethiopian Rift
LIP	Large Igneous Province
CFB	Continental Flood Basalt
REE	Rare Earth Element
LREE	Light Rare Earth Element
HREE	Heavy Rare Earth Element
HFS	High Field Strength
LIL	Large Ion Lithofile
ICP-MS	Inductively Coupled Plasma Mass Spectroscopy
ICP-AES	Inductively Coupled Plasma Atomic Emission Spectroscopy
LOI	Loss of Ignition
L.D	Detection Limit
ALS	Australian Laboratory Services
QC	Quality Control
CIPW	Cross, Iddings, Pirsson and Washington
PPL	Plane Polarized Light
XPL	Cross Polarized Light
TAS	Total Alkali Silica
FC	Fractional Crystallization
AFC	Assimilation Fractional Crystallization

CHAPTER – ONE

1. Introduction

1.1. Background

The Main Ethiopian Rift (MER) is the northern part of East African Rift System (EARS) which is attracting geologists due to the wide opportunity to study the variations in compositions and volumes of volcanism with in restricted area (Bekele Abebe et al., 2007). Rate and the total amount of extension of the MER increase northwards, being largest in the Afar triple junction (Bekele Abebe et al., 2007). According to Tsegaye Abebe et al. (2010) MER is approximately NE oriented segment of EARS extending from the Afar to Kenyan rift. MER is mainly composed of three segments (northern, central and southern).

The volcanic provinces from the margins of main Ethiopian rift and Afar cover an area greater than 600,000 km^2 dominated by 300,000 km^3 fissure-fed basaltic lavas forming volcanic plateau (Mohr, 1983 and Ebinger, et al 1993, cited in Kieffer et al., 2004). These volcanic products lie directly on the metamorphic rocks of Precambrian age or Mesozoic sedimentary sequences. The Ethiopian flood basalts cover an area of about 60,000km^2 with a layer of basaltic and felsic volcanic rocks; and the thickness of this layer is highly variable but reaches ~2 km in some regions (Kieffer et al., 2004).

Most of the northwestern Ethiopian flood basalts mainly erupted during 30 Ma, in a short 1 my period, to form a vast volcanic plateau (Hofmann et al., 1997). Immediately after peak of flood volcanics activity, a number of large shield volcanoes developed on the surface of the volcanic plateau. The northwestern part of Ethiopian Plateau comprises shield volcanics overlying the flood basalts. Currently about 20 % of the surface of the plateau is covered by shield volcanoes; with thickness ~ 1.5km at the summits of the volcanoes, above the flood basalt (Kieffer et al., 2004, and Addise Mekonnen, 2006). The common shield volcanics in the north western Ethiopian Plateau are Simien, Choke, Guguftu, Guna, and Megezez (see Fig.1.1). According to Kieffer et al. (2004) these large shield volcanics have different compositions and magma flux of lavas with age ranging from 30-10 Ma. This is the duration from the peak of flood volcanism to the onset of major rifting in the northern part of the volcanic Plateau.

Trachytic flows commonly containing lath- like feldspar phenocryst that emanated from Megezez volcanics are overlying the flood basalts on the flexural margin of Adama basin

(Wolfendene et al., 2004). These trachytic flows from the base of the Megezez have been dated as 10.5 ± 0.2 Ma from whole rock Ar^{40}/Ar^{39} (George, 1997, as cited in Wolfendene et al., 2004, Hofmann et al., 1997) and 10.4 ± 0.2 Ma from K–Ar (Tadiwos Chernet et al., 1998).

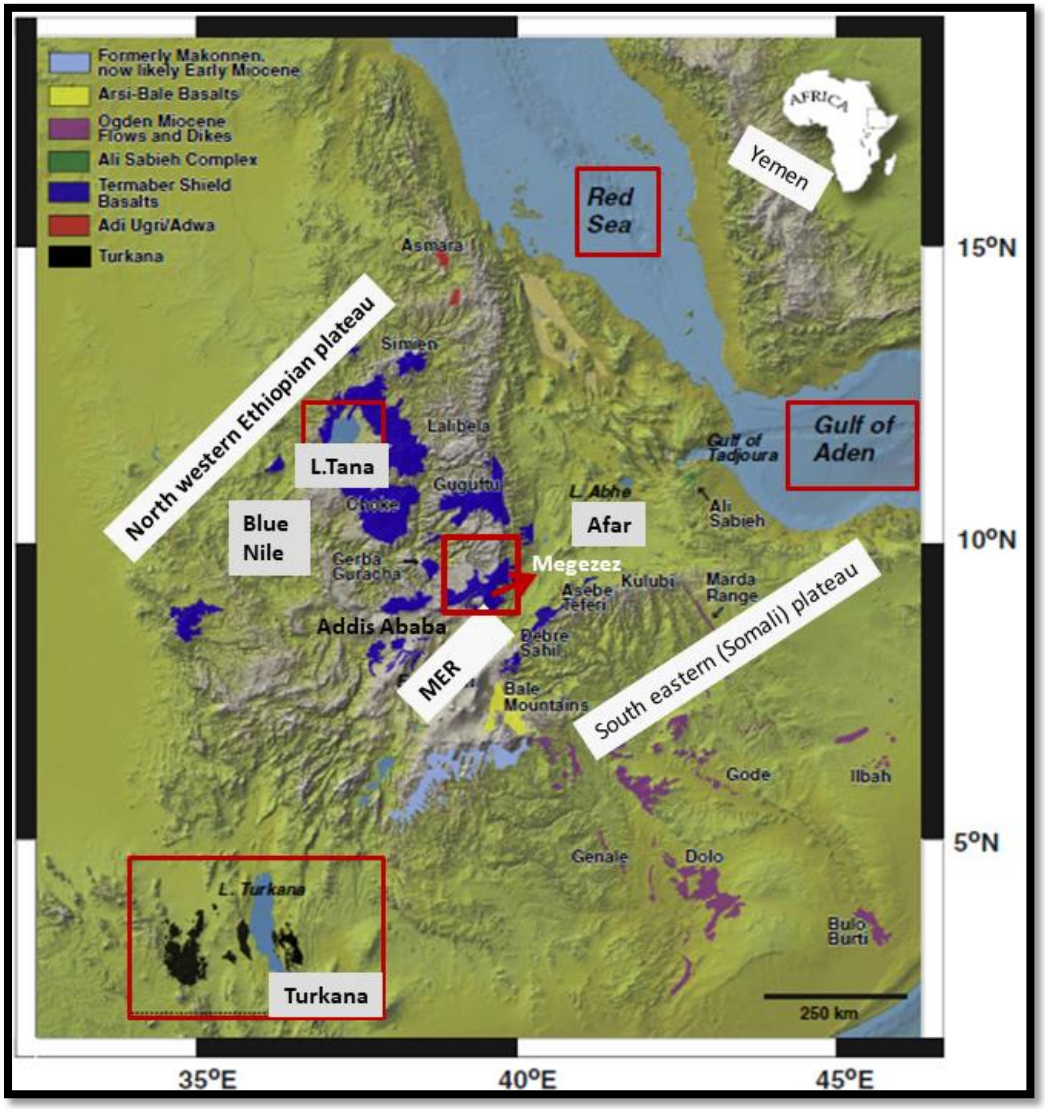

Fig.1.1. Magmatic activity in East Africa -Yemen during the Early Miocene resurgence Phase (26.9–22 Ma) from Rooney (2017).

1.2. Geographic setting of the Study Area

1.2.1. Location and accessibility map of study area

Megezez Mountain is a shield volcanic land form, located in North Shoa Zone, Amhara National Regional State, Ethiopia. The area is accessible with Addis Ababa-Dessie main road travelling from Addis Ababa –Sheno –Sembo asphalt road; and Kotu Gebeya- Gina Ager dry weather road. The total travel distance from Addis Ababa to Gina Ager town is about 125 km, northeast of Addis Ababa. The other alternative road to access Megezez is

from Debre Berhan-Sembo asphalt road to Sembo-Megezez dry weather road. The area falls in Gina Ager map sheet number 0939D1 of Debre Berhan area topographic map (Ethiopian Mapping Agency, 1986).

The area is roughly divided by dry weather road into northern and southern sections. The area is bounded by a grid of Easting from 556000 to 564000 m and Northing of 1024000 to 1034000 m in UTM (Universal Transverse Mercator) 37 P zone.

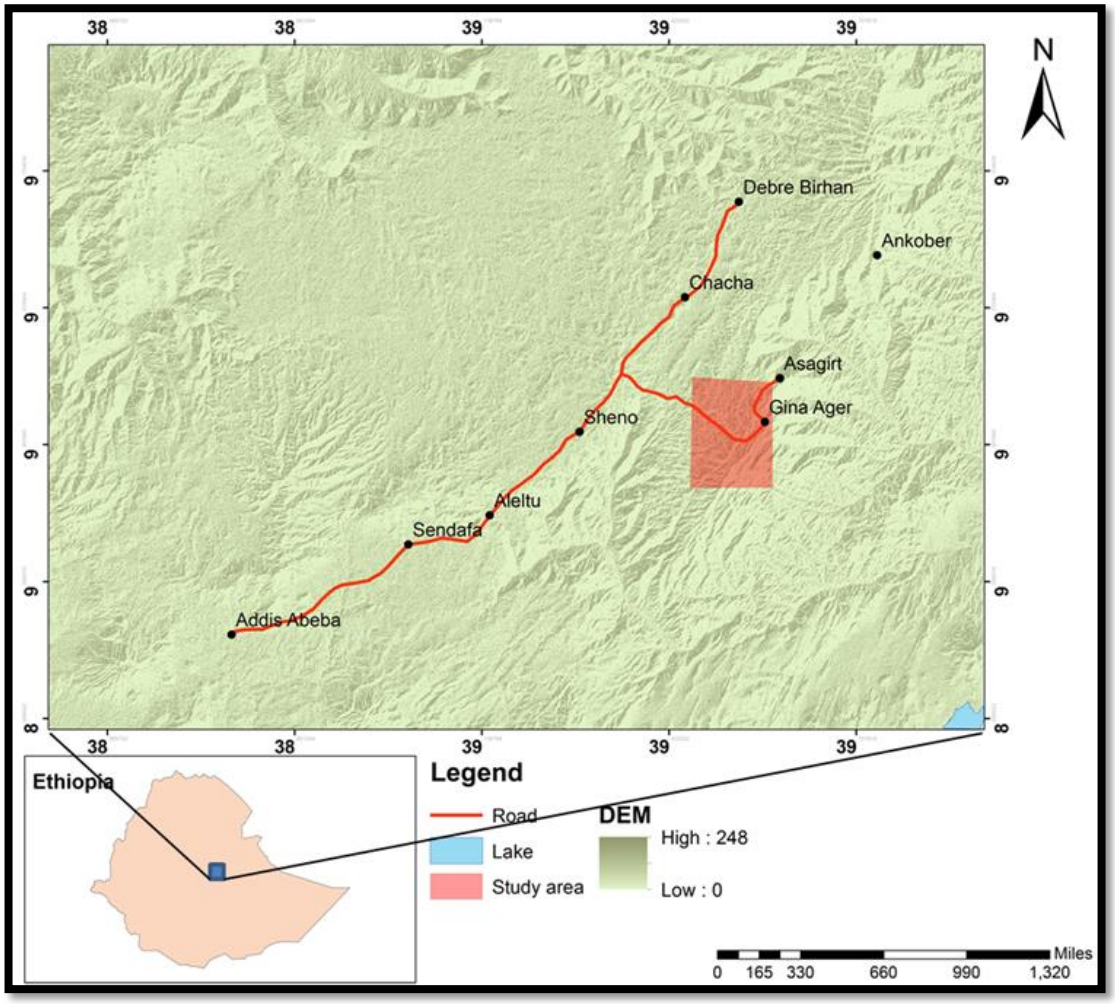

Fig.1.2. Location and accessibility map of the studied area.

1.2.2. Physiography of study area

The physiography of Ethiopia is generally grouped in to three geographical sectors: (1) Main Ethiopian Rift including Afar depression, (2) northwestern Ethiopian Plateau with adjacent low land areas, and (3) South- eastern (Somali) Plateau. The study area is part of northwestern Ethiopian Plateau, located in the western margin of Main Ethiopian Rift. The enormous volcanic and tectonic activities that took place in the Miocene – Pliocene period created distinct physiographic groups in the study area identified as the mountain,

ridges and cliff blocks bounding the rift floor. Megezez Mountain has highest elevation at the peak ~3,593 meter above mean sea level and bordered northeastern, eastern and southern flank with ragged gorges at fault escarpments of western rift margin (see Fig. 1.2).

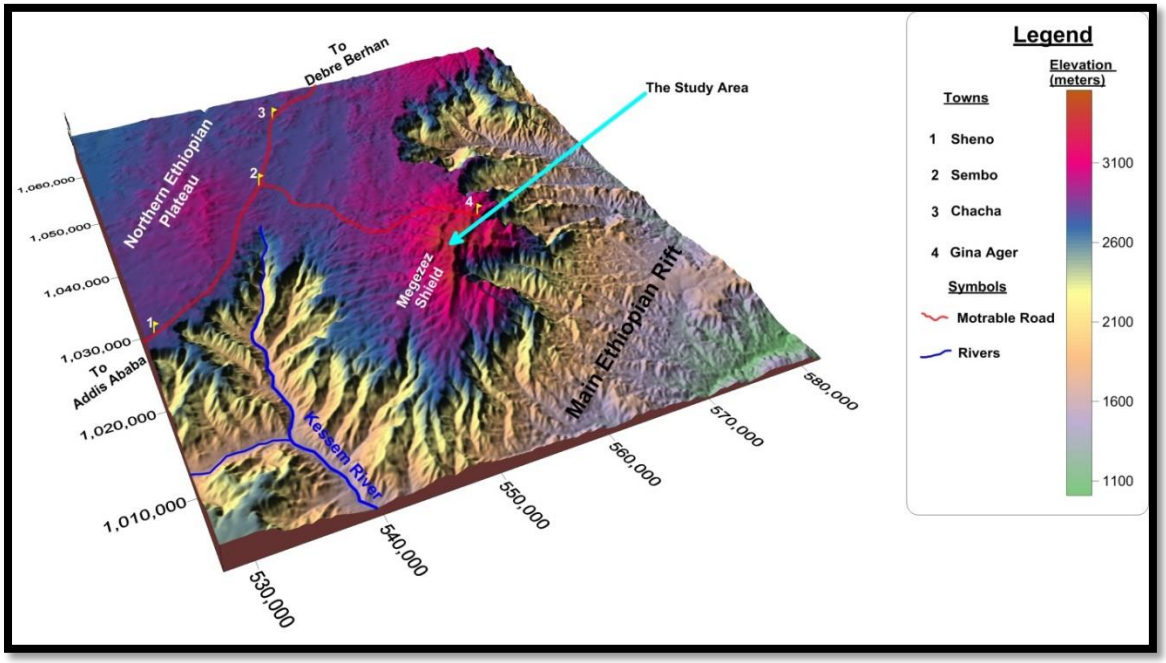

Fig.1.3. Physiographic map of Megezez shield volcanics

1.2.3. Climatic condition

The climate and weather condition in Debre Berhan and eastern side localities including Gina Ager, Asagirt, Ankober and Megezez-Weneberi are the cold temperature condition. The studied area is generally very cold and windy. The wind blowing east west direction is very pressurized increasing towards the Peak of mount Megezez. Ankober is situated eastern side of Debre Berhan town, and north of Megezez approximately having similar physiographic feature and higher elevation to Megezez. The climate data of Ankober station was used to explain the temperature and precipitation conditions to Megezez locality. The maximum and minimum monthly average temperature is recorded during months of May-June (17.3^0C) and December ($12.3\ ^0$C) respectively, with variation of $5\ ^0$C throughout the year. The driest and wettest months are December (5mm) and July (309 mm); and the variation in the precipitation is 304 mm.

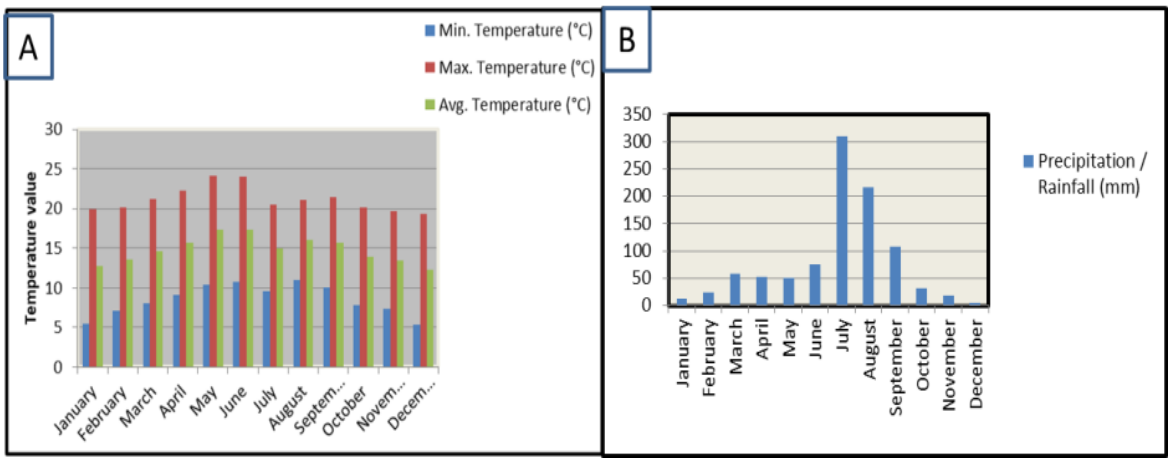

Fig.1.4.Bar charts showing climate (A) and precipitation (B) conditions of Ankober area, north of Megezez, north Shoa. Sourced from Climate.data.org: https://en.climate-data.org/location/928323/

1.2.4. Population and Settlement

The population density in the study area is generally low. Small kebeles like Megezez, Weneberi, Wena and Chiraro are within the study area. Among these small kebeles, Megezez is least populated relative to the above three. Based on the 2007 Census conducted by the Central Statistical Agency of Ethiopia (CSA), the total population of Asagirt wereda is 48,371. Gina Ager town which is the part of studied area, north of Mount Megezez; has total population of 2,482. The total ethnic group in the study area is Amhara; with spoken language of Amharic.

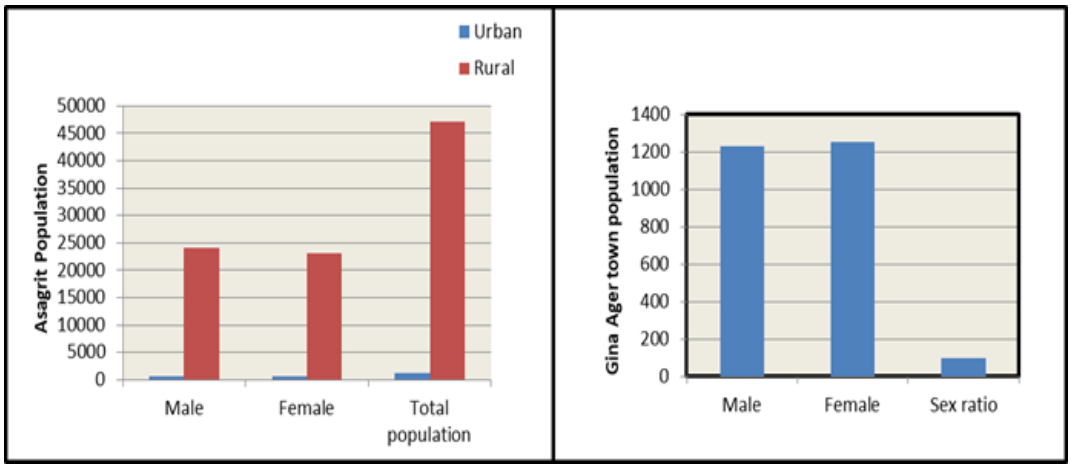

Fig.1.5. Bar charts showing population of Asagrit wereda (left) and Gina Ager (right), north Shoa zone, Amhara regional state. Data source is from 2007 Census conducted by the Central Statistical Agency of Ethiopia (CSA).

1.3. Problem Statement

Many researchers have conducted studies on northwestern Ethiopian plateau basalts including shield volcanics. The Main Ethiopian Rift (MER) bisects the Ethiopian highlands in to two; western and eastern Plateaus. These Plateaus comprise both trap

series and overlying shield volcanics. Conducting research on shield and Plateau volcanics give better geologic evidence about magmatism and volcanic history; because these volcanic areas are relatively tectonically more stable and can give continuous geological record.

Northwestern shield volcanoes like Simien, Guguftu, Choke, and Guna have been well studied by Kieffer et al (2004, and references there in). Megezez area has been mapped by different geologists with different objectives in regional scale. Basic understandings on the geochemistry of Megezez volcanics have been presented by Gezahegn Yirgu (1997). However, major scientific gaps remain unsolved like geological map, stratigraphic section, and sufficient petrographic and geochemical data to further characterize the compositional variability of volcanic products together with their succession, distribution and petrogenesis. These visible scientific gaps on the petrography, Petrology, and petrogenesis initiate to conduct research on Megezez shield volcanics.

Hence, this research aims to solve the following: (1) produce detailed geological map, composite stratigraphic log section, and petrographic interpretation of Megezez volcanics; (2) compile representative primary data collected from the studied area to address the petrographic and petrology of observed lithologic units; and (3) understand the petrogenesis of Megezez volcanic suite with their genetic relationship.

1.4. Objectives of the research study

1.4.1. General Objective

The general objective of this research work is to describe the petrograpic and geochemical composition of Megezez shield volcanics and to assess their petrogenesis.

1.4.2. Specific Objectives

- To produce detailed geological map with scale of 1:50,000
- To produce a composite stratigraphic log section of Megezez volcanics
- To recognize the mineralogical and petrographic features of the volcanic rocks in the area
- To assess the petrogenesis of observed volcanic suite supported with major and trace element signature using different chemical variation and spider diagrams.

1.5. Research Methods

The general framework of this thesis was in three divisions: 1) pre-field work, 2) field work, 3) post field work.

Previous works on Sheno – Megezez area (Gezahegn Yirgu, 1997), regional studies on Debre Berhan area (Feyissa Dejene Hailemariam et al., 2017); north western Ethiopian shield volcanics (Kieffer et al, 2004, Addise Mekonnen, 2006) thoroughly used to broaden the researcher's understanding on research approaches.

Both primary and secondary data discussed, interpreted, and finally written up in a final thesis report. Major research methods are presented separately in the following sections.

1.5.1. Literature survey

Relevant and annotated reading materials on magmatism, petrology and petrogenesis of flood and overlying shield volcanics in the western and eastern Ethiopian Plateau, Main Ethiopian Rift (MER), and marginal volcanic products have been thoroughly explored. Literature survey used to have comprehensive understanding on:(1) geochemical data analysis, presentation and interpretation techniques based on their accuracy, precision, and procedures; (2) the analytical methods used and their role in the present research. ICP-AES and ICP-MS combined methods adopted from taken from Kieffer et al. (2004); utilized on studies of northwestern Ethiopian flood and shield volcanics.

1.5.2. Field geology and geological mapping

Field work and geological mapping conducted with three phases to attain the objectives of the thesis work as: the first phase spending two consecutive days; second phase for 10 consecutive days; and the third phase took three days.

Base maps, remote sensing applications and GIS software (ERDAS, ArcGIS, Google earth, Global mapper), and DEM data utilized to produce location map, geological map, and physiographic map of the study area. Major faults analyzed in the study area delineated from DEM data and Google earth to support field observations.

1.5.3. Secondary data

Previous data collected and generated from different sources including climate data, and population data used as an input. Previous works like topographic and geological maps, literatures collected from advisor, staff members in school of earth sciences, and webpages also thoroughly used. Secondary geochemical data from Megezez (eight) and

underlying Alaji silicic(one) samples from Gezahegn Yirgu (1997) plotted in different variation and spider diagrams together with primary data to make comparison.

1.5.4. Laboratory and Primary data

The samples collected during field work prepared for two purposes: (1) for petrographic study; (2) for geochemical analysis.

1.5.4.1. Petrographic Analysis

A total of twenty representative rock samples were selected for petrographic analysis. These samples collected from porphyritic basalt (thirteen), rhyolite lava flow (one), trachy dacite (one), aphaneritic trachy basalt (one), trachy andesite (one), and the three samples for different dyke intrusions. Samples have submitted to Geological Survey of Ethiopia, laboratory center for thin-section preparation. Petrographic description is conducted in Mineralogy and Petrology laboratory, school of earth sciences, Addis Ababa University.

1.5.4.2. Analytical methods and sample preparation

- **Sample preparation**

The samples submitted to Australian Laboratory services (ALS), available in Ethiopia. First, samples finely crushed and powdered to 70% of <2mm size, and pulverized with riffle splitter to have whole rock geochemical analysis. Sample preparation was accomplished with the following procedures: samples received to ALS services – labeled with a bar code – finely crushed to 70 %< 2mm – pulverized with riffle splitter – crushing tested with Quality Control (QC) test – pulverizing split tested with QC test.

- **Geochemical Analysis**

To achieve the geochemical signatures of elements for whole rock chemistry, a total of nine representative and relatively fresh samples was selected. These samples submitted to ALS laboratory services. The powdered samples sent to ALS services, Ireland and analyzed for major, trace element chemical data. Geochemical data done with a combined method of ICP-MS and ICP-AES (ME-MS81d) to generate trace elements and major concentration respectively. Major elements SiO_2, Al_2O_3, Fe_2O_3, CaO, MgO,Na_2O, K_2O, TiO_2, MnO, P_2O_5, analyzed with ICP- AES (ME-ICP06) whole rock package ; and trace elements Ba, Ce, Cr, Cs, Dy, Er, Eu, Ga, Gd, Hf, Ho, La, Lu, Nb, Nd, Pr, Rb, Sm, Sn,Sr,Ta,Tb, Th, Tm, U, V, W, Y, Yb, Zr with whole rock package of Lithium Borate

Fusion by ICP-MS(ME-MS81). In addition, base metals Ag, As, Cd, Co, Cu, Li, Mo, Ni, Pb, Sc, Tl, Zn, analyzed with ICP-AES (ME-4ACD81) 4 acid digestions.

Table 4.1. Summary for analytical procedures.

Australian laboratory (ALS) services code	Analytical methods	Descriptions	Data
ME-ICP06	ICP-AES	Whole rock package ICP-AES	Major elements
OA-GRA05	WST-SEQ	Loss on ignition at 1000 ^{0}C	Total volatiles
ME-MS81	ICP-MS	Using lithium borate fusion ICP-MS	Trace elements
TOT-ICP06	ICP-AES	Total calculation for ICP06	Major elements
ME-4ACD81	ICP-AES	Using 4 acid digestions	Base metals

Three standards AMIS0304, ORAES-12, and ICP-4 have been used as quality control measurements; which are the certified reference material by Australian Mineral Standards (AMIS) available in Australia laboratory services (ALS) private limited company. Certified reference materials for trace elements used are AMIS0304 and ORAES-12; for major elements AMIS0304; and for base metals ICP-4. The precision of major oxides is better than 0.01%. The confidence interval for trace elements slightly varies in precision range. The precision is within a confidence interval of <0.2% for high field strength elements (HFS) like Ta, Nb, Th, La, Hf, U, Y; whereas Pb and Zr which is better than 2 and 3% respectively. The precision of large ion lithophile elements like Sr, Rb, and Ba is <0.25 average; rare earth elements like La, Ce, Eu, Gd, Yb, Dy show confidence interval of 0.01-0.9 precision; highly compatible elements like Ni, Co, <1, V<5, and Cr<10 confidence interval of precision.

1.5.5. Synthesis, interpretation and presentation

Data synthesis involves collecting and integrating different data sets into coherent information for final interpretation. Primary and secondary data synthesizing and interpretation were post field work tasks in this research work. Different software packages like petrograph2beta, GCDKit, Adobe illustrator (AI) Microsoft Excel, Stereo net, and GeoRose thoroughly used based on their respective purpose in this research.

This software finally gave coherent and meaningful information for final interpretation and discussion. Data presentation is in the form of text, table, graph and map. The text provides descriptions of the lithological, petrographic, and geochemical results presented

with graphs, tables and maps. The presented data put into a regional context by comparing relevant literatures on the study area or nearby volcanic products.

1.5.6. Research relevance and expected outcome

As stated above in the problem statement, the petrography and petrology of Megezez have not been studied well. Therefore, this research is expected to fill these gaps; and will have the following relevance for the scientific community and an input for further studies. The main research outcomes and relevance will be:

- Previous geological map on Megezez shield volcanics done regionally at scale 1:250,000; whereas, the present research tried to identify various lithologic units as mafic, intermediate and felsic volcanic products, with their spatial distributions at scale of 1:50,000.
- Will be the first to construct composite volcanic stratigraphic log section of Megezez shield volcanics and assessing volcanic history.
- To give the location, physiographic and accessibility map of the study area for different aspects of geological studies on Megezez and localities around.
- Understanding the petrography and petrology of Megezez with additionally investigated rock units than previously taught.
- To promote the understanding of the mineralogical and geochemical characteristics of these rocks in order to establish their genesis (source and history) with contributions on some data sets to the ongoing worldwide studies of Ethiopian Cenozoic volcanism.

1.6. Review of previous works

Much of Ethiopia and Djibouti has experienced Cenozoic hot spot tectonism, including plateau uplift, rifting, and flood basalt volcanism (Mulugeta Dugda et al., 2007). Wolfendene et al. (2004) have presented the tectonic and structural map of Main Ethiopian Rift (MER), rift-rift-rift triple junction (Red sea-Gulf of Aden-Afar), major border faults, central volcanoes of the rift axis (e.g. Boset, Cone, and Fentale). The rift floor is obliquely affected by a system of ~NE-SW-to N-S-trending border faults and ~NNE-SSW- to N-S-trending, en-echelon arranged faults (Mohr, 1962 and Gibson, 1969, cited in Cortti, G. et al., 2009).

Many geological studies have been conducted both on the Main Ethiopian Rift (MER) and the adjacent volcanic Plateaus in the western and eastern margin. Studies show the Main Ethiopian Rift (MER) is bounded by boundary faults with the orientation of $N40^0E$.

Boccaletti et al. (1998) suggested that faults form escarpments to the boundary of the rift and the Plateau. The petrogenesis of rock suits both in MER and Afar studied by many geologists (Gibson, 1972; Barberi et al., 1975; Gasparon et al., 1993, Boccaletti et al., 1995). These authors also shown the origin of large volumes of silicic extrusive rocks in Main Ethiopian Rift (MER) and Afar is attributed to fractional crystallization of basaltic magmas with limited crustal contamination.

Dereje Ayalew and Gezahegn Yirgu (2003), recognized four units (Wegel Tena, Jima, Lima Limo, and Debre Berhan areas), each with its own geochemical specificity. They have suggested the formation of Ethiopian continental flood basalt province (~30 Ma, >3 x 105 km3) was result from the impingement of the Afar mantle plume beneath the Ethiopian lithosphere. Pik et al. (1998) under take detailed geochemical studies on the Oligocene flood basalts of the northwestern Ethiopian trap series. The trap basalts grouped in to three distinct geochemical groups based on Ti- concentration (low Ti, High Ti-1 and high Ti -2) (Pik et al., 1998). Based on this classification scheme, Megezez shield volcanic products fall in the region of High-Ti1 (HT1). The mantle and crustal source involvements on the genesis of pre-rift continental flood basalts of northwestern Ethiopian Plateau have been identified by Pik, et al. (1999).

The volcanic units of the northern and central part of western Ethiopian Plateau have classified as Ashangi formation---Aiba basalts---Alaji formation---Tarmaber-Megezez formation(bottom to top chronology) (Kazmin, 1972,Mohr, 1967, Merla et al., 1979, Berhe et al., and 1987, Mohr).

Flood volcanism was succeeded by emplacement of large shield volcanoes and by continental rifting (Mohr, 1983 and Hoffmann et al., 1997). A number of large shield volcanoes including Simien, Guguftu, Choke and Guna from the northwestern Ethiopian plateau developed on the surface of the volcanic plateau overlying the thick sequence of flood basalt (Kieffer et al., 2004). Kieffer et al. (2004) suggested that the shield volcanoes from northwestern Ethiopia are magmatically similar to the underlying flood basalts. That is the tholeiitic Simien shield overlies tholeiitic flood basalts, and the alkaline Choke and Guguftu shields overlie alkaline flood basalts. Hofmann, et al. (1997), Coulie et al. (2001), Ukistins et al. (2002), Kieffer et al. (2004) provide absolute 40Ar/39Ar age determination on Oligocene-Miocene flood volcanics and Miocene - Pliocene volcanoes from the western Ethiopian Plateau.

The contact between Megezez and flood volcanics traced in imagery throughout the region (Wolfenden et al, 2004); and the pre-rift flood volcanics and syn-rift units show a regional SE dip. Some authors have conducted shallow studies on the geological distribution, petrology, geochemistry, age, and geological setting of Megezez volcanic products together with Tarmaber formation (Gezahegn Yirgu, 1997; Tadiwos Chernet and Hart, 1999; Tadiwos Chernet et al., 1998; Wolfendene et al., 2004, Geological survey of Ethiopia (GSE, 2009), and Feyissa Dejene Hailemariam et al., 2017).

Better work on the petrogenesis and geochemistry of Megezez shield comparing with the plateau basalt and Alaji silicics compiled by Gezahegn Yirgu (1997). Compositional variations of Megezez volcanics have been presented as mafic to intermediate suits (Gezahegn Yirgu, 1997 and Tadiwos Chernet et al., 1998). The Mid-Miocene Tarmaber–Megezez formation erupted from centers along the developing rift shoulder (Kazmin et al., 1980). Tadiwos Chernet and Hart (1999) have presented chronostratigraphic unit of Tarmaber-Megezez formation deposited overlying Alaji basalt with a hiatus. Megezez have been dated as 10.4 Ma as Ar-K compilations and Ar-Ar compilation as 10.5 Ma (George, 1997, as cited in Wolfendene et al., 2004, and Tadiows Chernet et al., 1998 respectively).

The petrographic and chemical composition of Megezez volcanics characterized by olivine, -pyroxene phyric basalt, plagioclase phyric basalt (Tadiwos Chernet and Hart, 1999). The compositional variations range from 45.1-52.5 silica content; with alkaline/transitional type.

Structural and stratigraphic relationships in the central sector indicate a two- stage rift development (Gidey Woldegebriel et al., 1990). This is characterized by an early phase (late Oligocene or early Miocene) of a series of alternating opposed half-grabens along the rift.

Table 1.1. Stratigraphic unit rock types (Tadiwos Chernet and Hart, 1999)

Age	Group nomenclatures	Phase of activity	Rock types	Distribution
Oligocene - Miocene	Alaji group and Plateau basalts	Pre-rift	Basalt to mugearite	NW & SE plateau
Miocene	Tarmaber group, Plateau basalts, Tarmaber-Megezez formation	Pre-rift	Basanite to mugearite	NW & SE plateau
Miocene-Pliocene	Nazret	Pre-rift/ post-rift	Basalt to mugearite	N.MER escarpments

Unit	Main petrographic types	SiO2(wt%)	TAS nomanclature	Nature of alkalinity
Tarmaber group	Olv. Basalt, Olv, -cpx basalt, plag. Phyric basalt	45.1-52.5	Basalt, basanite, hawaiite, mugearite	Alkaline/ transitional to subalkaline(alkaline olv. basalt to tholeiite)
Alaji group	Plag. Phyric basalt, olv. baslt, olv, -cpx basalt(± olv. basalt)	45-53	Basalt, basaltic andesite, hawaiite, mugearite	Transitional to sub alkaline(olv. tholeiite to quartz tholeiite)
Nazret group basalt	Olv, -cpx basalt,(± opx), plag. Phyric basalt, olv. basalt	46.5-53.2	Basalt, hawaiite, mugearite	Transitional to subalkaline(alkaline olv. basalt to tholeiite)

Table.1.2. Distributions of different volcanic products from north Western Ethiopian plateau (Kieffer et al., 2004, Addise Mekonnen, 2006, and references there in).

Rock type	Age	location	Data source
Mio-Pliocene Volcano	10.6-3.2Ma	North of Addis Ababa	Ukstine et al. (2002)
	10.7Ma	Mt.Guna	Kiffer et al. (2004)
	10.9-19.8Ma	Between Addis Ababa and Dese	Ukstine et al. (2002)
	18.7Ma	Simien Mt.	Kiffer et al. (2004)
	21.6Ma	Alem Ketema	Coulie (2001)
	22.3 Ma	Guguftu Mt.	
	22.4 Ma	Mt. Choke	
Flood Basalt	25.3 Ma	Between Addis Ababa and Dese	Ukstin et al. (2002)
	26.9-29.4 Ma	Blue Nile river	Hofmann etal. (1997)
	30.9-25.0 Ma	Near Dese	
Mid-Miocene volcano	10.5 Ma	Mt. Megezez	Ukstin et al.(2002), George (1997)

1.7. Thesis frame work

This thesis is framed with six main chapters. The first chapter gives general back ground; location; accessibility; climate; population and settlement of study area; problem statement; objectives of the study, significances and research methods followed in the research. The second chapter presents an overview on regional geologic setting. The third chapter is focusing on presenting geological map and composite stratigraphic section for mappable rock units; rock descriptions from exposures; and petrographic descriptions with interpretations of analyzed samples. Chapter four presents the geochemical data analysis, synthesis, presentations and interpretations using different geochemical models. The chapter five is the discussion part of the thesis to summarize and generalize field, petrographic, and geochemical results and interpretations given in separate sections. Finally, chapter six deals on the main conclusions on petrography and petrology of Megezez shield volcanics. Major scientific points have recommended for future studies.

CHAPTER -TWO

2. Regional Geological Setting

2.1. East African Rift System

The East African Rift System is a Miocene-Quaternary intracontinental extensional system composed of several interacting rift segments, from Mozambique to Afar. At Afar, the EARS join with the Gulf of Aden and Red Sea Rifts, characterized by a more advanced extensional stage. The East African rift system is a series of several thousand kilometers long aligned successions of adjacent individual tectonic basins (Chorowicz, 2005); which can be regarded as an intra-continental ridge system comprising an axial rift. The Rift System provides an advantage to investigate the compositional variation of erupted magma with the amount of extension (Bekele Abebe et al., 2007).

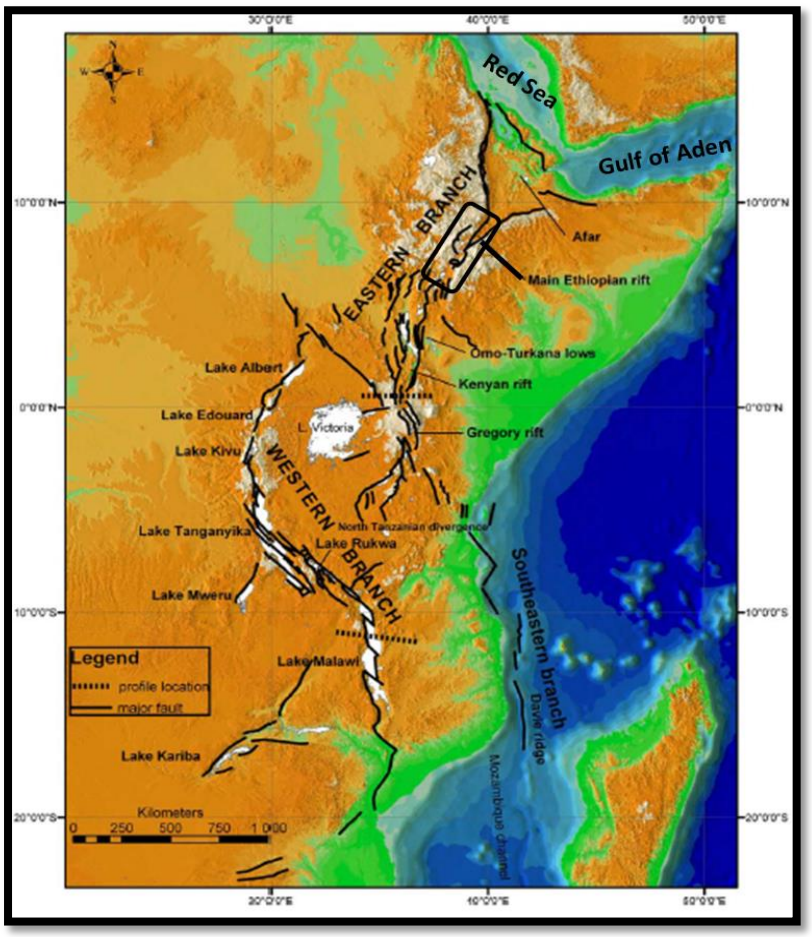

Fig.2.1. Hypsographic DEM of the East African rift system. Black lines are main faults; white surfaces indicate lakes (Chorowicz, 2005).

2.2. Main Ethiopian Rift

The Main Ethiopian Rift is the northernmost sector of the East African Rift System; connecting this continental rift to the oceanic spreading centers of the Red Sea and Gulf of Aden (e.g. Bonini et al., 2005, Corti et al., 2009). It is considered as an ideal place to analyze the evolution of continental extension, the rupture of lithospheric plates and the dynamics by which distributed continental deformation is progressively focused at oceanic spreading centers. The Main Ethiopian Rift (MER) constitutes a part of the East African Rift System (EARS) and merges with the oceanic Red Sea and Gulf of Aden rifts in a triple junction located in the Afar depression (Wolfenden et al., 2004). Rifting and volcanism has been considered to be related to mantle plume activity (e.g. Furman, 2007; Marty et al., 1996; Pik et al., 1999). The dominant part of the Main Ethiopian Rift volcanic is Plio-Quaternary in age and older volcanic massifs only limited to the rift margins. In Afar, basaltic lavas predominate over intermediate and acid products, while a number of intrusive granites have also been emplaced during the early evolution of the rift. In the Main Ethiopian Rift (MER), basic products are subordinate to evolved lavas and pyroclastics. Contemporaneously to the connection between the MER and Red Sea rifts, a flood basalt event has been occurred (Chernet et al., 1998). The MER is also characterized with a volcanically active region in east African rift; marked with the transition from continental rifting process in East African rift to incipient sea floor spreading in Afar (Maguiere et al., 2006).

Different studies show, MER is characterized by roughly NE-oriented segments of the East African Rift system, extending from Afar to Kenya rift system. It is mainly composed of northern, central and southern segments with a rift propagation progressed northward (Tsegaye Abebe et al., 2010, Wolfendene et al., 2004, Abate and Sagri, 1980, Abbate et al., 2015, Kier et al., 2006 and references there in).

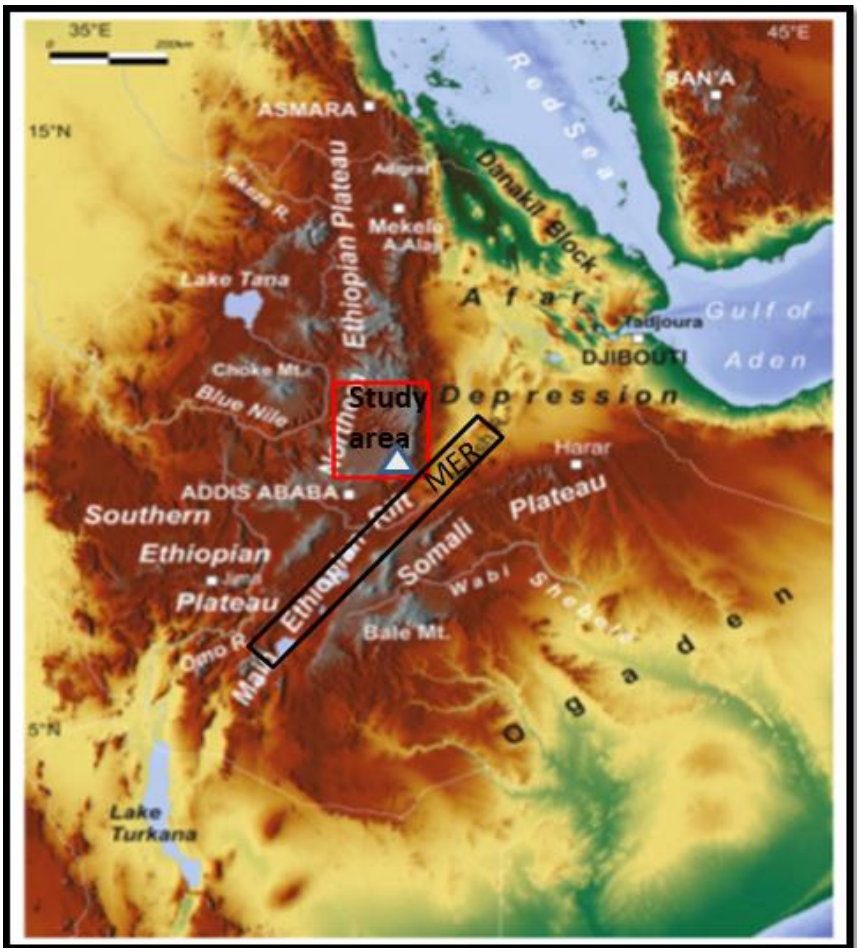

Fig.2.2. Digital elevation map of Ethiopia (SRTM data) with the main physiographic elements, mainly to represent north western and eastern (Somali) Ethiopian plateau, main Ethiopian rift (MER), (Abate et al., 2015).

2.3. Continental flood basalt provinces

Much of Ethiopia and Djibouti has experienced Cenozoic hot spot tectonism, including flood basalt volcanism, plateau uplift, and rifting (Mulugeta Dugda et al., 2007). The East African rift system is of particular interest as large Continental Flood Basalts (CFB) were erupted during the Tertiary associated with regional uplift (Ethiopian and Kenyan domes). These volcanics have been attributed to one or two distinct mantle plumes (Ebinger and Sleep, 1998; Rogers et al., 2000; Gezahegn Yirgu et al., 2006, cited in Beccaluva et al., 2009). The Early Oligocene Northern Ethiopia-Yemen volcanic province comprises the entire range of CFB magmas, from Low-Ti to High-Ti and very High-Ti basalts and picrites (Beccaluva et al., 2009). Also suggested that CFB erupted in a well-defined space-time interval, and overlain by younger alkaline basalts with peridotite xenoliths, providing a direct evidence of the nature of the mantle beneath the plateau. This CFB province corresponds to the region where Afro-Arabia continental break-up took place with the formation of the Red Sea-Gulf of Aden-East African rift system centered on the

Afar triple junction, where a possible deep mantle plume has been suggested on the basis of geophysical data (Hofmann et al., 1997; Davaille et al., 2005).

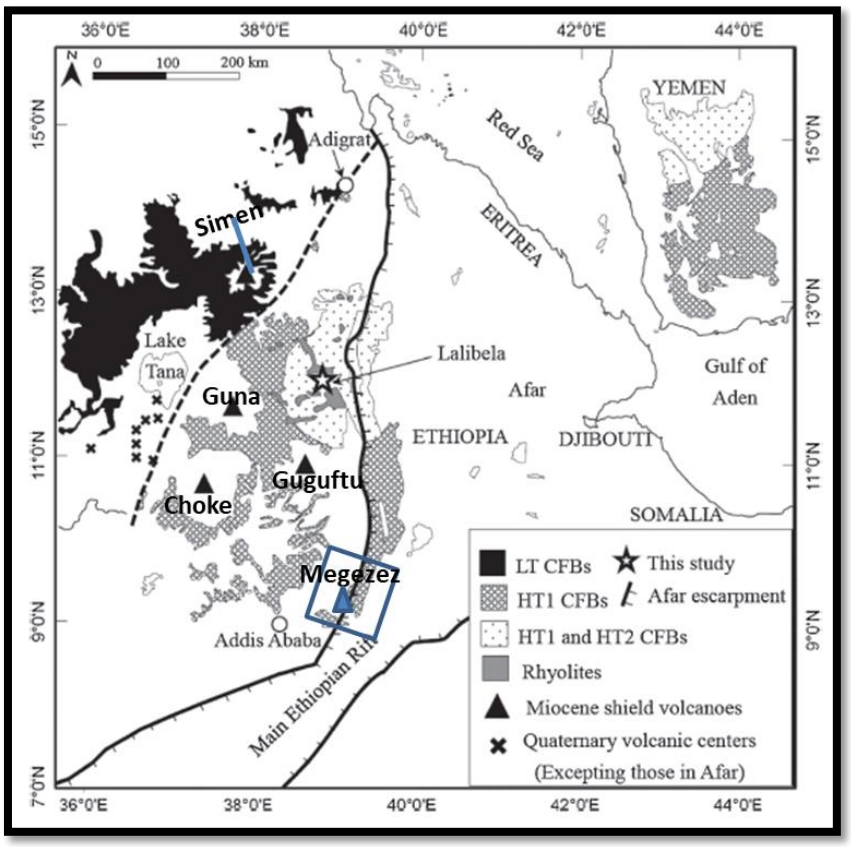

Fig.2.3. Sketched geological map of Ethiopian large igneous provinces (LIP) including Yemen conjugate margin, showing distributions of continental flood basalts and shield volcanics: LT= low -Ti tholeitic basalts, HT1= high-Ti tholeitic basalts, HT2=very high-Ti transitional basalts and picrites (Minyahl Teferi et al., 2014 and references there in).

Northern Ethiopia and the conjugate Yemen margin, CFB generation was favored by several factors: 1) lowered solidus temperatures of plume metasomatized mantle sources; 2) heat transfer by the plume buoyancy flux that raised the regional geotherm; and 3) decompression of the upwelling mantle (Beccaluva et al., 2009).

Cenozoic flood basalt volcanism, plateau uplift, the development of the Main Ethiopian and Afar rift systems have been attributed to the upwelling of a mantle plume with a potential link to the African Super plume (Pik et al., 1998, Kieffer et al., 2004, and references there in).

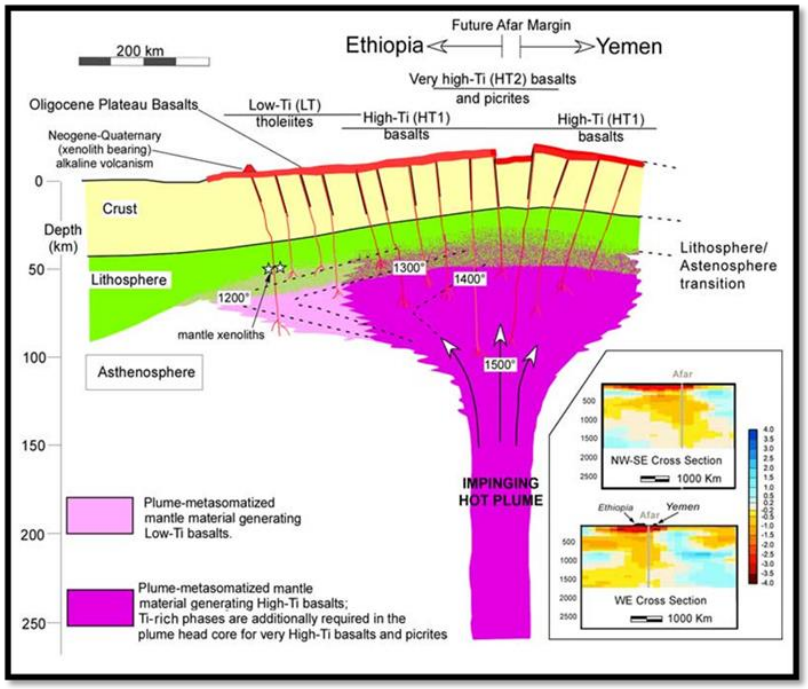

Fig.2.4. Illustration showing the Afar plume impinging on the Afro-Arabian lithosphere and the generation of Oligocene Northern Ethiopia-Yemen CFBs from a thermally and compositionally zoned plume head (Beccaluva et al., 2009). The inset shows mantle tomographic cross-sections beneath Afar, based on models for shear-wave velocity variations (Davaille et al., 2005).

2.4. Northwestern Ethiopian Plateau

The Afar and MER cut the plateau volcanics of Ethiopia in to two major sectors as western and south eastern (Somali) plateau. The western plateau comprises northern, central and south western plateau; whereas the south eastern is divided as eastern, south eastern and southern most sectors of the Ethiopian flood volcanic province (Corti, 2009).

The volcanic units of the Northwestern Ethiopian Plateau (Kieffer et al., 2004) mainly classified as: (1) the Oligocene flood volcanics (Trap series) including Oligocene – Miocene basalts and rhyolites; (2) Miocene- Pliocene shield volcanoes; (3) Volcanic plugs and domes; (4) Quaternary volcanics.

Quaternary plateau basalts and volcanics comprise all Quaternary alkaline basalts and trachyte emplaced on the northwestern and southeastern plateaus. Alkaline basalts and trachytic lavas prevail in the region south of Lake Tana (see Fig. 2.5). As suggested in Kieffer et al (2004) and Pik et al (1998, 1999) the northwestern Ethiopian Plateau is covered with different date of eruptions, magmatic fluxes and compositions of volcanic products. It can be subdivided in terms of Ti- compositional variations (Pik et al., 1998, 1999) as low-Ti-provinces exposed in the northwestern and high-Ti- basalts provinces exposed in the south eastern plateau (see Fig. 2.5).

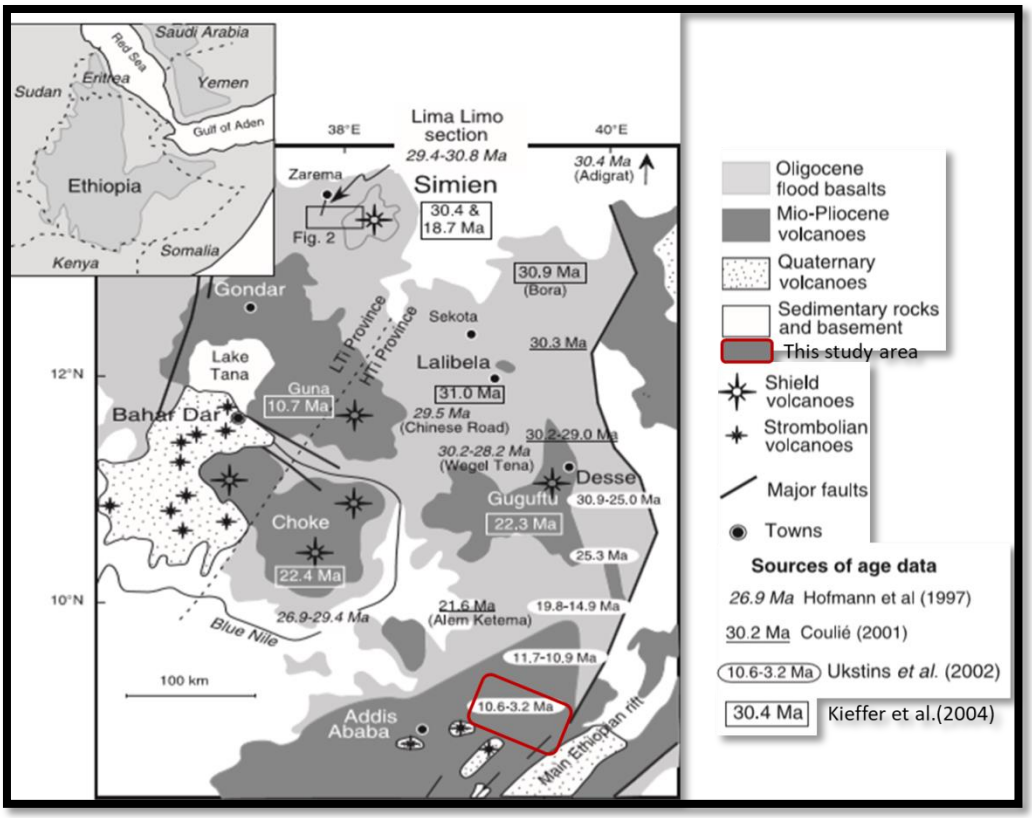

Fig.2.5. Geological Map of north western Ethiopian plateau showing the extent of the flood volcanism and the location and ages of the major shield volcanoes (Kieffer et al., 2004, after Zanettin, 1992 and Pik et al., 1999,).

2.4.1. Tarmaber-Megezez Formation

In the NE, thick sequences of 30 Ma flood basalts are overlain by the 30 Ma Simien shield volcano (Kieffer et al., 2004). The flood volcanism was succeeded by emplacement of large shield volcanoes and by continental rifting (Hoffmann et al., 1997, Kieffer et al., 2004, and references there in). The ages of the Tarmaber shield volcanoes are Early and Middle Miocene, ranging from 23 to 11 Ma (Kieffer et al., 2004), with the exception of the Simien dated as 30 Ma to the base and 19 Ma to the top. Megezez and Guna shield volcanics are exceptionally young in age for which Guna is 10.7 Ma (Kieffer et al., 2004), and Megezez dated as Ar^{40}-Ar^{40} of 10.5 ±0.2 (George, 1997, cited in Wolfenden, 2004) and K-Ar of 10.4±0.2 (Tadiwos Chernet et al., 1998). Choke and Guguftu Shield Mountains have ages of 22 Ma (Kieffer et al., 2004,). Tarmaber-Megezez basalts are overlying the Sela Dingay-Debre Berhan-Gorgo ignimbrites (Geological Survey of Ethiopia (GSE, 2009) and Feyissa Dejene Hailemariam et al., 2017). In the southwestern part of the plateau highly alkaline lavas were erupted from a number of Quaternary volcanic centers. Tarmaber formation is localized in the northern Ethiopia (Tigray) and Central Ethiopia (Blue Nile) in all cases overlying Alaji silicics (see Fig. 2.6).

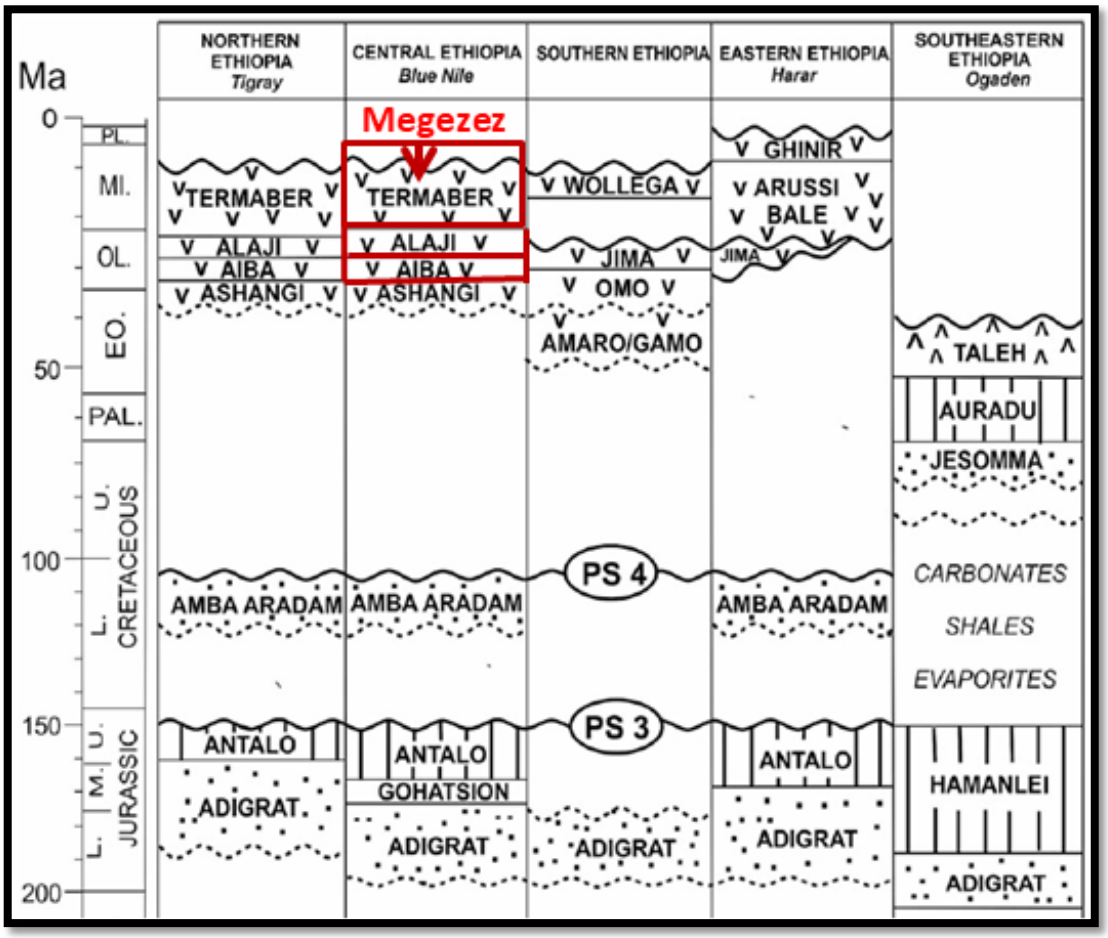

Fig. 2.6. Schematic stratigraphic chart of Ethiopia (from Abbate et al., 2015) with the major planation surfaces (PS) of Coltorti et al (2007).

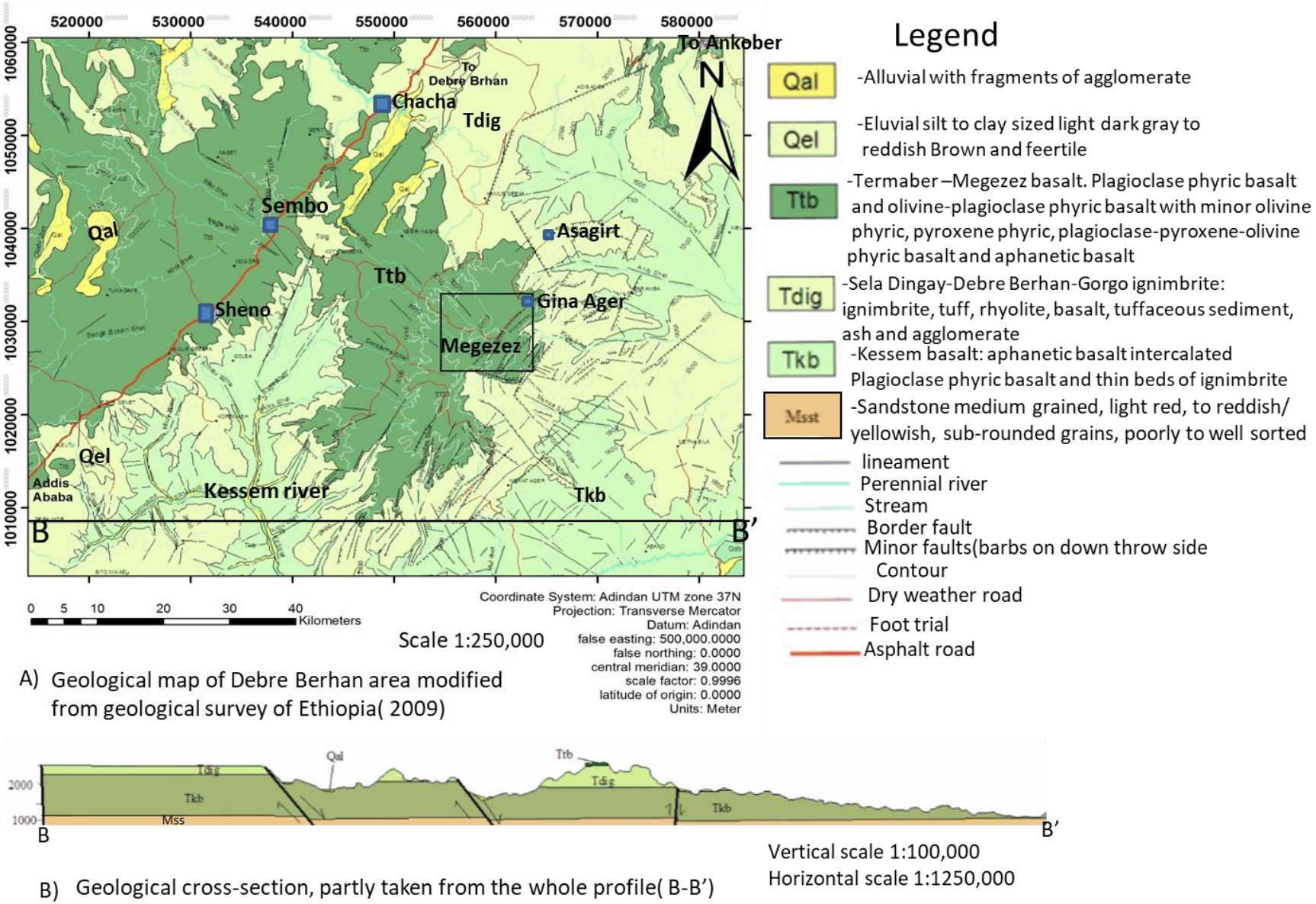

Fig. 2.6. Geological map and Cross-section of Debre Berhan Area (Modified after Geological Survey of Ethiopia (2009))

CHAPTER -THREE

3. Geology of study area

3.1. Introduction

Megezez Mountain is one of the Mid Miocene age volcanic centers in western Ethiopian plateau formed as shield volcano, northwestern sector of main Ethiopian rift (part of Tarmaber formation). Megezez shield has age of 10.5 Ma (George, 1997, cited in Wolfendene, 2004 and Kieffer et al., 2004). Geomorphologically, this volcanic area is characterized by slope angle ~ 5^0; which is a relatively flat topography (Wolfendene et al., 2004). This study shows the shield volcano comprises lava flows with mafic, intermediate, and felsic composition. Highly porphyritic basalts show dyke intrusions with different composition to the surrounding rock. The distribution and volcanic succession of observed rock units are shown in the geological map of Megezez with a geological cross section and composite stratigraphic log section respectively (Fig.3.1, 3.2 and 3.3).

3.2. Volcanic successions and petrographic descriptions

From the combination of studies in the field observations, geological mapping, petrographic, and geochemical analysis; the Megezez shield volcanic products from youngest to oldest are basalt, rhyolite, trachydacite, trachybasalt, and trachyandesite. In addition, dyke intrusions are also common in porphyritic basalt unit; and these dykes sampled and analyzed. The dykes compositionally determined as glassy rhyolite, trachyandesite and basaltic trachyandesite. Representative and fresh samples utilized for the suit of petrographic and geochemical analysis. This chapter presents field descriptions in out crop scale, litologic units with geological map, geological cross-section, composite stratigraphic log section and petrographic description of study area.

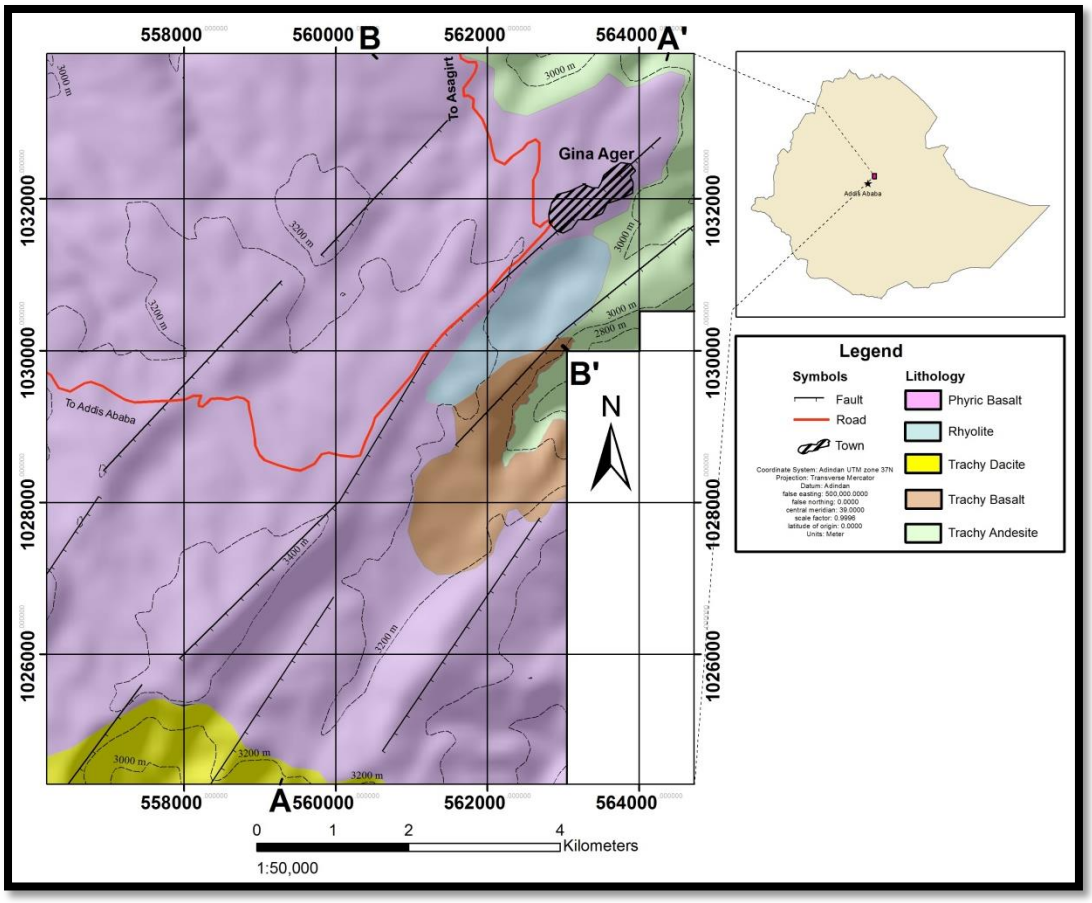

Fig.3.1. Geological map of shield volcanics, Gina Ager-Megezez locality.

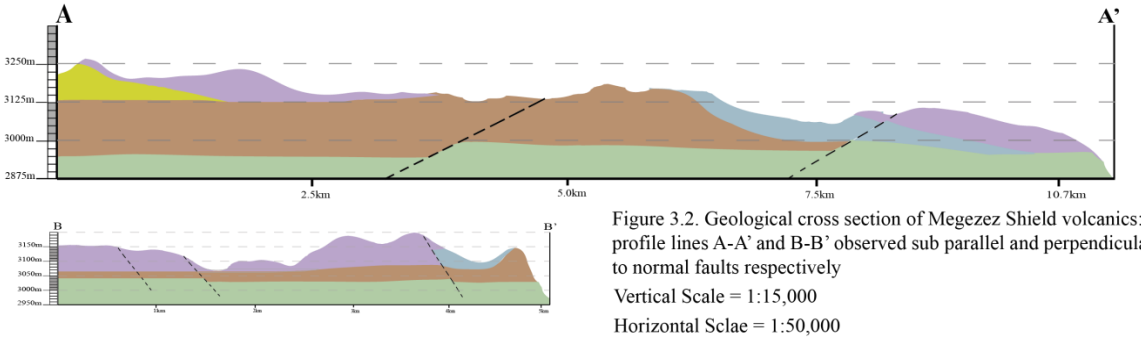

Figure 3.2. Geological cross section of Megezez Shield volcanics: profile lines A-A' and B-B' observed sub parallel and perpendicular to normal faults respectively

Vertical Scale = 1:15,000

Horizontal Sclae = 1:50,000

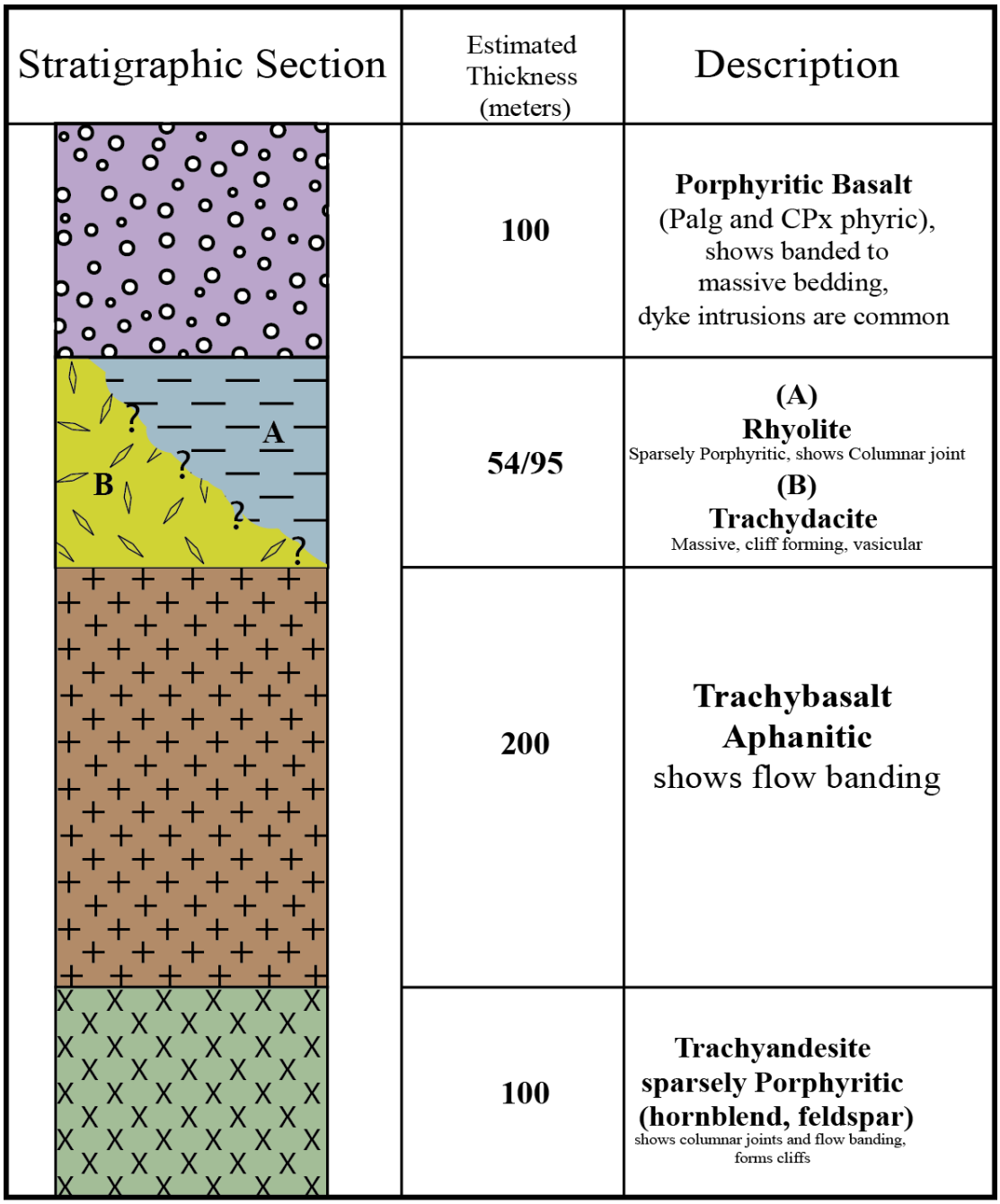

Fig.3.3. Composite stratigraphic section of Gina Ager-Megezez locality, Megezez shield volcanics, (not to scale).

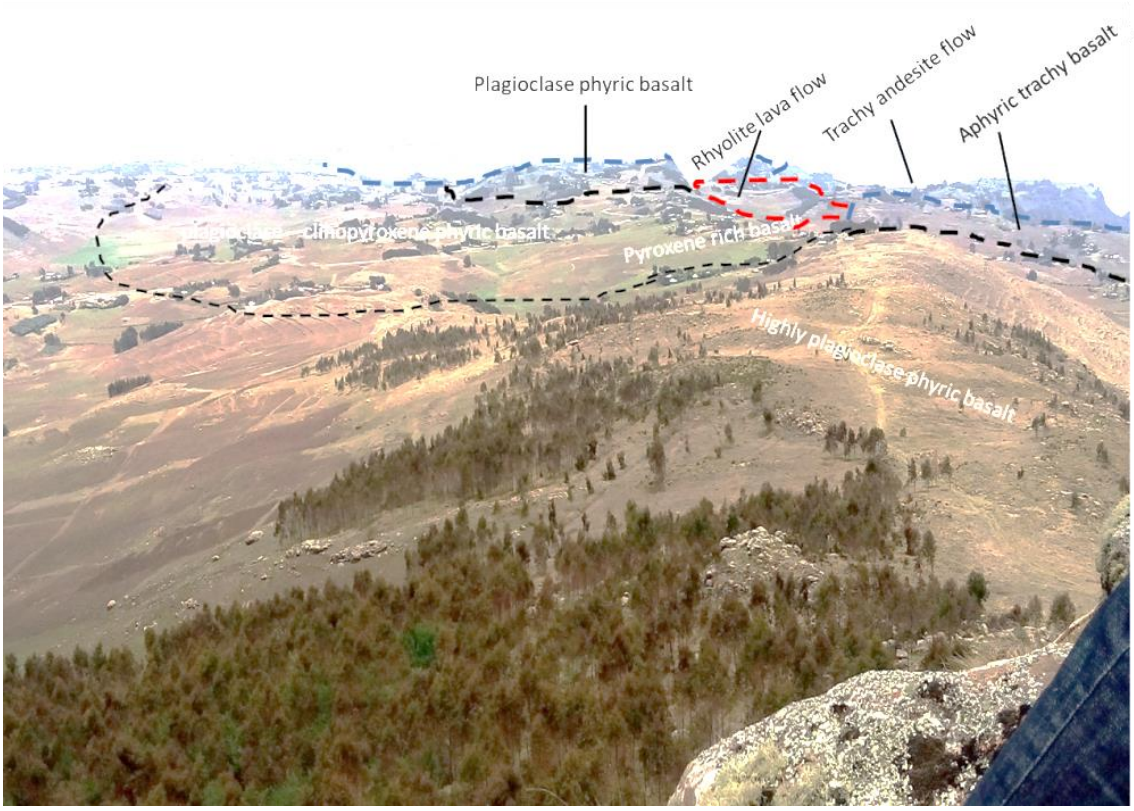

Fig.3.4. Panoramic view of the northern section of the study area showing the distribution of mappable units classified based on field observation and characterization of rock units confirmed also in petrographic study and geochemical results; northern sector of Megezez Mountain.

3.2.1. Sparsely porphyritic Trachyandesite

This unit is exposed in the northern part of the studied area following the lower elevation along Ankober border faults. It varies from phyric – sparsely phyric and aphyric texture. Within ~5m elevation difference to the bottom of the same unit it shows sparsely phyric nature with feldspars, no visible amphibole minerals are observed as phenocryst. The unit is overlain by plagioclase phyric basalt, rhyolite, and trachy basalt unit in the area they cover. Small portion of this unit has visible phenocryst of very coarse hornblende and feldspars. Amphibole grains show randomly distributed tabular and lath-like shape in the field, confirmed also from petrographic study. Paleosol is the distinguishing feature used to delineate the contact between trachyandesite and flow banded plagioclase phyric basalt. The porphyritic andesite unit is intensively weathered at top and slightly weathered with flow banding at the bottom.

In petrographic analysis and description; the stumpy groundmass of alkali feldspars (sample M-TA) show parallel to sub-parallel alignment, and partly following the outline of the hornblende phenocrysts.

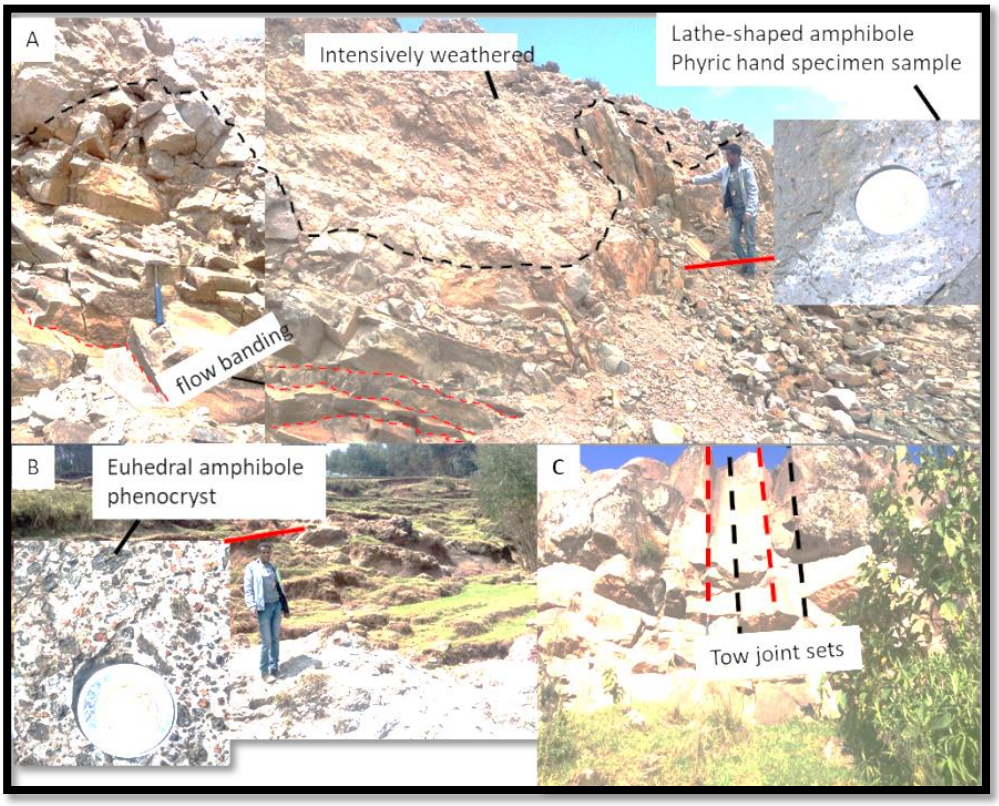

Fig.3.5. Close up view of trachy andesite flow unit with different nature; A) Quarry exposure of lath- shaped amphibole and slightly altered feldspar phyric trachyandesite topped by intensively weathered flow of the same unit; coin scaled sample shows hand specimen rock with amphibole and feldspars phenocryst observed with necked eye in the field B) euhedral amphibole and pyroxene phenocryst (coarse grain) with in the same unit of trachyandesite is observed and it is weathered; south of Gina Ager Egziabiherab church; C) exposure with pronounced columnar joint northern margin of the area.

As shown in microphotograph in Fig 3.17 (A&B), euhedral hornblende forming reaction rim of opaque minerals. The lath-shape, feldspars show sub alignment wrapping phenocryst minerals. Petrographic study shows sparsely phyric with euhedral hornblende, alkali feldspars, plagioclase, and opaque minerals. The modal percentage of mineralogical composition is determined as ~9% phenocryst and ~91% groundmass. From this proportion phenocrysts comprise 4% hornblende, 1% plagioclase, 2% alkali feldspar, 1% opaque (accessory minerals). Plagioclase is altered and fractured showing simple and multiple twining, less pronounced zoning with euhedral tabular form of grain. Quartz is not visible as phenocryst size under petrographic study; however the norm value of minerals in geochemical data results the present of ~11% quartz mineral. Phenocryst

phases have maximum grain size: ~5.5 mm hornblende, ~5 mm plagioclase, ~1.5 mm alkali feldspars, and ~1.2 mm opaque minerals.

Trachyandesite dyke is also observed intruding porphyritic basalt unit (see exposure view in section 3.2.5.1, Fig. 3.12) with the microphotograph view (Fig. 3.6, C&D, M-D2). It is classified based on petrographic and geochemical analysis. It is composed of nearly equal proportions of plagioclase and alkali feldspar with coarser groundmass of lath-shaped feldspars compared to sample M-TA. It is composed of less phenocryst with no visible amphibole minerals, less opaque minerals, few clinopyroxene. Lath- shape feldspar groundmass crystals are coarser and comprising 92%. The modal composition is ~8% phenocrysts composed of 2.5% plagioclase, 1% clinopyroxene, 0.5% quartz, 3% alkali feldspars, and 1% opaque. Phenocryst phases show grains with Subhedral clinopyroxene with ~1.5 mm, euhedral, tabular, altered plagioclase with ~ 3 mm; and tabular and subhedral alkali feldspars with ~4 mm diameter maximum grain size in a long side measurement.

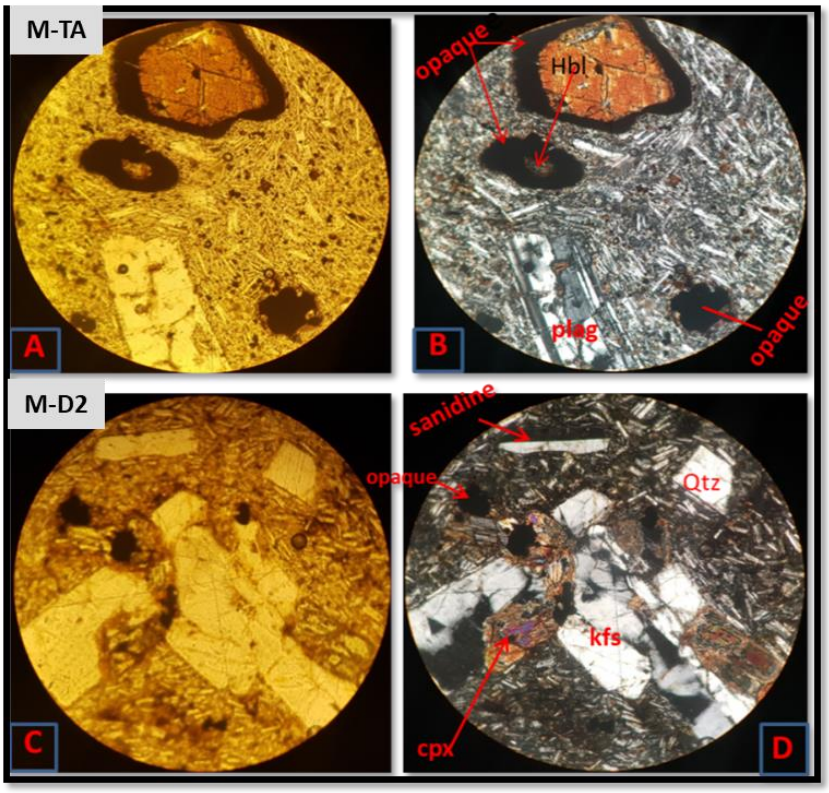

Fig.3.6. Microphotograph of trachyandesite flow, samples M-TA (A & B) and M-D2 (C & D) under optical microscope with different view in XPL (A & C) and PPL (B & D), at 10 X magnifications. The labels stand for: B) Hbl- subhedral and rimed dehydrated hornblende in to Fe-Ti oxide; plag- slightly altered prismatic and euhedral plagioclase feldspar with albite twin; (D) Qtz- subhedral Quartz, kfs- subhedral with inclusion of pyroxene (augite) labeled as (Cpx), samples taken northern side of Gina Ager town (A & B); south of Wena Michael village (eastern side of Megezez mountain(C & D).

3.2.2.Trachybasalt

This unit is exposed covering the north eastern part of studied area. It is exposed in localities of Chiraro with flat topography and cliff forming on the side of border faults, towards the rift margin. Field descriptions of volcanic products show characteristic features of dark to gray color, and aphanitic texture. It is characterized by rugged topography which is difficult to access. Flow banding and polygonal joints on the gentle slope part, with poor exposure are common. It is overlain by plagioclase – pyroxene phyric basalt to south west, rhyolite lava flow to western side and underlain by sparsely phyric trachy andesite. Sample M-TB is taken from Chiraro village for petrographic and geochemical analysis at altitude of 3158 m.

This unit is dominantly composed of dominant microcrystalline groundmass of feldspars and mafic minerals with few clinopyroxene phenocrysts. Therefore, rock classification is using geochemical data and differentiated from the remaining analyzed rock units in the study area.

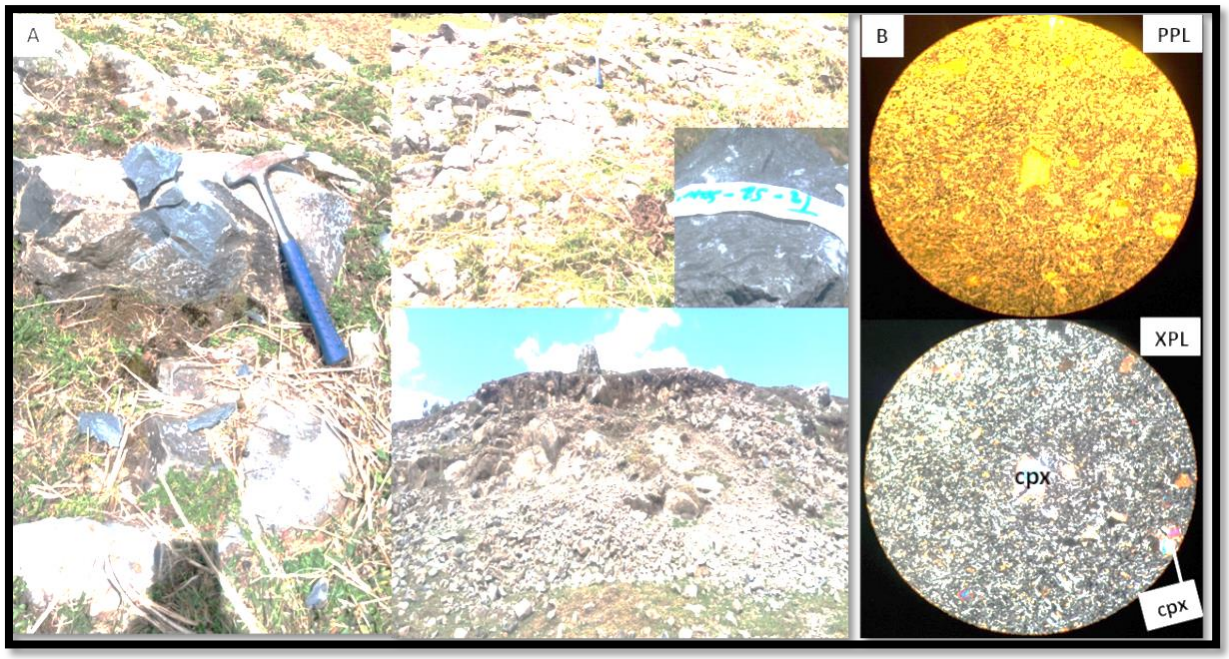

Fig.3.7. Field and microphotograph of aphanitic trachybasalt unit. A) Different exposure sections from aphanitic trachy basalt unit; (B) Microphotographs of sample M-TB showing microphenocrysts of feldspars and pyroxene (clinopyroxene~0.3mm size), viewed under optical microscope, at 10X magnification, Chiraro village, north eastern side of Megezez Mountain.

3.2.3. Sparsely porphyritic Trachydacite

This volcanic product exposed in the southern side the study area (mountain peak) with a ragged topography and difficult to field traverse It is highly weathered brownish, and overlain by plagioclase phyric basalt to the north. Sample M-TD collected for geochemical and petrographic study on the top and northern part of Meti village at location of grid E-0558284 and N-1028836.

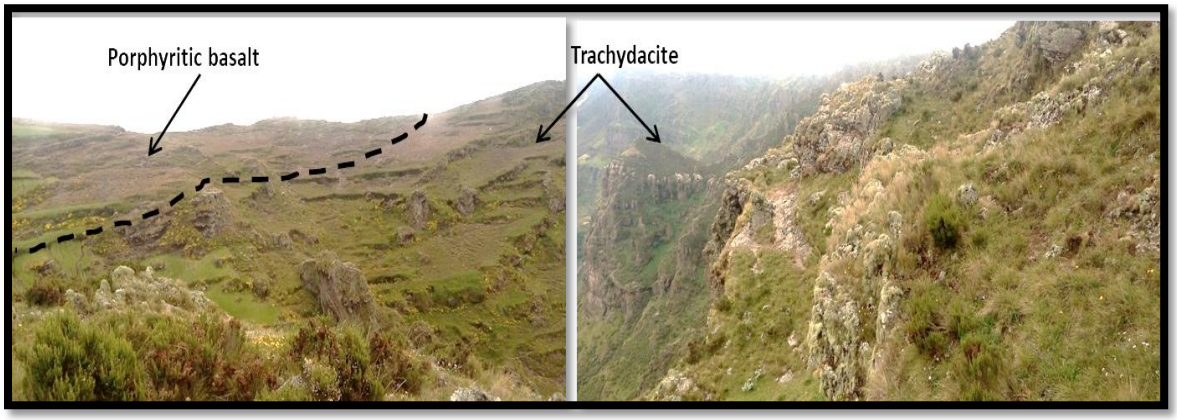

Fig.3.8. Exposure of trachy dacite lava flow and the contact with plagioclase phyric basalt, south of Megezez peak (part of Meti village).

The trachydacite is composed of 17.5% phenocrysts and 83% glass rich groundmass. It is sparsely porphyritic rock comprising phenocrysts of 3% clinopyroxene, 6% plagioclase, 5% alkali feldspar and 3% opaque minerals. It is vesicular with percentage volume of ~6% in the rock. There is slight variation in rock name with geochemistry results; assumed to be due to cryptocrystalline nature of some alkali feldspars and quartz minerals in petrographic analysis. Modal percentage of plagioclase and alkali feldspars shows nearly proportional.

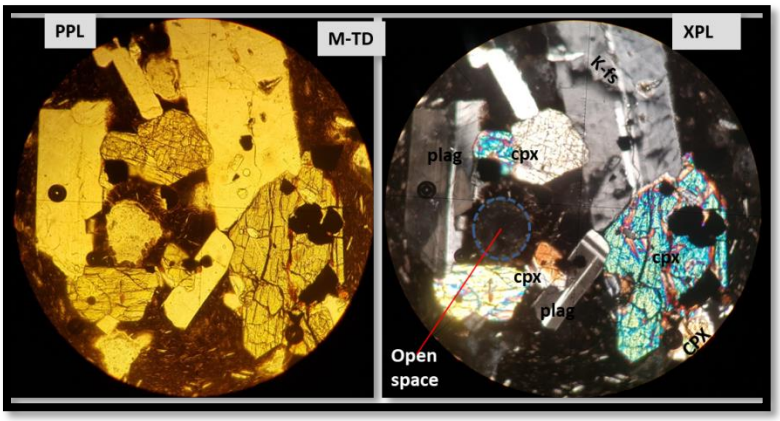

Fig.3.9. Microphotograph of trachydacite. Sample M-TD under optical microscope with different view, at 10X magnification. Labels stand for: k-fs- tabular shape alkali feldspar with inclusion of Fe-Ti oxides, cpx- subhedral clinopyroxene with subophitic texture and inclusions of Fe-Ti oxide, plag- euhedral, lath-shaped plagioclase feldspar with simple and albite twin. Broken circles in red show Fe-Ti oxide (opaque) minerals. Samples are from Meti village, southern side of Megezez Mountain.

3.2.4. Rhyolite lava flow

This unit clearly exposed between basalt and intermediate (trachyandesite and trachybasalt) Gina Ager town and Chiraro villages respectively. The rhyolite contact with basalt and trachybasalt unit is marked by paleosol. The products exposed by quarry and hill side exposure; showing columnar joint structures. From field observations, this unit can be described as sparsely porphyritic. It is relatively less cliff forming, small area coverage, brownish weathering color and light gray fresh color.

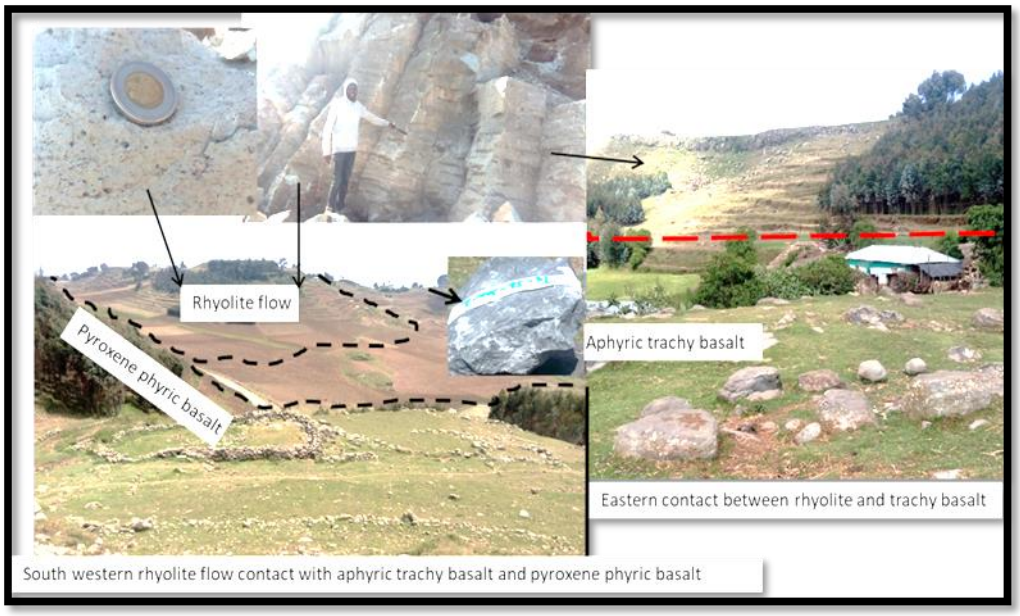

Fig.3.10. Different exposures of rhyolite lava flow with intensive columnar joint, and light gray color hand specimen (top left); and contacts with trachybasalt and basalt unit, from Chiraro locality, north eastern margin of studied area.

A petrographic result from rhyolite lava flow (sample M-R) shows that this unit is composed of ~8% microphenocrysts, ~92% crypto crystalline groundmass. Groundmass partly show flow banding resulting from slowly moving magma during its emplacement on the surface. The modal percentage of microphenocrysts is 4.5% alkali feldspar, 1% quartz, 0.5 clinopyroxene, 1% opaque, and 0.8% hornblende. Textural arrangement described as euhedral, tabular hornblende (~0.5mm), subhedral alkali feldspar (~3mm), subhedral-euhedral clinopyroxene showing Carlsbad twin (~1.1mm), and anhedral quartz (~ 1.25mm).

Sample M-RD collected at coordinate of E-0559903 and N-102125, eastern side of mountain peak for the suit of thin dyke intruding the porphyritic basalt unit, around Wena locality. Field and Petrographic analysis show that it is described as glassy rhyolite in composition (see Fig. 3.11). It is composed of modal proportions of ~11% phenocryst and

~89% glassy groundmass. The groundmass is mainly composed of glass materials. Constituting phenocryst minerals identified under petrographic microscope with modal percentage include ~2%, alkali feldspar, ~3% plagioclase feldspar, ~5% glass, ~0.2% rock fragment, ~1% clinopyroxene, and~0.2% opaque minerals.

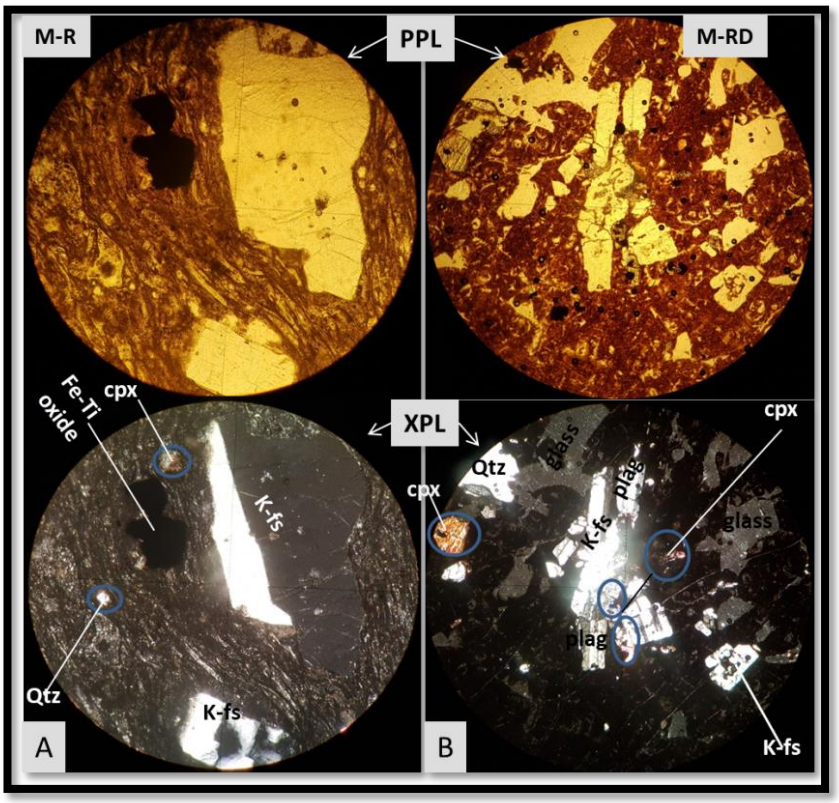

Fig.3.11. Microphotograph of rhyolite (A) and glassy rhyolite (B) under optical microscope. Labels stand for: Qtz- anhedral Quartz, k-fs- subhedral alkali feldspar; cpx- subhedral and partially altered clinopyroxene forming intergrowth with alkali feldspar; viewed at 10 X magnifications.

3.2.5. Porphyritic basalt

3.2.5.1. Plagioclase phyric basalt

This rock unit comparatively covers wide area in this study. It is mainly exposed from the Megezez –Weneberi localities to the west of Gina Ager town, eastern and southern part of Megezez Mountain. The rock unit is characterized by dominant and large size phenocryst of plagioclase; which are visible from hand specimen scale and supported with petrographic microscope. It is poorly exposed, covered by grass and farm land, showing massive structure. It is exposed at the highest elevation ~3593 m at the mountain peak, and gentle slope towards eastern and north western part. Samples collected from different parts of this unit show alternate weathering and are highly friable, contain identifiable feldspars. Close to the mountain continuing to the village of Weneberi and Wena show

very coarse grain size of plagioclase phenocryst relative to northern sector of the same unit.

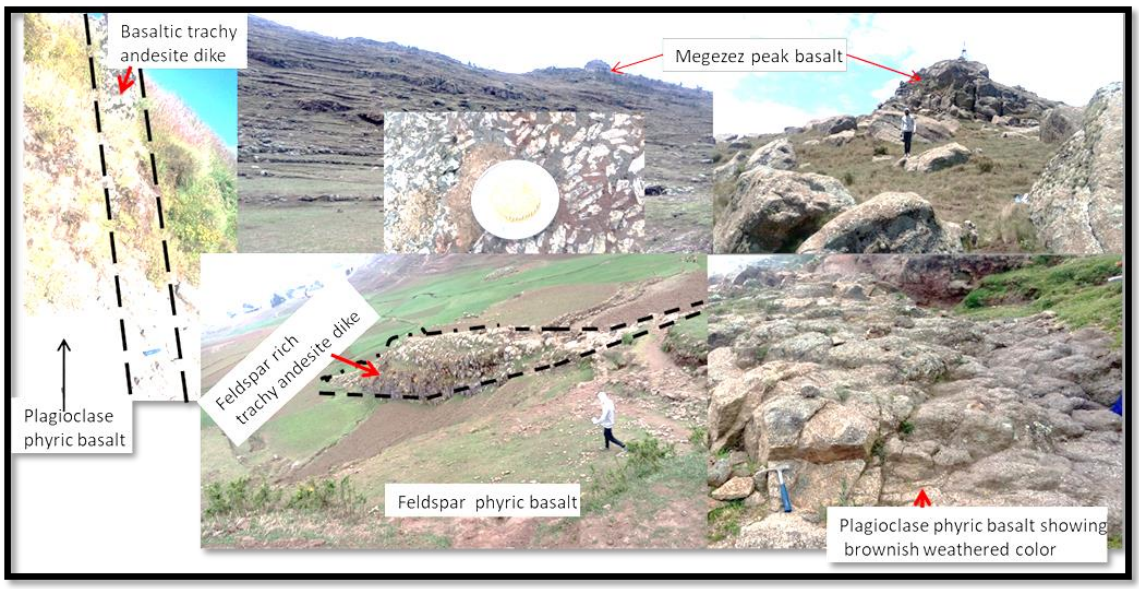

Fig.3.12. Close-up views of Megezez porphyritic basalt from northern, southern and eastern side of the mountain. Composed of very coarse size tabular and lathe-shaped plagioclase and few pyroxenes as phenocryst. The dyke intrusions labeled with in phyric basalt encountered and samples analyzed show different mineral and chemical composition from the host rock.

Sample M-B4 (see Fig. 3.13 A) and M-B13 (Fig. 3.13 B) are collected from south eastern and western side of Megezez mountain respectively. Petrographic analysis shows the dominant phase being plagioclase phenocryst. It shows characteristic pronounced polysynthetic twin and zoning. Samples show pokiolitic inclusion of pyroxene which is slightly altered in to accessory mineral, and enclosed with plagioclase. Subhedral clinopyroxene (~1 mm) also shows intergrowth texture with zoned and twinned plagioclase.

The other sample (M-B4) shows modal proportion of ~37% phenocryst and ~63% groundmass, and the phenocrysts are composed of 29% plagioclase, 3.6% slightly altered clinopyroxene, 1.5% alkali feldspar, 3% opaque. The porphyritic basalt with sample M-B13 show less mineral alteration compared to the same unit of sample M-B4. This rock unit has a modal percentage composition of 33% phenocryst and 67% groundmass. The phenocrysts consist of 26% plagioclase, 4% clinopyroxene, 2% opaque, and 1% alkali feldspars. Plagioclase shows pronounced polysynthetic twin and zoning with light core and darker rim compositional change. Sample MW-B (see Fig. 3.13 C) collected at latitude 3150 m, around the village of Weneberi, northwest of the studied area, showing the continuity of porphyritic basalt dominantly of very coarse plagioclase visible in

outcrop. This volcanic product exposed on the stream side and road with poor exposure. Plagioclase is the maximum phenocryst modal percentage having euhedral shape and tabular form of texture with long direction size of ~ 8 mm, pronounced polysynthetic twin, zoning, poikilitic inclusion and alteration. Clinopyroxene is also the second phenocryst with euhedral to subhedral shape, alteration in to accessory minerals. The modal composition of this rock unit is described as 31% plagioclase, 3% clinopyroxene, 1.5% opaque, 0.6% alkali feldspar, that is ~36% phenocryst and 64% groundmass. The groundmass is composed of microcrystalline textures of mafic minerals as a maximum abundance and some colorless crystals.

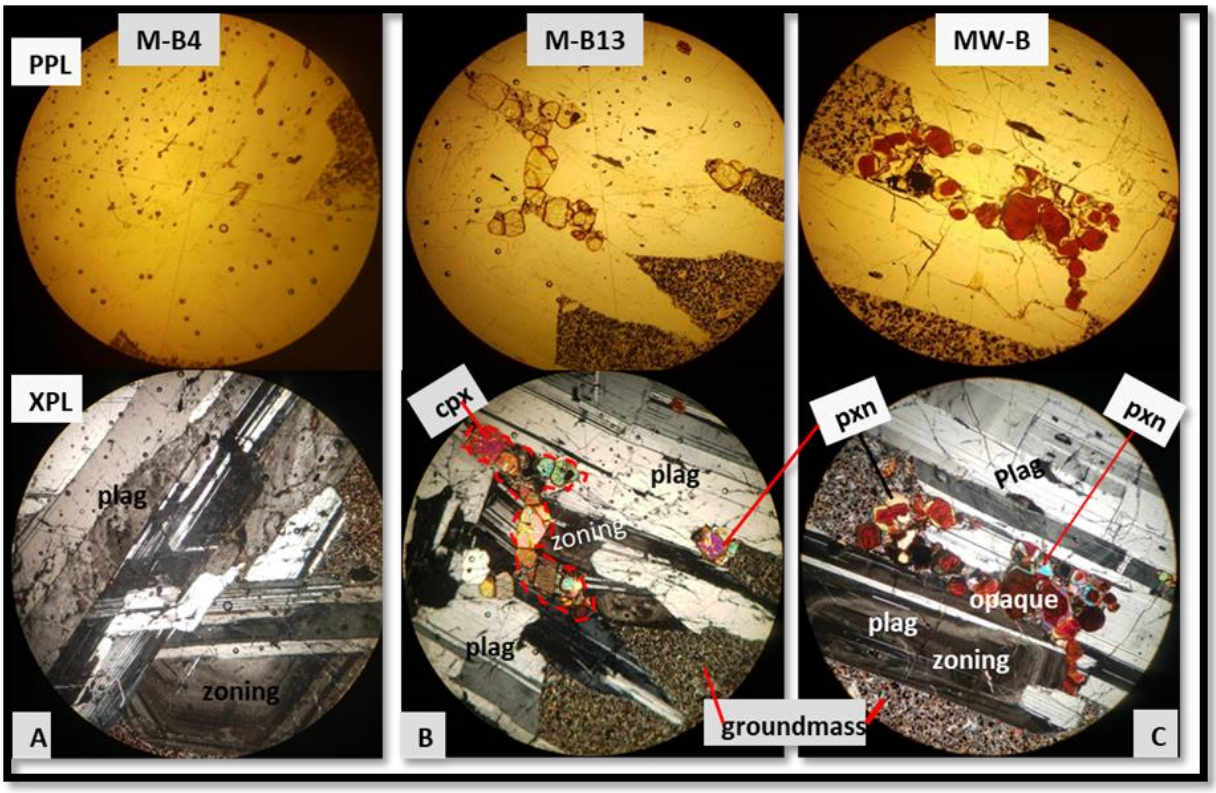

Fig.3.13. Microphotographs of plagioclase phyric basalt. Sample M-B4 (A) showing polysynthetic twinning and zoning in tabular plagioclase; sample M-B3 (B) showing poikilitic inclusion of pyroxene (labeled in broken line as cpx) in plagioclase feldspar grains forming multiple twin and zoning; and MW-B (C), showing less pronounced zoning and replacement of clinopyroxene with Fe-Ti oxide minerals indicating poikilitic texture as pyroxene enclosed by plagioclase, samples collected from eastern, western and north western sector of Megezez mountain.

The same basalt unit observed (sample M-B1) from northern margin of the studied area, in and close to Gina Ager town. It is overlying trachyandesite unit and geochemical investigation results show lowest silica content in geochemical data relative to the other samples. Plagioclase phyric with significant vesicles and some pyroxene, flow banding primary structures are common. It is relatively fresh in outcrop with dark to light dark

color. Visible minerals from hand specimen include feldspars/ plagioclase, quartz forming vein, and pyroxene.

Petrographic study on sample M-B1 shows modal compositions of 26% phenocrysts composed of 19% plagioclase, 3% pyroxene, 1% alkali feldspar, 2% accessory minerals and 74% microcrystalline groundmass. It is rich in vesicles (9%) relative to the other basalt samples, and almost all plagioclase grains are larger size, minimum ~ 1 mm diameter. Plagioclase is strongly zoned with light core and dark rim recognized from extinction angles under XPL view. Plagioclase is characterized with pyroxene and opaque mineral inclusion, simple to multiple twining; tabular, lath-shaped, euhedral shape with maximum rang of ~6.5 mm grain size. Euhedral to subhedral, slightly altered clinopyroxene forms subophitic texture in which pyroxene grains partially enclosing subhedral plagioclase feldspar (see Fig. 3.14. B). Grain size of clinopyroxene is ~1 mm in a long side of euhedral grain.

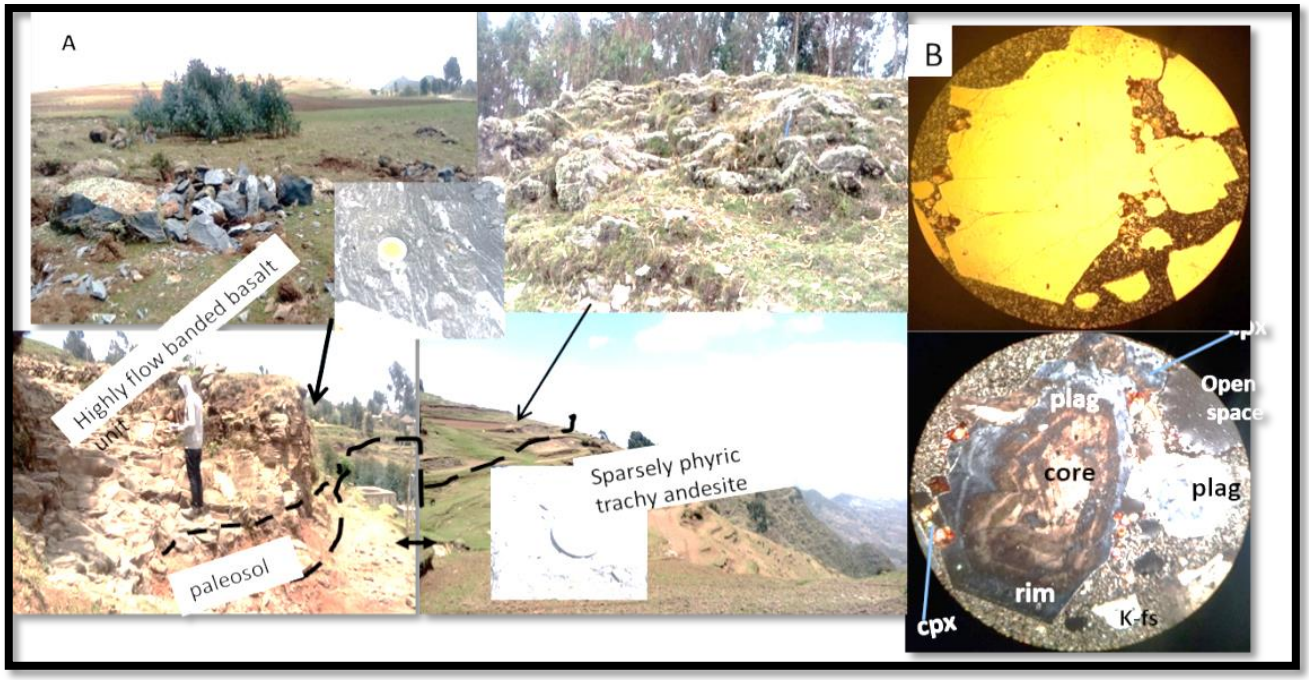

Fig.3.14. A) Close-up views of plagioclase phyric basalt showing lower contact with trachyandesite unit from different exposures with hand specimen; northern side of Gina Ager town. B) Microphotograph of plagioclase phyric basalt with sub ophitic texture plagioclase feldspar, zoning (light core-to-dark rim).Labels stand for: plag- subhedral, tabular plagioclase, cpx- subhedral euhedral clinopyroxene; viewed at 10X magnification.

Samples collected around Woy Abo church (sample M-B5-1) from the same porphyritic basaltic unit with different grain size of minerals and sieved plagioclase feldspars. Plagioclase shows strong alteration, polysynthetic twin and zoning. The mineralogical composition of this volcanic product is similar to the above samples with differences in grain size and abundance of plagioclase phenocryst. The modal composition is described as ~19% phenocryst and ~81% groundmass. Phenocryst phases comprise 13% plagioclase, 2% clinopyroxene, 1% alkali feldspar, 3% accessory minerals. The groundmass is composed of microcrystalline mafic minerals, lath-shaped feldspars. Twinning, zoning sieve texture, euhedral shape, and tabular form are observed characteristic feature in plagioclase. Plagioclase is with size of ~5 mm long side length, clinopyroxene ~0.6 mm with subhedral shape, alkali feldspar ~1.75 mm grain size with subhedral tabular form, and accessory minerals are subhedral to euhedral shape. Clinopyroxene shows alteration inward from rim to core and outward from core to rim.

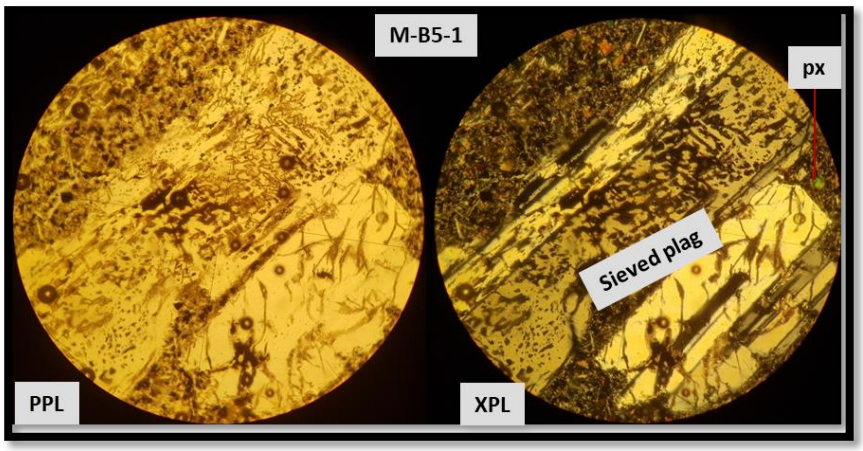

Fig.3.15. Microphotograph of plagioclase phyric basalt. Sample M-B5-1; plagioclase phyric basalt with sieve texture in tabular and polysynthetic twin plagioclase (plag); and pyroxene (PX) with micro phenocryst size; Optical microscope view at 10X magnification; locality of Woy Abo church, North West of the studied area.

3.2.5.2. Plagioclase-clinopyroxene phyric basalt

This unit is mapped as plagioclase phyric basalt, exhibiting different mineralogical composition. It is composed of abundance of clinopyroxene with coars grain size. Samples are collected in different locations from the basalt unit following gentle topographic area; between Megezez mountain and Gina Ager town. It is covered with farm land and was difficult to collect fresh samples for analysis. Pyroxene and feldspar mineral phases were visible in outcrop level and confirmed with petrographic analysis. Plagioclase is randomly distributed in some analyzed samples, and replacement reaction is common resulting accessory minerals (e.g. hematite, magnetite, and ilmenite).

From field investigation, minerals were less visible with necked eye compared to the previous porphyritic basalts. From petrographic investigation, however it show sparsely porphyritic with feldspar and increase in pyroxene and decreasing of plagioclase phenocryst. This sample is rich in clinopyroxene and opaque minerals. Mineral modal composition comprises 9% plagioclase, 10% clinopyroxene, 4% alkali feldspar, 3% opaque minerals; with a sum total of 26% phenocryst and 74% groundmass. Plagioclase exhibits textural features of euhedral, tabular, weak zoning, and simple and multiple twin, and alteration. Clinopyroxene and opaque mineral inclusion are observed in plagioclase feldspar with a maximum grain size of ~ 3.5 mm for this sample. Pyroxene shows oxidation (alteration) both inward and out ward to accessory minerals keeping their euhedral to subhedral shape, with unaltered mineral grain size ~1.5 mm. Alkali feldspar shows Carlsbad twin with euhedral and tabular form of grain ranging with a maximum grain size of ~4.8 mm.

This unit also sampled from the northern side of mountain to check if there is variation in spatial distribution towards Gina Ager town. These samples petrographically show similar phenocryst and mineralogy but variations in abundances. It is a continuity of Megezez mountain porphyritic basalt with increasing clinopyroxene and decreasing plagioclase both in grain size and modal proportion compared to the porphyritic basalts analyzed as samples M-B4, MW-B, M-B13, and M-B5-1. Common mineral textures include inclusion of slightly altered pyroxene, zoning, albite twinning in plagioclase, less pronounced Carlsbad twin in alkali feldspar. The modal composition is presented as 18% phenocryst and 83% groundmass. The phenocryst modal composition is a combination of plagioclase (11%), alkali feldspars (2%), clinopyroxene (4%), and opaques (1%). The groundmass is composed of microcrystalline matrix in which mafic minerals are polarized. Maximum grain size of each mineral is determined as plagioclase ~6 mm, clinopyroxene ~1 mm, alkali feldspar ~2.5 mm, opaques ~0.6 mm, and quartz ~0.25 mm.

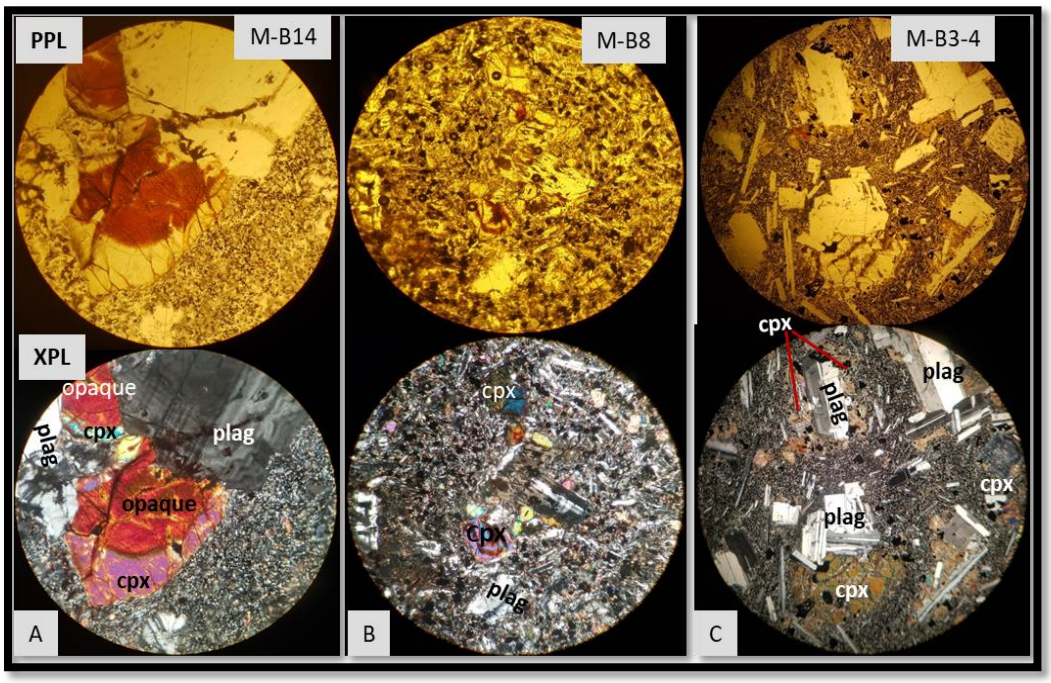

Fig.3.16. Microphotograph of plagioclase-clinopyroxene phyric basalt. It is characterized by relative abundance of clinopyroxene and replacement reactions (A), and intergrowth of plagioclase; and;(B) sparsely phyric rock with abundance micro phenocrysts of pyroxene; (C) inter-granular texture shown with randomly distributed phenocrysts and subophitic texture as plagioclase is partly enclosed by pyroxene(red lines), samples collected northern flank of the mountain; optical microscope view with 10X magnification. Labels stand: plag - tabular and euhedral plagioclase, cpx- subhedral pyroxene.

Sample M-B3-4 collected at altitude of 3,415 m (above mean sea level) just below the mountain about 178 m altitude difference from the Megezez peak in the north. The rock is light dark and with small size feldspar grains; randomly distributed and embedded in the groundmass. The abundance of feldspars shows progressive decrease in plagioclase phenocryst in the rock between Charie primary school and Megezez mountain; instead it shows clinopyroxene. Mafic minerals and oxide minerals make the microcrystalline groundmass. The modal percentage is 21% phenocryst and 79% groundmass. The phenocrysts comprise 11% plagioclase, 2% alkali feldspars, 7% clinopyroxene, and 1.4% opaque minerals.

3.2.5.3. Clinopyroxene – olivine phyric basalt

This volcanic product is taken from restricted location intercalated in basalt unit northern margin of the studied area, west of Gina Ager town. Mafic minerals including olivine, feldspar (plagioclase), and pyroxene are visible in hand specimen examination.

As shown in Fig 3:17 below, these volcanic products are explained as remnants of mafic rocks as soft and less resistant rocks removed by different agents. There is little

relationship with the local volcanic product as examined both in the field and petrographic study with: a few alkali feldspars and plagioclase, dominant pyroxene and some olivine phenocrysts make this product different in mineralogical composition and physical features relative to the local studied volcanic rock units. Mineralogical composition determined with modal percentage of 19% phenocryst and 81% microcrystalline groundmass. This percentage of phenocryst constitutes11% clinopyroxene, 4% olivine, 2% plagioclase, 1% orthopyroxene, 0.7% opaque, 0.3% alkali feldspars. Open spaces observed with petrographic microscope constitute 1% of the total volume of analyzed sample may be spaces left as coarse minerals removed during sample preparation.

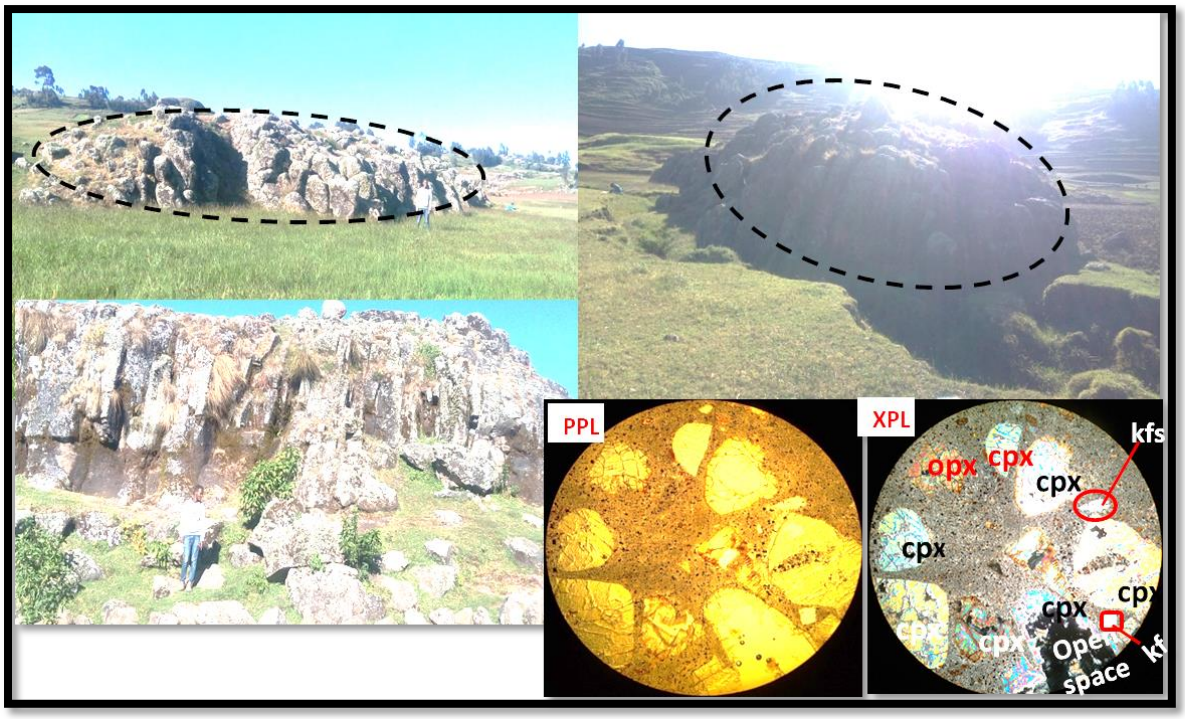

Fig.3.17. Close-up view of intercalated porphyritic basalt volcanic products; and microphotograph of sample M-B5-3: Labels stand for: cpx- subhedral clinopyroxene, opx- subhedral orthopyroxene, k-fs- alkali feldspar; olv- altered subhedral olivine, western side of Gina Ager town, viewed with optical microscope at 10X magnification.

3.2.6. Basaltic trachyandesite dyke

In the southern flank of Megezez mountain near the contact between porphyritic basalt and sparsely porphyritic trachydacite there is dyke intrusion (see section 3.2.5.1, Fig 3.12). The dyke intrudes porphyritc basalt unit following the orientation of normal faults; and show aphanitic field texture in hand specimen. Petrographic analysis shows the sample is not fully aphanitic rather it is composed of microphenocrysts forming intergranular texture. It is composed of approximately equal abundance of lath- shaped

plagioclase and alkali feldspar and other mafic minerals like pyroxene and opaque mineral phases. Lath-shape feldspars show sub parallel alignment forming flow pattern. Generally, this dyke intrusion has no relation to the surrounding porphyritic basalt both in field, petrographic and geochemical features investigated in the study.

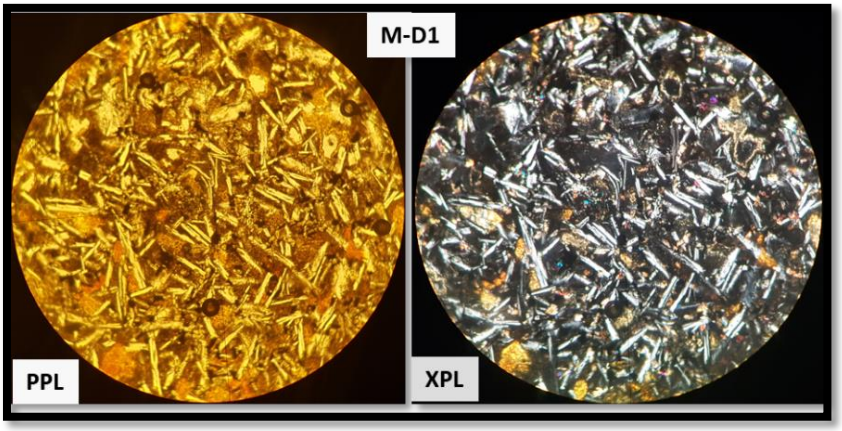

Fig. 3.18. Microphotograph of basaltic trachyandesite dyke. Sample M-D1 taken from basaltic trachyandesite intrusion with intergranular texture, viewed at 10X magnification.

3.3. Geological structures

Primary and secondary geological structures are common in the study area. Primary structures analyzed are flow banding formed during rock formation/ magma cooling stage. Whereas, secondary structures are joints (columnar and polygonal) and normal faults which resulted from crustal extension.

The area is affected with well-developed normal faults following the regional fault orientations in the Main Ethiopian Rift (MER) and Ankober border faults. The Red sea-Gulf of Aden- MER triple junction is exhibits left lateral oblique-slip, Quaternary fault zone; separated with E-W extension in the south (MER) from the NE-SW extension in the northern part (Wolfenden et al., 2004).

Structural measurements for the following geological structures presented in APPENDIX-C with a table format.

3.3.1.Flow banding

This is the primary geological structure resulted from slowly flowing of lava during emplacement. It is common in basalt unit around Gina Ager town; trachy andesite unit in outcrop scale and flow patterns shown by lath-shaped feldspar grains supported also with petrographic microscope. Trachybasalt unit also show banding observed at micro scale with hand specimen rocks.

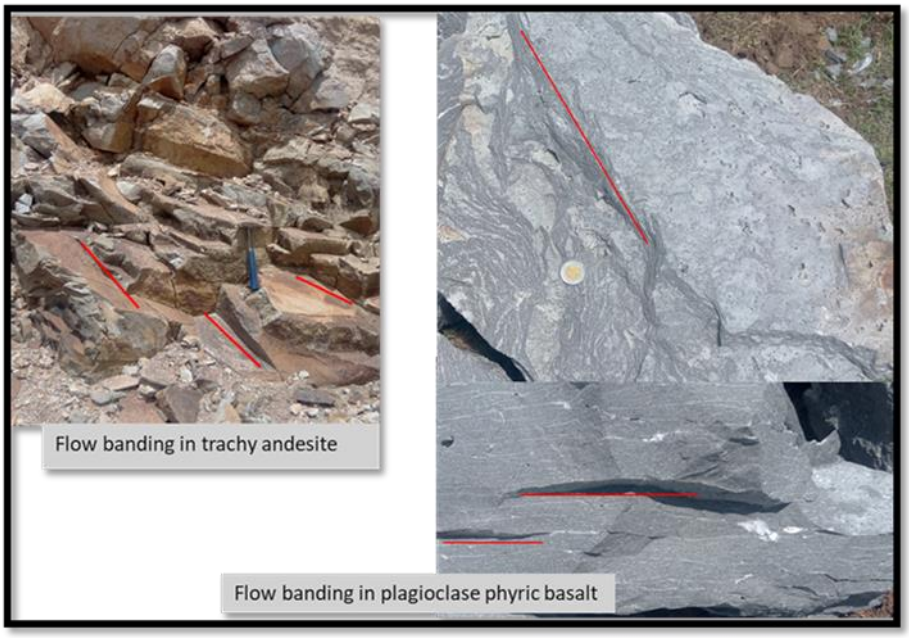

Fig.3.19. Close up view of flow banding with different magnitude from trachyandesite (left) and plagioclase phyric rocks (right), northern margin of the studied area.

3.3.2. Joint

This type of geological structure is the result of magmatic activity formed due to magma cooling but it can also result from crustal extension. Field observation shows the joints are systematic and non-systematic with different sets trending variably as NE to SE strike and NW, SW, NE, and SE dipping; mainly affecting trachy andesite and rhyolite lava flow.

Fig.3.20. Close view of systematic joints with two sets of joint in rhyolite lava flow (A), arrows show opposite joint faces to indicate two joint sets; trachyandesite(B); and Polygonal joint in trachybasalt (C).

3.3.3.Faults

The study area is characterized with normal faults trending NE-SW strike and SE dip direction (see Fig. 3.21, A&B). The trend imitates the regional faults of Ankober border fault system and Main Ethiopian Rift marginal faults. A total of eight normal faults have been identified and analyzed during this study as presented in the stereonet plots (see Fig 3.21, A&B).

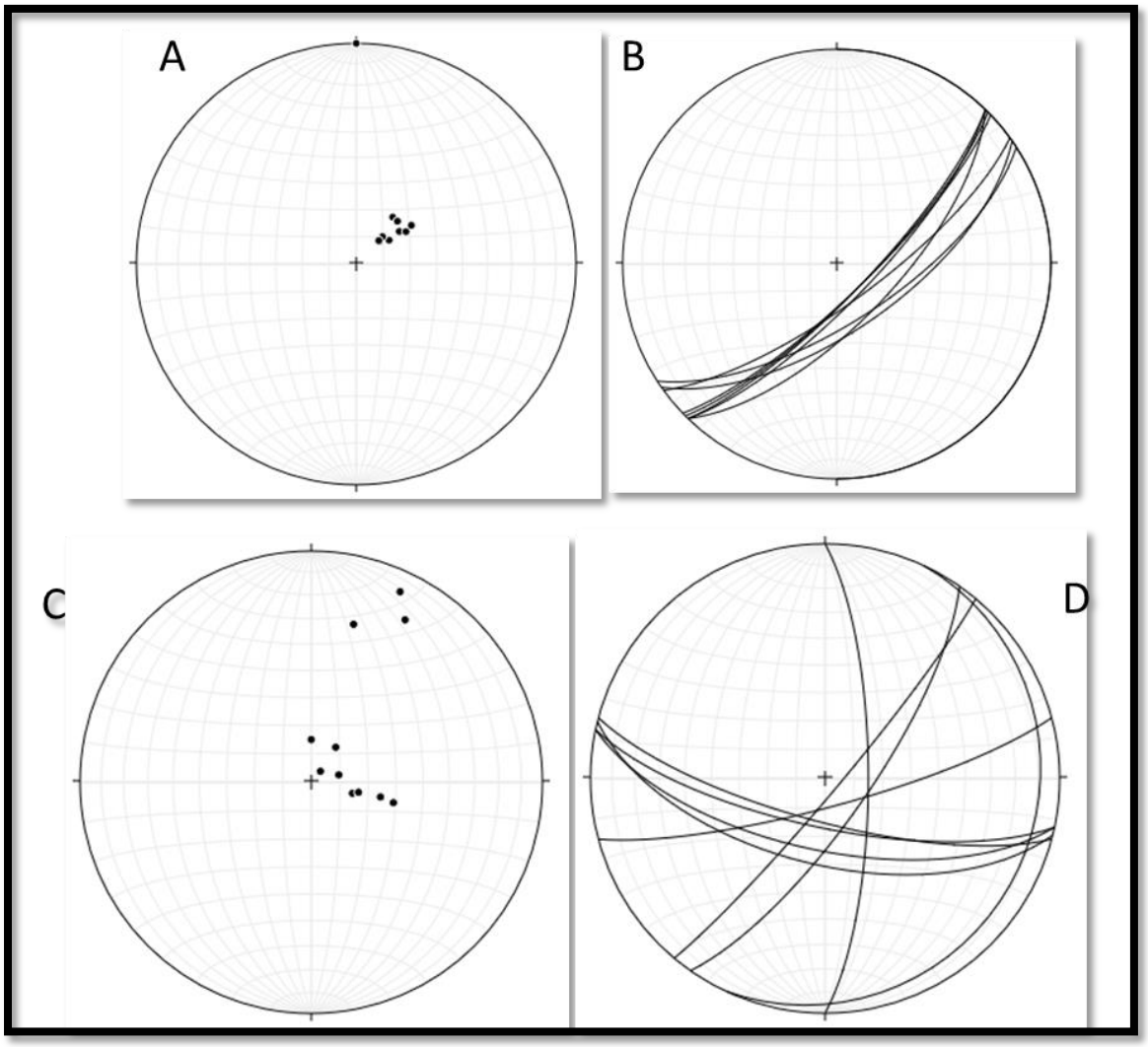

Fig. 3.21. Equal area plots of strike and dip direction of normal faults (A and B) and joints (C and D), analyzed from Megezez shield volcanics.

CHAPTER- FOUR

4. Whole Rock Geochemistry

4.1. Introduction

Geochemistry is vital tool to study elements signature in rock; and the magmatic evolution of any volcanic product. This method mainly depends on the relative signature of the elemental composition that enables to understand the geologic process.

Three types of geochemical data (major, trace, volatile) are identified for nine primary samples analyzed in this study. Among these, major and trace element geochemical data types are the main objective of this study to understand the evolution of Megezez volcanic products. Volatiles used to determine the alteration effects on analyzed samples and the behavior of mobile and immobile elements presented by Loss on Ignition (LOI). LOI represents the total volatile content of the rock that is generated by igniting the analyzed rock sample with temperature of 1000 ^{o}C.

Lava flow from Megezez volcanic center show distinctive geochemical characters where basic lavas are dominant in the study area. Based Total Alkali Silica (TAS) classification of volcanic rocks, after Le Bas et al, 1986, Megezez volcanic suite encompass trachyandesite, rhyolite, trachybasalt, trachydacite, rhyolite and basalt as mappable units plus trachyandesite, and basaltic trachyandesite dike intrusions encountered from different locations within basaltic unit. Analytical data for major element, trace element, LOI, and CIPW norms presented in Table 4.2. Several variation diagrams for major element oxides versus silica, trace element versus silica, trace element versus trace element presented. Chondritic normalized rare earth elements (REE) abundance patterns and primitive mantle normalized incompatible trace elements patterns in multi element spider diagrams are also used for presentation and interpretation of the Megezez volcanic rocks.

Table4.1.Geochemical data of Megezez volcanics presented as major element data with LOI (wt %), CIPW normative mineral data (wt %), and trace element data (ppm) respectively. The notation stands for L.D- Detection Limit, and m-meter.

Field code	M-B1	M-B3	M-B5	M-TB	M-D1	M-TA	M-D2	M-TD	M-R
Rock name	Basalt	Basalt	Basalt	Trachy basalt	Basaltic-trachy andesite	Trachy andesite	Trachy andesite	Trachy dacite	Rhyolite
East(m)	0564622	0558560	0562980	0562973	0557888	0564751	0560604	0558284	0562118
North(m)	1033668	1026571	32850	1030249	1025697	1033743	1026592	10288836	1030422
Altitude(m)	3031	3593	3045	3158	3445	3013	3163	3422	3175
SiO_2	45.5	47.5	47.6	48.5	53.2	59.3	59.6	65.4	72.2
TiO_2	3.4	2.92	2.45	3.24	2.55	1.41	1.5	0.81	0.37
Al_2O_3	15.15	15.25	14.7	15.45	14.3	15.35	17.95	15.95	9.82
Fe_2O_3	16	14.45	13.2	13.6	11.6	6.39	6.77	5.22	5.35
MnO	0.17	0.18	0.18	0.19	0.2	0.18	0.06	0.13	0.19
MgO	6.47	4.24	5.68	4.06	2.6	1.74	0.73	0.55	0.15
CaO	9.51	9.58	10.3	7.99	6.29	3.79	3.71	2.13	0.18
Na_2O	2.55	3.09	2.59	3.64	3.82	4.03	4.91	4.64	3.8
K_2O	0.79	0.94	0.86	1.36	2.4	3.56	3.24	3.89	4.36
P_2O_5	0.33	0.34	0.26	0.51	0.81	0.49	0.59	0.25	0.02
LOI	0.73	0.62	0.35	0.33	1.65	1.54	2.47	1.63	1.33
Total	**100.6**	**99.11**	**98.17**	**95.63**	**99.42**	**97.78**	**101.53**	**100.6**	**97.77**

Continued…. CIPW Normative minerals for analyzed samples (wt %)

Apatite	0.78	0.81	0.62	1.21	1.92	1.4	1.16	0.59	0.05
Ilmenite	0.37	0.39	0.39	0.41	0.43	0.13	0.39	0.28	0.41
Sphene	7.87	6.67	5.51	7.43	5.71	--	1.88	--	0.38
Orthoclase	4.67	5.55	5.08	8.04	14.18	19.15	21.04	22.99	25.76
Albite	21.58	26.15	21.92	30.8	32.32	41.55	34.1	39.26	26.24
Anorthite	27.56	24.97	25.94	218	14.78	14.85	13.28	9.2	--
Hematite	16	14.45	13.2	13.6	11.6	6.77	6.39	5.22	3.55
Diopside	5.07	8.65	12.32	3.31	2.6	--	--	--	0.17
Hypersthene	13.76	6.55	8.44	8.58	5.27	1.82	4.33	1.37	0.29
Quartz	2.27	4.37	4.46	3.44	9.03	11.11	13.3	18.7	34.28
Rutile	--	--	--	--	--	1.43	0.44	0.66	--
Acmite	--	--	--	--	--	--	--	--	5.21
Sum (wt %)	**100**	**98.6**	**97.9**	**98.7**	**97.9**	**99.2**	**96.4**	**99.1**	**96.7**
Li	10	10	10	10	10	10	10	20	30
Sc	24	27	29	19	15	7	7	7	9
V	488	418	335	289	128	29	56	15	<L.D
Cr	50	30	50	10	10	<L.D	10	<L.D	<L.D
Co	62	48	52	40	22	1	6	2	<L.D
Ni	54	29	63	2	1	<L.D	1	3	<L.D
Cu	42	96	126	13	71	<L.D	<L.D	<L.D	<L.D
Zn	127	131	111	139	62	127	132	114	220
Ga	25.5	26	20.9	26.8	27	25.2	26.6	24.4	36.3
As	7	<L.D	<L.D	<L.D	<L.D	<L.D	<5	<L.D	<L.D
Rb	16.5	15.8	16.2	27.5	38.6	74.4	77.5	105	117
Sr	570	545	430	624	553	626	506	314	3.9
Y	24.1	27.8	28.6	37.2	55.5	47.5	38	40.6	89.9
Zr	196	201	161	279	469	389	443	476	1530
Nb	27.1	26.3	20.7	49	54.1	46.5	65	55.9	165

Mo	1	1	1	3	3	2	3	2	1
Ag	<L.D	<L.D	<L.D	<L.D	<L.D	<L.D	<L.D	<L.D	<L.D
Cd	1	0.8	0.72	1	0.7	<L.D	<L.D	<L.D	<L.D
Sn	2	2	2	2	3	3	3	3	11
Cs	0.14	0.07	0.1	0.2	0.65	2.13	0.8	1.9	0.12
Ba	179	272	202	409	652	730	671	790	18.5
La	23.8	24.1	23.7	39.3	55.3	60.5	66.2	67.5	99.7
Hf	4.6	5.1	4	6.3	10.1	8.3	10.6	11.6	34.7
Ta	1	0.9	0.7	1.8	2.8	2.4	3.7	3	9.6
W	1	1	1	1	1	2	2	2	2
TI	<L.D	<L.D	<L.D	<L.D	<L.D	<L.D	<L.D	<L.D	<L.D
Pb	2	<L.D	10	6	13	12	7	16	23
Ce	49	52	43.8	77.2	115.5	119.5	124.5	139	231
Pr	6.52	7.02	6.28	10.1	15.6	15.6	16	16.7	27
Nd	29.5	31.3	26.6	41.1	65.6	62	63.3	63.7	102
Sm	6.34	6.79	5.95	8.5	13.75	12.65	12.3	12.1	18.9
Eu	2.08	2.23	2.06	2.88	3.98	3.21	3.23	3.09	2.83
Gd	5.9	6.49	6.13	8.65	13.1	11.05	9.81	10.05	15.05
Tb	0.83	0.92	0.91	1.22	1.9	1.57	1.38	1.5	2.88
Dy	4.78	5.31	5.14	6.51	10.55	8.69	7.59	8.35	17.65
Ho	0.94	1.05	1.02	1.38	2.08	1.71	1.39	1.61	3.73
Er	2.27	2.53	2.56	3.37	5.59	4.77	3.76	4.19	11.4
Tm	0.31	0.3	0.3	0.5	0.77	0.68	0.51	0.59	1.98
Yb	1.7	2.08	2.14	2.47	4.79	3.83	2.82	3.47	12.4
Lu	0.23	0.24	0.28	0.34	0.68	0.53	0.46	0.47	1.9
Th	2.57	2.52	2.68	4.45	6.14	9	10.35	13.2	22.5
U	0.65	0.54	0.76	1.04	2.23	2.32	2.43	3.09	2.4

4.2. Chemical Variation diagrams

4.2.1.Classification variation diagram

Igneous rocks classified using silica content (SiO_2%), into acidic>66 wt%, intermediate 52-66 wt%, basic 45 to 52 wt% and ultra-basic<45 wt%. Based on this classification criteria, analyzed rock samples from Megezez volcanics classified as basic (45.5 – 48.5 wt %), intermediate (53.2 – 65.4 wt %), and acidic (72.2 wt %). Major element variation diagram of SiO_2 versus Na_2O + K_2O (wt %) used to classify rock suites based on chemical composition. Using Total Alkali Silica (TAS) classification diagrams (after Le Bas et al, 1986); the rocks are classified as basalt, trachybasalt, basaltic trachyandesite, trachyandesite, trachydacite, and rhyolite. Mafic and intermediate samples show general characteristic compositions fall in transitional field. Acidic volcanic products fall in sub alkaline/ tholeiitic field. Geochemical data symbols used in all plots throughout this chapter are the same.

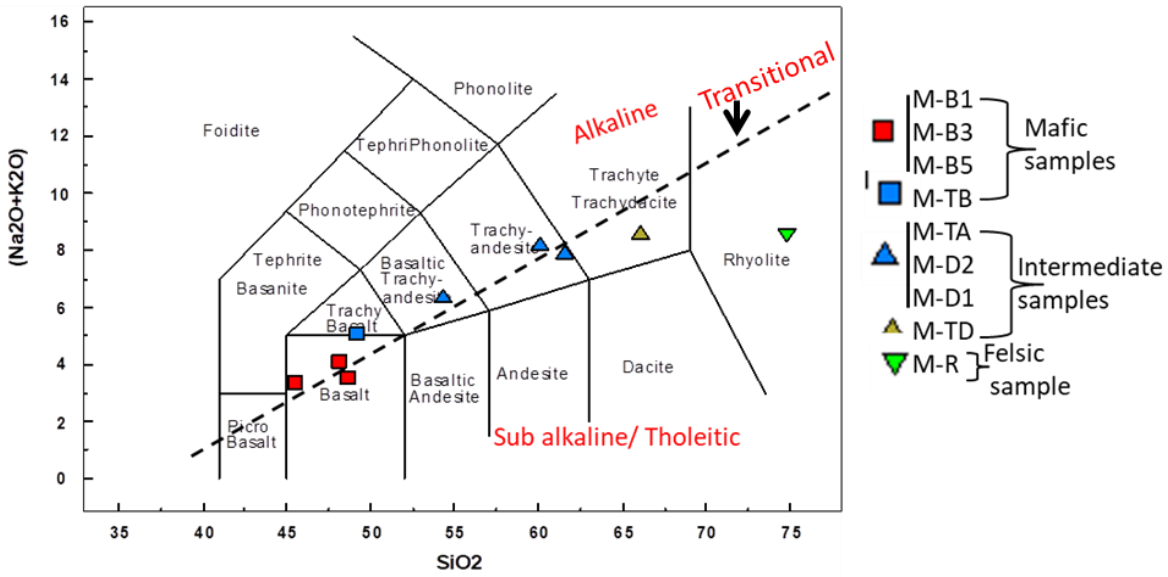

Fig.4.1. TAS (total alkali silica) classification diagram after Le Bas et al., (1986) for analyzed Megezez shield volcanics. Broken line is to classify samples as alkaline and subalkaline, after Irvine and Baragar (1971).

4.2.2. Major element variation diagrams

The purpose of using variation diagrams is to define and model products of partial melting and crystallization with interpretation of chemical differences and trends on related rocks. The SiO_2 is taken as the X-axis (abscissa) and used as a differentiation index in the variation diagrams constructed for major element oxides; because it shows reasonably wide range of variation (45.5 – 72.2 wt%). Variation diagrams constructed below in major element as a function of silica content generally show well defined trends.

Major element concentration is variable for analyzed rock suite. Basalt units constitute 15.2-15.7% Al_2O_3, 13.5-16% Fe_2O_3, 4.1-6.5% MgO, 8.1-10.5% CaO, 2.6-3.7% Na_2O, 0.8-1.4% K_2O, 0.3-0.5% P_2O_5, and2.5-3.4% TiO_2. After recalculating and normalizing to volatile free base; intermediate samples show 5.3-11.9% Fe_2O_3, 0.6-2.7% MgO, 2.2-6.4% CaO, 14.6-18.1% Al_2O_3, 3.9-5%Na_2O, 2.5-3.9% K_2O, 0.3-0.8% P_2O_5,and0.8-2.6%TiO_2. Rhyolite constitute MgO, CaO, and Fe_2O_3=5.5%, A_2O_3=10.2%, Na_2O= 3.9%, K_2O=4.5%, and 0.4%TiO_2. The values of Mg# range 24.47-32.2% for basalts; 10.41-23.11% for intermediate samples; and 3% for rhyolite samples of observed suites. The degree of alteration for rocks is low as shown by the value of LOI (<2.5%). The major element variation plots show both negative and positive correlations. Plots of MgO, Fe_2O_3, TiO_2 and CaO as a function of SiO_2 show negative correlation. K_2O versus SiO_2 variation diagrams show well-defined positive correlation trend; whereas diagrams in Na_2O, and P_2O_5, against SiO_2 show positive correlation for some stage and becoming negative correlation with inflection points.

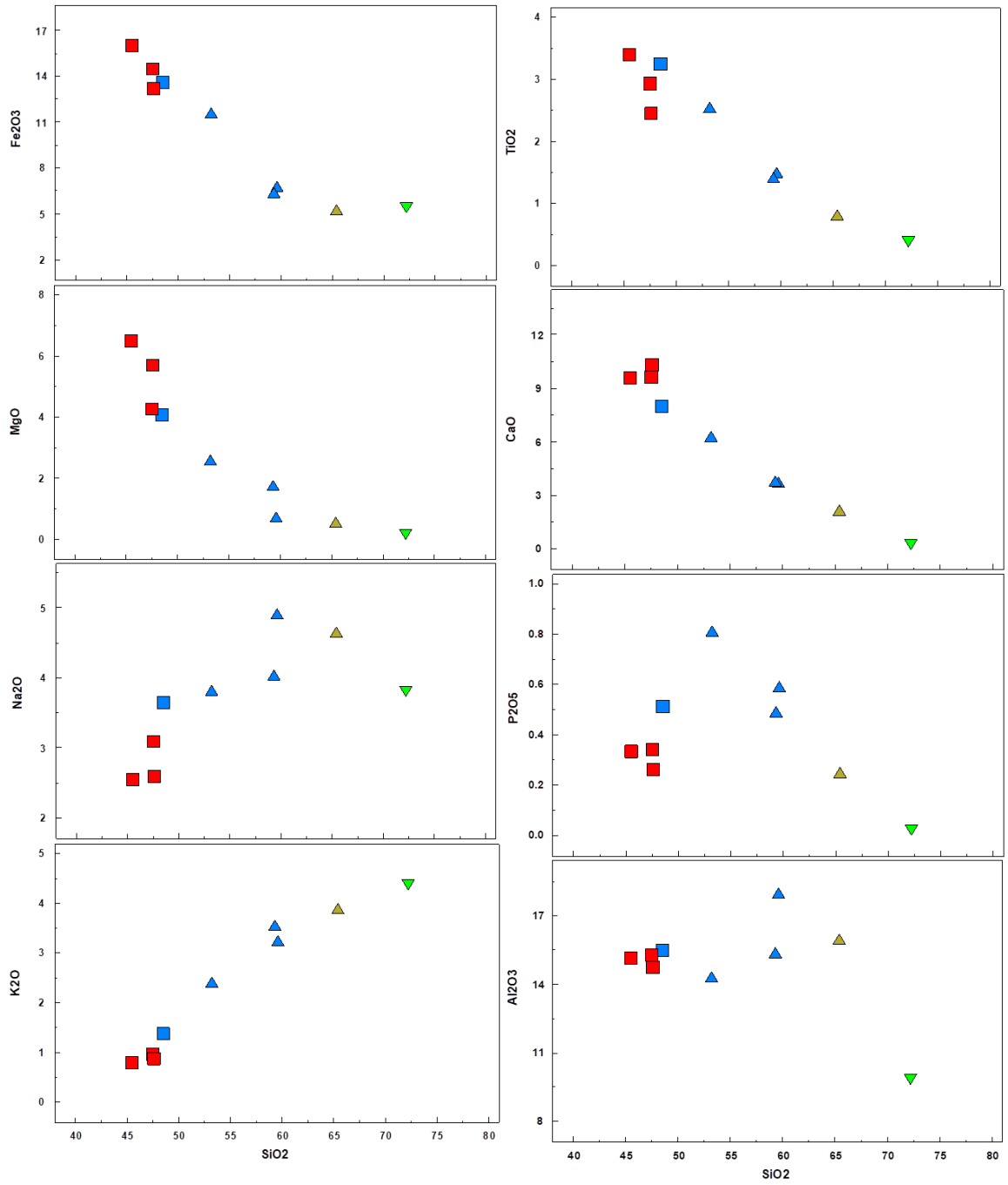

Fig.4.2. Variation diagrams of major element abundances (wt%) as function of SiO2(wt%) content for analyzed Megezez volcanics(symbols as in Fig.4.1).

4.2.3.Trace element variation diagrams

Trace elements are the second geochemical data analyzed, synthesized and presented in this study. They constitute small fractions in the phase with concentrations <0.1 wt% expressed in ppm. Regardless of their abundance in the system of interest they give geochemical and geological information. Trace elements generally can be grouped as compatible (concentrated in solid phase) and incompatible (concentrated in the melt). High field strength (HFS) elements (e.g. Th, U, Ce, Pb, Zr, Hf, Ti, Nb, and Ta) and low field strength elements (K, Rb, Cs, Ba, Sr, and Eu) are common incompatible elements

going to be used in this section. Spider diagrams constructed using these elements are useful for understanding the petrogenesis of Megezez volcanic rock suits.

Incompatible trace element (ppm) variation diagrams as a function of silica concentration (wt %) plotted in Fig.4.3, show defined trend for magma evolution. Variation diagrams in Rb show positive correlation with positive trend, whereas Sr shows negative trend. Positive trend in Eu and Ba as a functions of SiO_2 continues for some stage (up to ~60 wt %) and starts to negatively trending after an inflection point. Positive steep slope trend show increasing in incompatible elements (Rb, Ba) from basalt towards rhyolite. Ca is the accommodating major element for Ba and Rb in mafic magma, whereas K is an accommodating element for Rb and Ba in felsic magma.

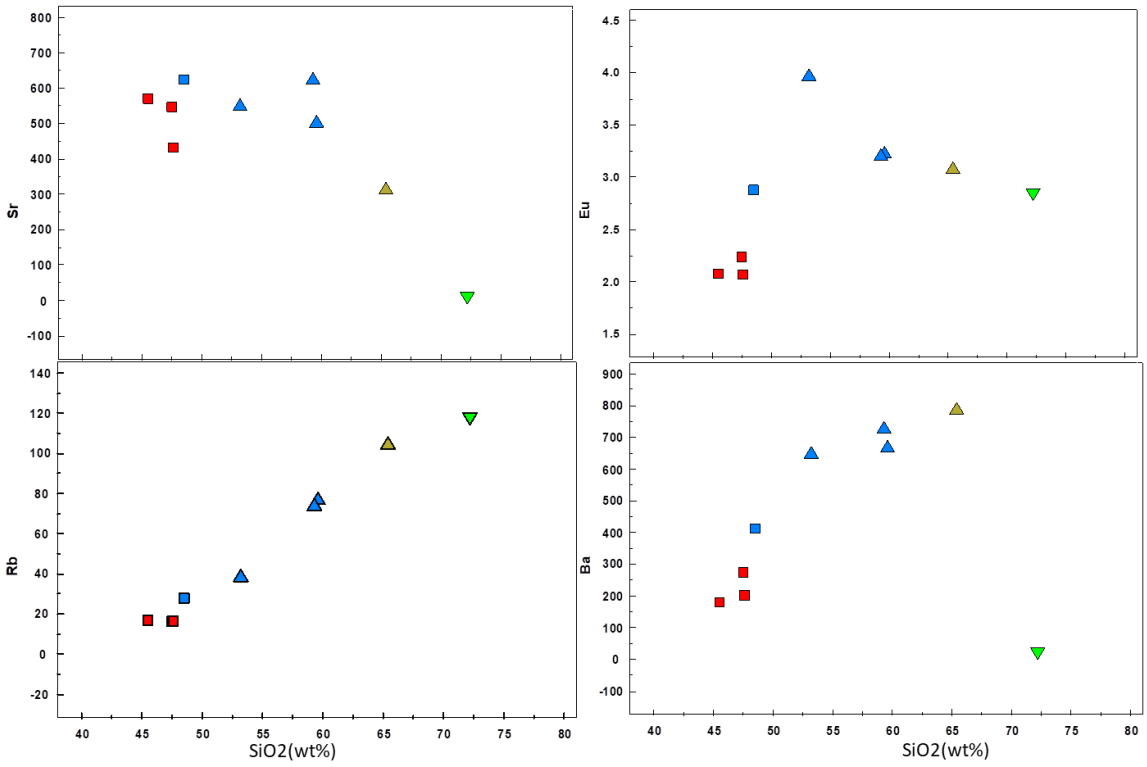

Fig.4.3. Large ion Lithofile (LIL) trace element (ppm) variation diagrams as a function of SiO2 (wt %), for analyzed Megezez volcanic products (symbols as in Fig. 4.1.).

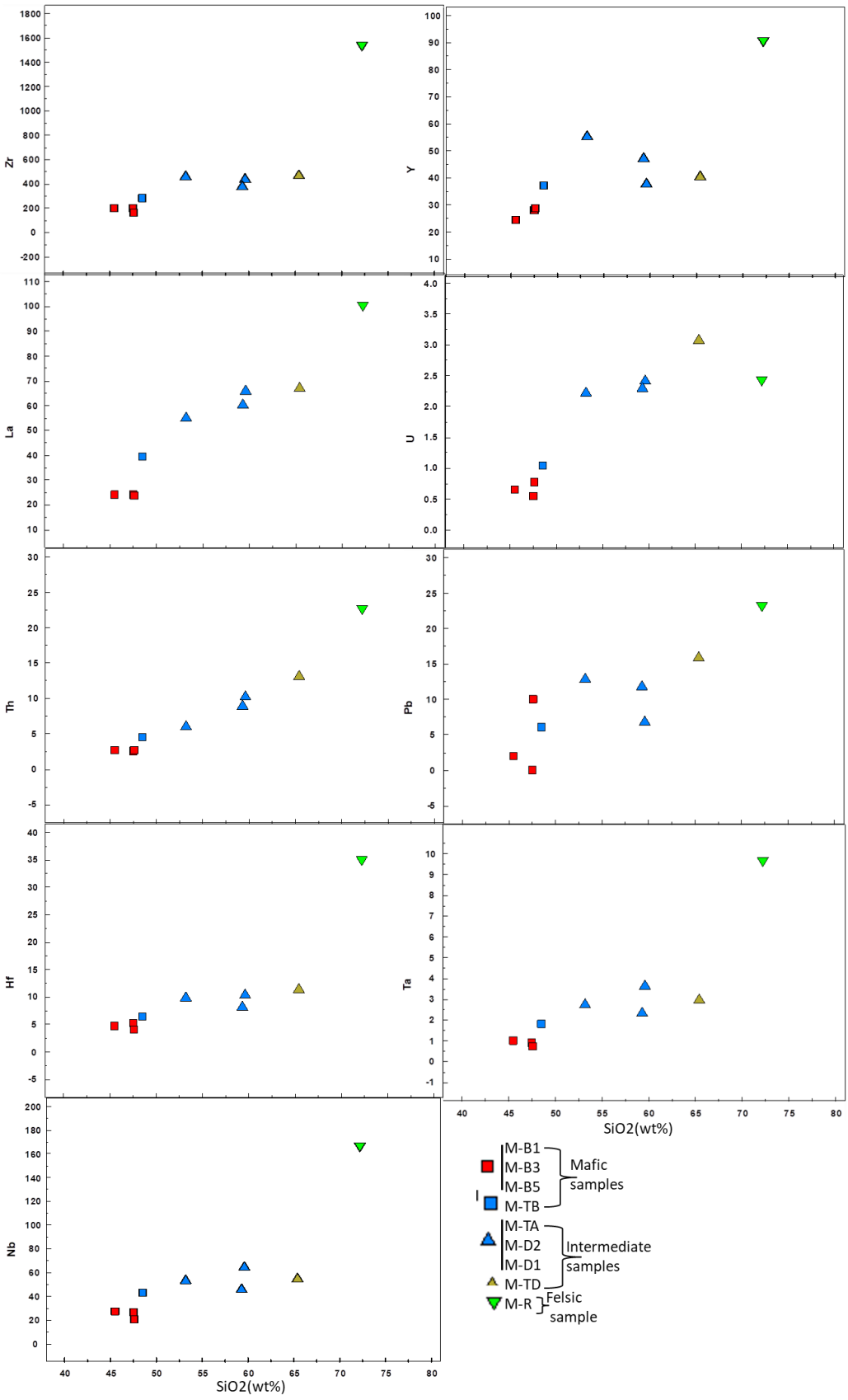

Fig. Fig.4.4. High Field Strength (HFS) trace element variation diagrams (ppm) as a function of SiO_2 (wt %), samples analyzed from Megezez volcanics.

Variation diagrams of HFSE (Th, Pb, U, La, Zr, Y, La, Nb, Hf) plotted against SiO_2 (Fig. 4.4 above) show positive correlations variably with well-defined evolution trend. Plots of Zr, Hf, Nb, and Ta versus SiO2 show positive, but narrow variation for those incompatible elements as silica increase; whereas, Th and La show well defined positive correlation.

The magma evolutions of the volcanic products can be additionally determined from highly compatible trace elements (Ni, Cr, Co, V). Six samples from Megezez volcanics have compatible element concentrations of Ni 1-63 ppm and Cr 10-50ppm; whereas, the remaining three samples have <1ppm and <10ppm respectively. From this concentration values, basalts have Ni 29-63ppm and Cr 30-50ppm, intermediate and acidic rocks have Ni ≤3ppm and Cr ≤10ppm concentration values. All compatible elements in the variation diagrams (Fig. 4.5) show slightly varying negative correlation forming curvilinear trend plotted as function of silica content (wt %).This shows almost similar characteristics to corresponding accommodating major elements having negative correlation trends (e.g. Fe_2O_3, MgO, CaO, TiO_2. Magma differentiation traced from the concentrations of these highly compatible trace elements and Mg# (24.47-32.2% for basalts, 10.41-23.11% for intermediates, and 3% for rhyolite) values as basalts have higher values and intermediate and felsic suites have lower concentration through differentiation processes of magma. Generally, these elements are enriched in basalts, progressively depleted in intermediate and rhyolite.

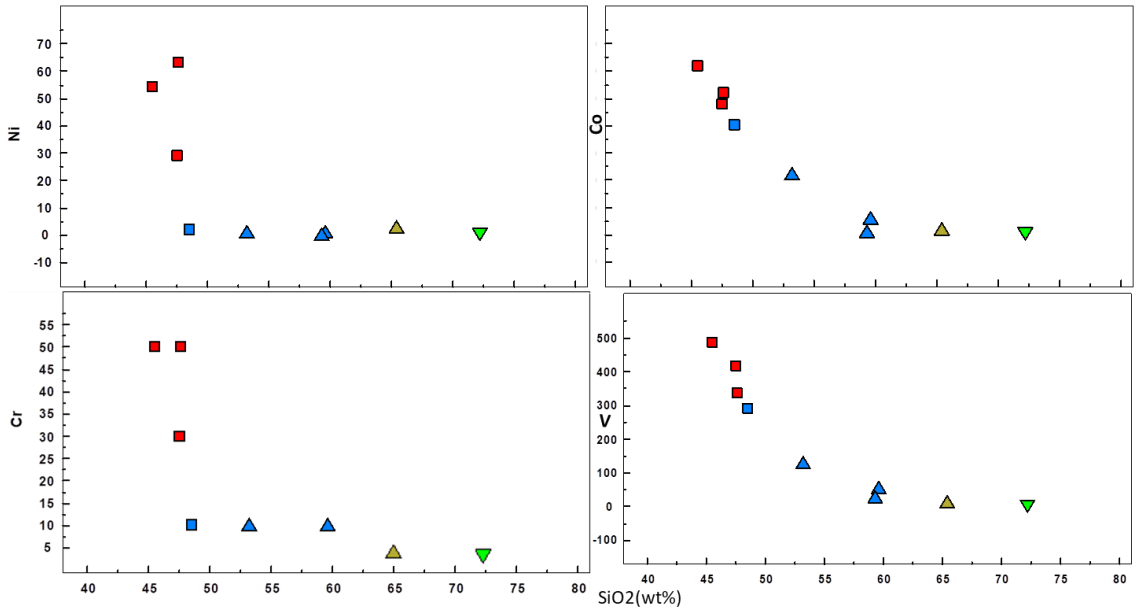

Fig.4.5. Variation diagrams for compatible trace elements (ppm) as a function of SiO2 (wt %) content (symbols as in Fig. 4.1. and Fig. 4.4.).

Selected incompatible trace elements also plotted as functions of incompatible element (Zr), showing increasing trend. Variation diagram in Nb and Y as a function of Zr show well defined positive correlation trend starting from basalts to rhyolite suits; having narrow differences in basic to intermediate samples and high concentration value for acidic sample. Generally, from the different plots Zr has relatively high concentration in acidic rocks; in contrast Ba show very low concentration value for acidic sample and higher for basic and intermediate samples.

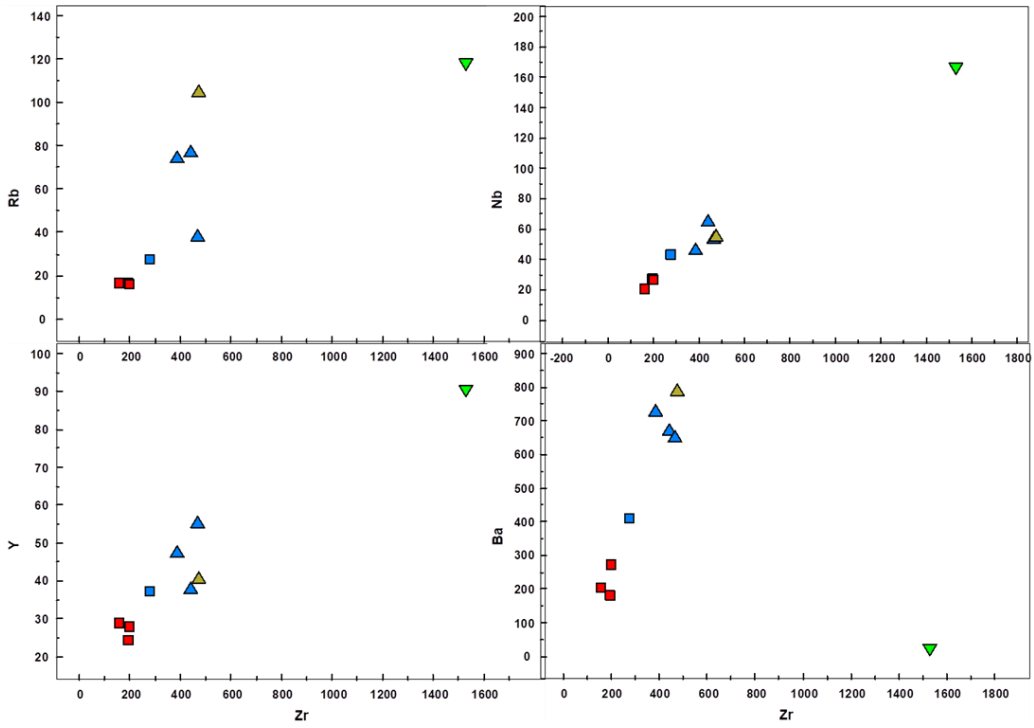

Fig.4.6. Variation diagrams for selected incompatible trace elements as a function of Zr, concentrations expressed in ppm (symbols as in Fig. 4.1).

4.3. Chemical Spider diagrams

4.3.1. Rare earth element patterns

REE element patterns plotted using Chondritic-normalized diagrams (Sun and McDonough, 1989). Variations within the data set provide information about the extent of crystallization and fractionation of magma. The break in pattern below is due to the concentration of Pm being below detection limit during sample analysis for trace elements. The negative anomaly in Eu (Eu/Eu* = 0.5) is pronounced for acidic volcanic products. The pattern of REE show steep slope trending in LREE (La – Sm) and become slightly flat slope in HREE (Gd – Lu) with concentration increasing from basic to intermediate to acidic suite. Acidic sample distinctly show relative enrichment both in LREE and HREE compared to mafic and intermediate volcanic rocks. Felsic samples show pronounced flat slope in HREE (Gd – Lu);

and all the samples show parallel to sub-parallel magma evolution trend. Normalized value of Eu/Eu* is 1.02-1.04 for mafic and <1(0.5-0.9) for intermediate and acidic analyzed samples in the present study. The LREE are highly enriched and HREE depleted relatively with 10 times greater than the Chondritic value of logarithmic scale (i.e. 100 times greater).

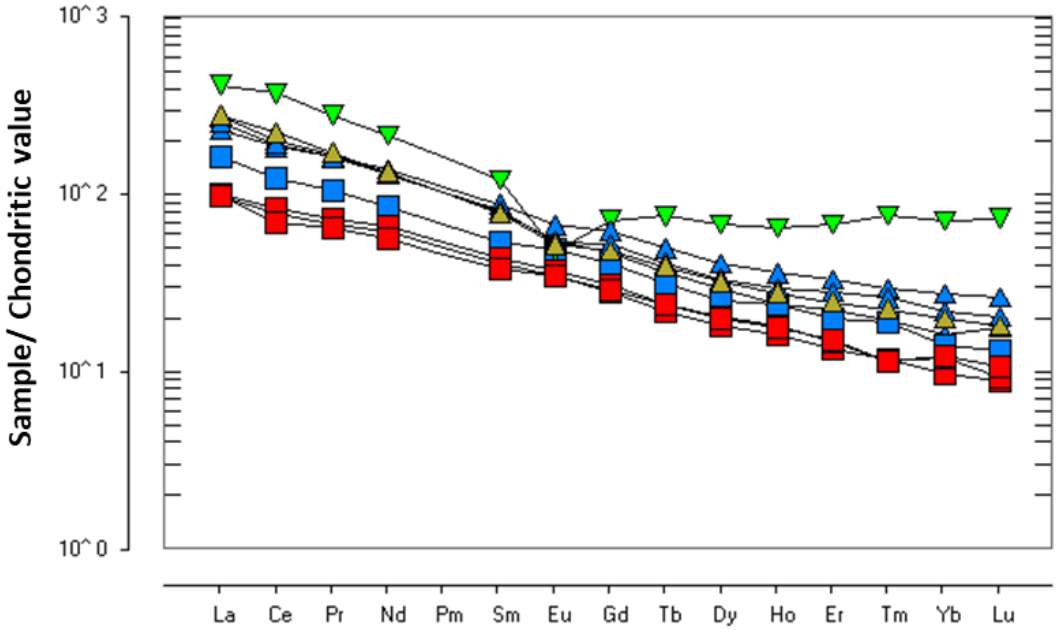

Fig.4.7. Multi element diagrams of Chondritic- normalized (Sun and McDonough, 1989) Rare Earth element patterns of analyzed Megezez volcanic products (symbols as in Fig. 4.1).

4.3.2. Multi elements spider diagrams

The evolution of Megezez volcanic products can also be understood from multi element (Spider) diagrams constructed using primordial mantle (McDonough and Sun, 1995). Strong depletion shown from strong negative spikes in trace elements Ba, Sr, and Ti (see Fig. 4.8) with a trend of acidic samples analyzed from studied area. Trace elements like Rb, Th, K, Sm, Nd, and Nb show higher positive anomaly for acidic rocks than intermediate and basic rocks. The incompatible trace elements fit to residual melt during magma crystallization and preserve their concentration higher in felsic rocks relatively. Analyzed rhyolite sample is variably enriched in trace elements including Zr, Hf, Ce, La, Ta, K, Rb, Nb, Th, and strongly depleted in Ti, Sr, Ba.

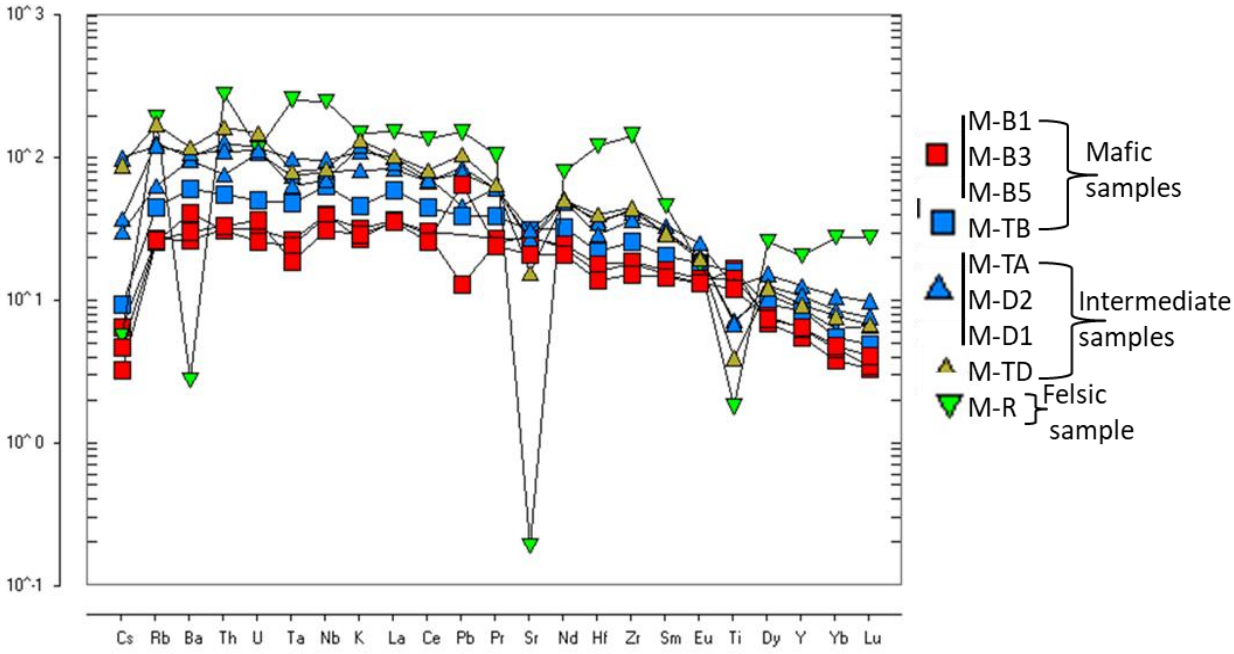

Fig.4.8. Spider plot for trace element patterns normalized to primordial mantle McDonough and Sun (1995), analyzed samples from Megezez volcanics (symbols as in Fig. 4.4)

CHAPTER- FIVE

5. Discussion

This research mainly presents detail geological map of the study area with geological cross-section; composite stratigraphic log sections; petrographic and geochemical compositions of Megezez shield volcanic. The petrography and mineralogical compositions, and petrogenesis of volcanic rocks from Megezez Shield volcanic area thoroughly discussed in this chapter. The relative volcanic successions of observed volcanic suite outlined from youngest to oldest as basalt –rhyolite - trachydacite - trachybasalt - trachyandesite. This needs dating supported with isotopic data.

The combination of field, petrographic, and geochemical data utilized in this study show Megezez shield volcanic rocks dominantly composed of basalt unit followed with intermediate and felsic composition.

5.1. Petrography

The modal composition of analyzed samples shows wide range of mineralogical composition and textural features presented in chapter three. Rock units in this study constitute different mineral phases at phenocryst, microphenocrysts, and groundmass level having different modal percentage. Plagioclase, clinopyroxene, hornblende, alkali feldspar, and quartz are the major phenocryst and microphenocryst mineral phases identified in basalts, intermediate (trachyandesite, trachydacite) and rhyolite units.

Megezez volcanic products composed of minerals having petrographic characteristics of different nature. The textural arrangements, the zoning in plagioclase, poikilitic inclusions, sub ophitic and reaction rims in hornblende, alteration effects in clinopyroxene and plagioclase, wide range of phenocryst phase variations, euhedral-Subhedral-anhedral shape are very common in the analyzed volcanic rocks. These petrographic characteristics testify fractional crystallization, mineral stability condition (exhibited by hornblende), and order of magma crystallization for basalt, trachyandesite, trachydacite and rhyolite rock suite. The observed volcanic suites exhibit differences in crystal shape; implying the order of magma crystallization as euhedral to Subhedral minerals assumed to be the first to crystalize and anhedral crystals crystalize later.

Basalt unit show mineral composition of phenocryst with modal percentage 18-37% as a leading phenocryst of plagioclase followed by clinopyroxene mineral phases. Plagioclase

show complex zoning, polysynthetic twin, poikilitic inclusion of clinopyroxene, and sieved texture (effect of alteration). It is characterized by euhedral shape, tabular and elongated crystal form observed with larger phenocryst; and lathe-shape small phenocryst embedded in microcrystalline groundmass. The groundmass constitutes mafic minerals like clinopyroxene, plagioclase, and opaque (ilmenite, hematite). Clinopyroxene phenocryst in most basalt samples shows replacement reaction in its core region by opaque minerals indicating the alteration effect. Different textures like poikilitic inclusion are indicative of order of crystallization resulted from difference in nucleation and growth rate during magma cooling. This can be explained as the enclosed mineral grain (clinopyroxene in this case) is assumed to be the first to crystalize followed by enclosing mineral (plagioclase) which is in agreement with fractional crystallization trend in geochemical variation plots. Zoning is a compositional variation which is common in minerals those exhibit solid solution behavior (e.g. plagioclase, pyroxene, and olivine). As presented in chapter three, plagioclase is normally zoned with a compositional change from high temperature mineral phase at the core (Ca-plagioclase) and to low temperature composition mineral at its rim (Na-plagioclase). This can be explained as normal zoning formed when early formed calcium plagioclase feldspars coated progressively with sodium plagioclase feldspar as magma cools.

The analyzed trachyandesite samples show opacitic rim in prismatic hornblende mineral grains, common in hydrated mineral phases like amphibole. The reaction rim observed in hornblende from trachy andesite resulted from disequilibrium reaction of phenocryst phase (hornblende) with the embedding groundmass and dehydration effect. This is because this hydrated mineral is unstable at lower pressure and temperature environment.

5.2. CIPW Normative minerals of Megezez volcanics

Petrographic descriptions and interpretations obtained from Megezez volcanics have associated with CIPW normative of minerals determined from major element geochemical analysis. The norm values coincide with petrographic modal abundance minerals; however, slight deviations can be expected. This is assumed because of taking only visible phenocryst mineral phases in petrographic modal compositions; whereas, CIPW calculations take the wt% of major oxides for mineral phase at groundmass and phenocryst level. This norm value important to characterize basalts, intermediate, and rhyolite rocks analyzed from Megezez area. Normative mineral abundance is the calculated wt% of particular mineral;

excluding hydrous minerals in the calculation. The normative data of analyzed rocks presented in chapter four (table 4.1), show that basalts are Hypersthene normative (13.76-6.55 wt %) and contain normative of quartz (2.27- 4.46 wt %). The presence of hypersthene and quartz in the norm can justify Megezez basalts classified as silica oversaturated rocks. Whereas, rhyolites classified based on CIPW normative of quartz = 34.28; implying the rock is silica oversaturated; and normative of acmite = 5.21 wt% to classify the rhyolite as peralkaline rock. From the norm calculation sphene ranges 5.51-7.87 wt% testifying the accumulation of plagioclase/ anorthite and titanite. Total alkali silica (TAS) and petrographic naming of trachy dacite unit in the studied samples also supported by normative quartz = 20.74%. This is because it is possible to classify using the range of quartz normative value is >20%; obtained from recalculation of Quartz + Anorthite + Albite + Orthoclase =100% (see Table 4.1).

5.3. Petrogenesis of Megezez volcanic rocks

Total alkali silica (TAS) classification diagrams in chapter four (Fig. 4.1) show, the analyzed samples fall in mafic, intermediate and felsic compositional field based on silica content. Basic and intermediate rock suites are transitional type while acidic samples classified as tholeiitic/ sub alkaline (but number of acidic samples is not sufficient to generalize).

The distribution of trace elements can be geologically controlled with fractional crystallization, partial melting, mixing, and crustal contamination. Two important models are basic tools to explain the petrogenesis of felsic rocks (Dereje Ayalew et al., 2002, Peccerillo et al., 2003: 1) Fractional crystallization of initially basaltic magma; 2) Partial melting of mafic lower crustal rocks with or without subsequent fractional crystallization.

This section presents the petrogenesis of mafic-intermediate-felsic rock suite with fractional crystallization (major effect), assimilation fractional crystallization, and crustal contamination models. Variable evolution trend observed from major element versus silica, trace versus silica content, and trace versus trace. In addition to this, spider diagrams of Chondritic normalized REE, primordial mantle normalized trace elements and other combinations used and interpreted following their signature. This is important to testify the source/genesis of Megezez shield volcanic rocks.

Parent magma derived from high temperature small melt fraction characterized with high concentration of Fe_2O_3=12-16%, TiO_2= 3-7%, and primary MgO=14-15% (Rogers et al., 2010). Megezez Volcanic rocks of the present study show distinctly lower concentration of Fe_2O_3 =5.3-16%, TiO_2 =0.4-3.4%, and MgO =0.2-6.5% implying the derivation of parent magma from lower temperature condition. In addition, Megezez volcanics characterized with MgO <6.51%, Mg# = 42-67%, Ni=7-37 ppm (Gezahegn Yirgu, 1997) and MgO = 0.2-6.5%, Mg# = 10.4-32.2% for intermediate and mafic samples, very low (3.4%) for felsic, Ni = 29-63 ppm for mafic and lower to low detection limit for intermediate and felsic samples (data from this study). This reasonably explains the significant magma differentiation during upraise to the surface.

Major oxide variation diagrams (chapter four, Fig. 4.2) like MgO, Fe_2O_3, CaO, and TiO_2 vs SiO_2 show negative correlation with defined trend; indicative of fractionation of Mg, Fe, Ca, Ti bearing minerals (like pyroxene, plagioclase, and Fe-Ti oxide). Variation diagram of K_2O against SiO_2 show positive correlation indicating the accumulation of alkali feldspars in the system due the increasing properties of K with increasing SiO2. Variable trend as positive for some stage and negative trend after inflection point is observed in P_2O_5, Na_2O and less in Al_2O_3 plotted against SiO_2 diagrams. This testifies the change in crystallizing mineral assemblage.

Fractional crystallization of mafic magma is capable to generate magma depleted in highly compatible elements (Cr, Co, Ni, V) showing pronounced negative trend in the genesis of Megezez volcanic rocks. These compatible trace elements variation diagrams (chapter four, Fig. 4.5) like Ni, Cr, Co, V also show pronounced negative correlation with well-defined trend of magma evolution. This is the same as their accommodating major element (Fe, Mg, and Ca) trends to imply the process of fractional crystallization, progressively decreasing concentration from mafic-intermediate-felsic mineral. Megezez volcanics are evolved from basaltic parent magma and their compositions controlled by the accumulation of plagioclase in the system; in agreement with features from Choke volcanics (Kieffer et al., 2004). Rocks derived from mantle source are enriched in highly compatible trace elements (Ni = 250-300 ppm, and Cr = 500 – 600 ppm). However, geochemical data from Megezez basalts show very low concentration in these compatible elements (Ni=29-63ppm, Cr=30-50ppm, Co=48-62 ppm), testifying the removal of mafic minerals like olivine and pyroxene. This leads to be interpreted as the fractional crystallization of mafic minerals (clinopyroxene, plagioclase)

derived from depleted magma source. Especially the declining of Cr concentration value in mafic samples is an indicative of fractionation of spinel and or clinopyroxene.

More evolved samples have high concentration; intermediate samples lower concentration and least evolved basalts are more depleted in highly incompatible trace elements Ba, Rb, Zr, and Nb (Mulugeta Alene et al., 2017). This is best explained with variation diagrams of these elements as a function of MgO% (Fig. 5.1). Adopting this, the present result show Megezez shield volcanics have Rb, Zr, and Nb concentration higher in felsic samples which are more evolved, moderate in intermediate samples and mafic samples are generally depleted (showing defined negative correlation trend (Fig.5.1.). This indicates the progressive enrichment of incompatible trace elements as magma evolved starting from basaltic parent magma into intermediate and felsic magma.

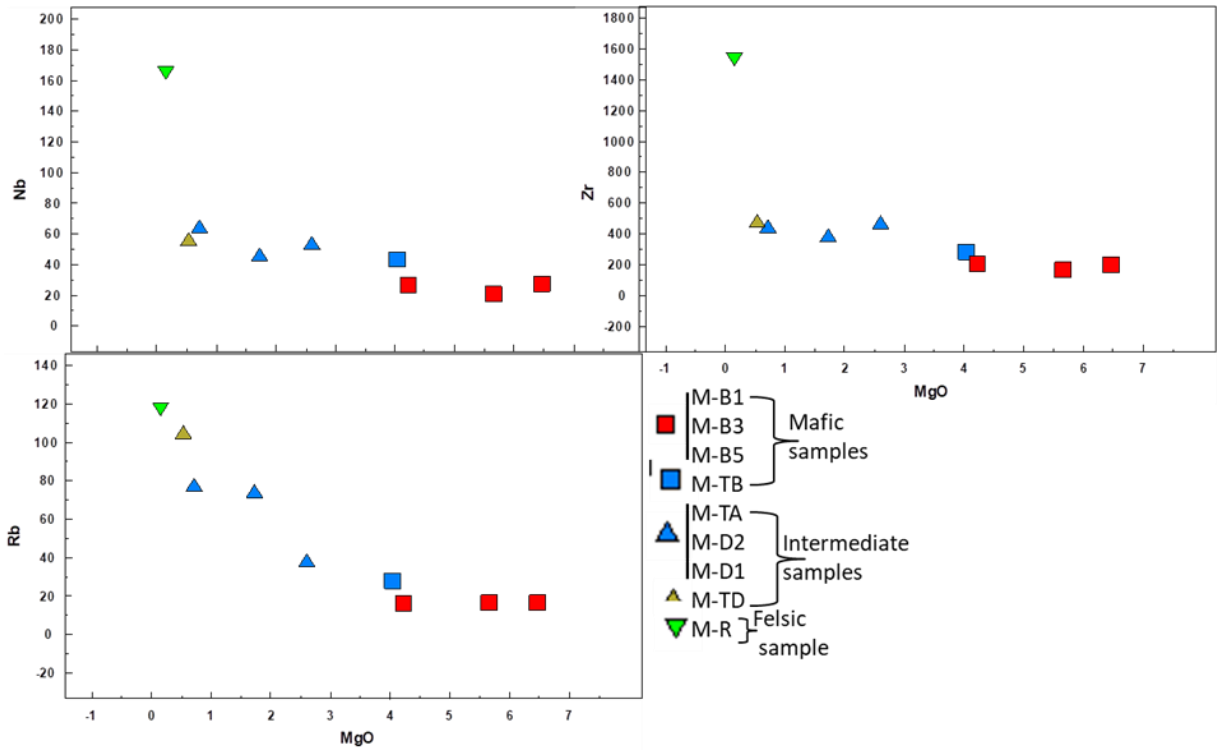

Fig.5.1. Variation diagrams for selected incompatible trace elements (ppm) as a function of MgO (wt %), samples from Megezez shield volcanics.

Variation diagrams constructed using high field strength elements (HFS) Nb, Th, Y, Hf, against Zr (Fig 5.2) display a good correlation of positive trend. This can be justified as the derivation of Megezez volcanics is from the same source (Co-genetic) related by crystal fractionation. Positive trend also indicate these elements fit to residual liquid with increasing concentration in felsic minerals than mafic during fractional crystallization.

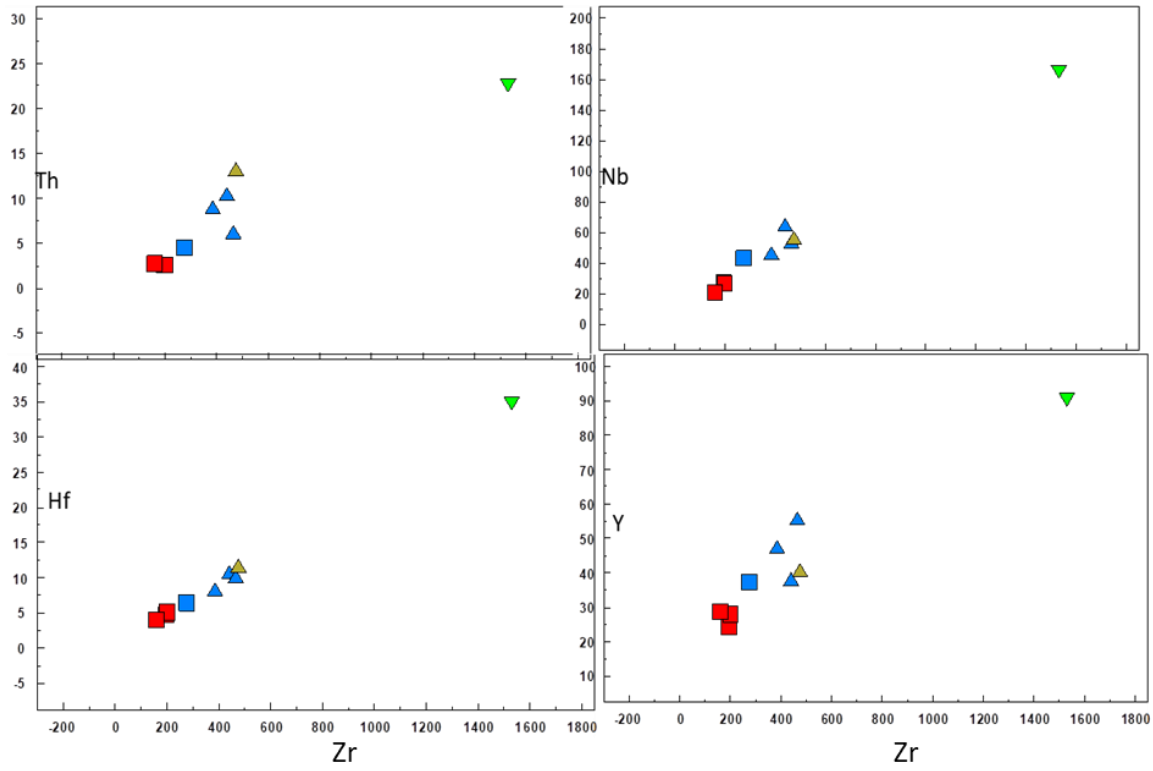

Fig. 5.2. Incompatible versus incompatible trace elements variation diagrams (ppm), Megezez analyzed samples (symbols as in Fig. 4.1 and 4.4).

Megezez basalts exhibit similar REE patterns with plateau basalts both in abundances and fractionation (Gezahegn Yirgu, 1997). The present analyzed samples of Megezez rhyolite lava show similar characteristics with Alaji rhyolite samples having pronounced negative anomaly at Eu; indicative of the fractionation of plagioclase in agreement with petrographic results. The REE spider diagram (Fig. 4.7) normalized with Chondritic value (Sun and McDonough, 1989). Megezez felsic suite displays flat trend for HREE (Dy-Lu) distinctly separated from intermediate and mafic suite of analyzed sample; may suggest the variation in degree of fractionation. There is also a variation with enrichment of both LREE and HREE in felsic samples compared to mafic and intermediate rock suite. Both LREE and HREE are enriched (>10 times as log scale) than Chondritic value (Fig. 4.7) with distinctly varying trend as steep for LREE and weak flat for HREE, implying spinel source (or garnet free). The evolution trend is parallel to sub parallel with intermediate and mafic rocks implying the co-genetic source.

Trace element spider diagrams (Fig. 4.8) normalized to primordial mantle of McDonough and Sun (1995) presented in chapter four (Fig. 4.8), show Megezez felsic rocks exhibit pronounced troughs/ depletion of Ba, Sr, and Ti. This testifies the fractionation of plagioclase, accessory minerals (like hematite, titanite); whereas, Ta and Nb, Pb exhibit

enrichment/ no troughs indicative of the presence of little or no crustal contamination during magma emplacement to surface. Similar results observed from felsic rocks of Guna shield volcanics (Adise Mekonnen, 2006), felsic rocks of Debre Berhan area (Dereje Ayalew et al., 2002), and Choke and Guguftu lavas (Kieffer et al., 2004). The presence of K negative anomalies observed in trace element spider diagrams of alkali basalts in East African rift and many other ultrapotassic magmas are indicative of melting in the presence of amphibole (Kieffer et al., 2004, and references there in). This is reasonably due to the stability of these minerals only under relatively low temperatures and pressures. The presence of such anomalies is evidence of a lithospheric source of the rift basalts. In lavas from northern Ethiopia, K negative anomalies are absent (Kieffer et al., 2004); and geochemical spider plot for the Megezez lavas show the absence of K negative anomalies; which is an indicative of the non-lithosphere source of rift basalts; in agreement with Kieffer et al. (2004).

5.4. Selected Trace element ratios

Petrogenesis of Megezez rock suite can be determined with the characteristic concentration of selected trace element ratios. For this study, La/Nb, Rb/Nb, La/Yb, Dy/Yb, Tb/Yb, Ce/Pb, K/Rb, and Eu/Eu* ratio values have been used to understand petrogenesis in terms of fractional crystallization, crustal contamination, source, and partial melting of studied rocks from Megezez shield volcanics. The degree of crustal contamination as magma emplaced to surface can be determined by considering the ratio of La/Nb, for the uncontaminated (La/Nb < 1) and contaminated magma (La/Nb >1). Therefore, Megezez volcanics show this ratio 0.6-1.02 and two samples 1.14-1.21 leads to conclude the minimum crustal contamination, confirming the lack/no negative anomaly of La and Nb from trace element spider diagram (Fig. 4.8). This is similar in terms of this element ratio with data presented from Guna Volcanics (Addise Mekonnen, 2006).

Chemical element ratios of Ce/Pb has important role to investigate magma generation/source. Mantle derived magma is characterized with 20-30 Ce/Pb ratio (Dereje Ayalew et al., 2016, 2018 and references there in). Analyzed samples from this study show 4.38-17.8 and only one sample has 24.5 values. This can be concluded as the source of Megezez volcanic rocks is not generally from mantle derived magma but some samples indicate the mantle source. This requires additional data to generalize and using other way of source indicators.

The ratios of Dy/Yb, Tb/Yb, and Tb_n/Yb_n have been used to assess the source rock; from the enrichment of HREE plots relative to Chondritic normalized value. The rift wall basalts characterized by HREE patterns ($Tb_{n/}Yb_n$= 1.4-1.9) with HREE concentration >10 times Chondritic values; likely suggesting mantle source containing spinel. Following this concept Megezez basalts show this characteristic feature in the range Tb_n/Yb_n =1.88-2.1, the total analyzed samples are 0.9-2.1 value together with HREE concentration >10 times Chondritic value as discussed in Fig. 4.8. This leads to generalize those volcanic rock units of Megezez shield derived from spinel source rather than garnet.

For rhyolites originated by crustal melting comprise Rb/Nb >10; whereas, the Alaji rhyolites of previous study and Megezez rhyolites of the present study show very low Rb/Nb ratio (<1) and (see Table 5.1), indicate these felsic rock suites could not be originated by partial melting of the continental crust (Gezahegn Yirgu, 1997). This argument may also work for intermediate and mafic rock suits analyzed from Megezez volcanics having Rb/Nb ratio in the narrow range (1.19-1.88 and 0.6-0.78 respectively). Alaji rhyolites have similar Rb/Nb ratios as basalts from both Megezez and plateau (Gezahegn Yirgu, 1997). This is an indicative of the derivation of those felsic rocks is from fractionation of basaltic magmas. The Eu/Eu* ratio show narrow variation determined as felsic (=0.5), intermediate samples (=0.81-0.9), and mafic samples (=1). Pronounced Eu negative anomaly observed from trace element spider diagram is an indicative of fractionation of plagioclase; and lack of this anomaly in the mafic rocks is due to the accumulation of plagioclase.

Incompatible trace element ratios used to compare and contrast Megezez volcanic rocks with north western Ethiopian volcanics (flood basalts, Wegel Tena rhyolites and Guna volcanics; see in Table 5.1). Megezez rock suite have Rb/Nb ratio proportional to flood basalts, Wegel Tena rhyolites, Alaji rhyolites and Guna volcanics; indicating the petrogenesis of those volcanics can explain the petrogenesis of Megezez volcanics.

Variation diagrams plotted for highly incompatible trace element ratios against incompatible trace element (see Fig. 5.3) to investigate the effect of fractional crystallization and source of volcanic rock products from Megezez. These plots show positive linear correlation trend interpreted as the lavas from Megezez shield volcanics are from the same magmatic source/co-genetic by differentiation process. From the three plots of trace ratios Th/La vs Rb shows well-defined positive trend; whereas, the remaining two show scattering trends. Since all elements are highly incompatible their correlation trend best explains the same magmatic

source/co-genetic of Megezez rock suites with dominant process of fractional crystallization.

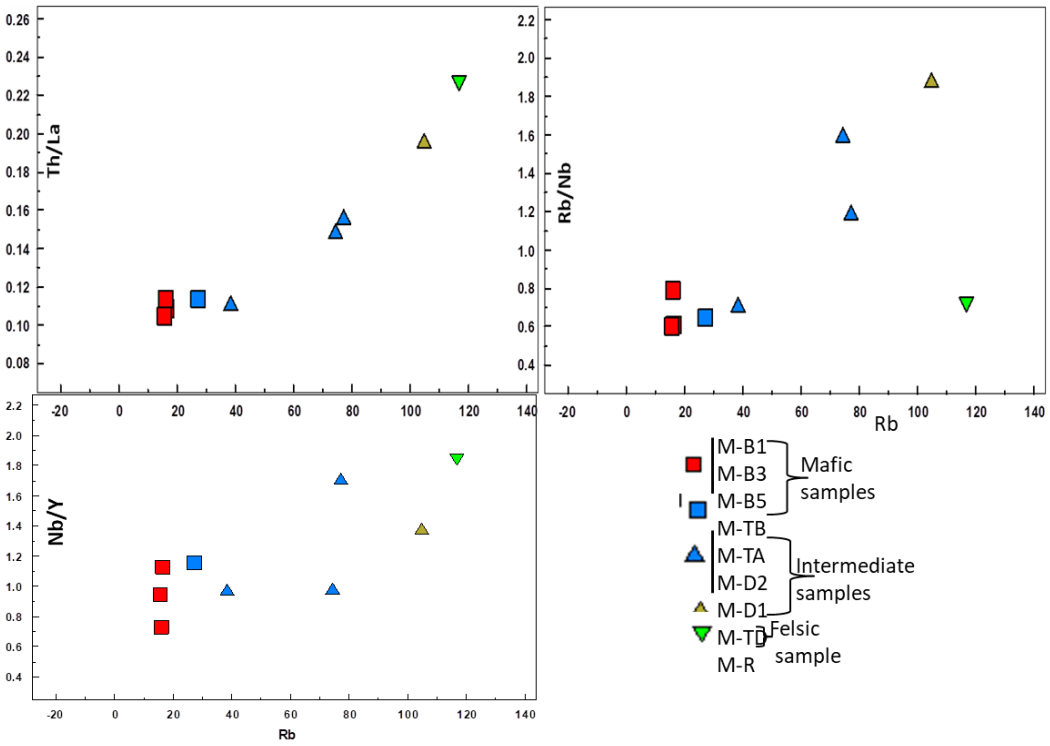

Fig. 5.3. Variation diagrams of trace ratio as a function of trace element, analyzed Megezez volcanics.

5.5. Comparison of Primary data with previous works

As stated in the research methods (chapter one), previous data from Megezez shield volcanics and one sample from Alaji rhyolite (Gezahegn Yirgu, 1997) used as a comparison. The samples show general agreement in results with the primary data analyzed in the present research approach. Eight samples from Megezez, and one sample from Alaji silicic rocks that is a total of nine samples used in various diagrams together with primary samples. Variation diagrams of different trace and major elements show analyzed primary basalts of Megezez plotted with secondary basalts; and Megezez primary felsic sample show the same signature with Alaji felsic sample.

The present study shows wide variation in composition of Megezez volcanic suites compared to previously taught that is geochemical data generated by previous works (Gezahegn Yirgu, 1997) (see Fig. 5.4).

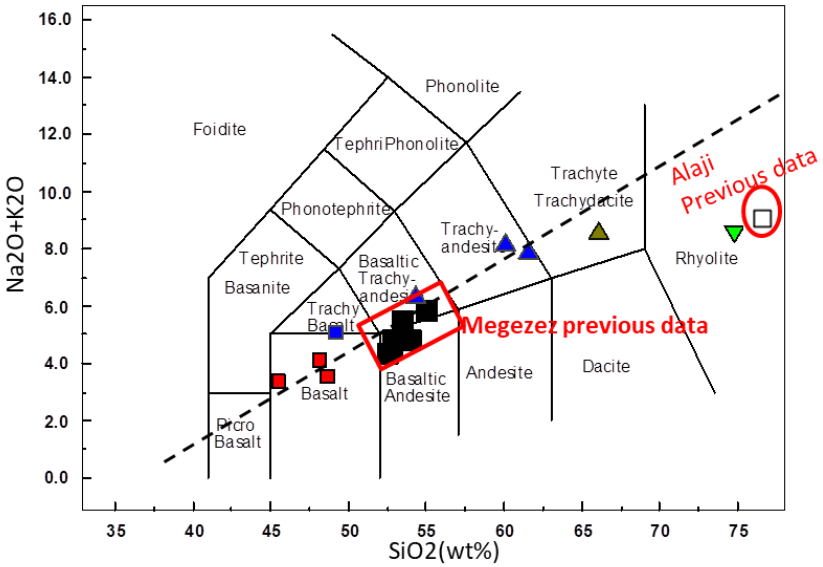

Fig. 5.4. Total alkali silica (TAS) diagram (Le Bas et al., 1986) to show compositional variations of primary data compared to previous data of Gezahegn Yirgu (1997).

The variation diagrams for MgO, CaO, Na_2O, and K_2O against SiO_2 (see Fig. 5.4, A) for primary data show wide variation in composition compared to previous work data compiled by Gezahegn Yirgu (1997). Strongly Negative trends in MgO and CaO Vs SiO_2 is an indicative of fractionation of Mg and Ca bearing minerals (like pyroxene, plagioclase). The decreasing trend of Na_2O as a function of SiO_2 after some amount of silica concentration is an implication of plagioclase fractionation (albite); whereas K_2O is continuously increasing trend with increasing SiO2 which implies fractionation of alkali feldspar. Ferromagnesian elements like Cr, Co, Ni, V and Sc show a sharp decrease to very low values within the Megezez mafic suits (Gezahegn Yirgu, 1997, and this study) and immediately drop down to very low concentration values in evolved volcanic products (intermediate and felsic samples). The controlling effect of fractional crystallization is also supported with strong negative trend in highly compatible element (Ni,V) plots as a function of SiO_2 which is indicative of rapid removal of mafic minerals from the magmatic system during crystallization. Both primary and secondary samples of Megezez show steep negative trend of these compatible trace elements and the accommodating major elements (Fe, Mg, Ca); show pronounced evolution trend starting from basalt-intermediate –rhyolite suites. The primary data result shows wide variation and more evolved magma crystallization compared to those previous data results in Megezez. Even though the sampling in the present research for felsic suits is not sufficient to generalize the relationship; the available primary data show Megezez rhyolites show similar signature of major and trace element abundance with Alaji silicics analyzed in previous works.

Basaltic systems show Sr depletion in response to the fractionation of plagioclase and or crustal assimilation (Haliday et al, 1991); and Rb increases corresponding to the more or less vertical trend (see Fig. 5.4, B). Incompatible trace elements like Sr drops to very low concentrations both in Alaji and Megezez felsic rocks; whereas strongly incompatible trace elements like Rb, Nb, and La reversely respond showing very high concentration. Previous work results have presented that, the felsic rocks of Alaji formation display distinctly higher enrichment in incompatible elements, but showing similar patterns with Megezez and plateau basalt. This study also show the same argument to which the Megezez and Alaji rhyolite samples exhibit similar patterns with Megezez basalts and intermediate samples but with highly enrichment of incompatible trace elements and depleted in compatible elements.

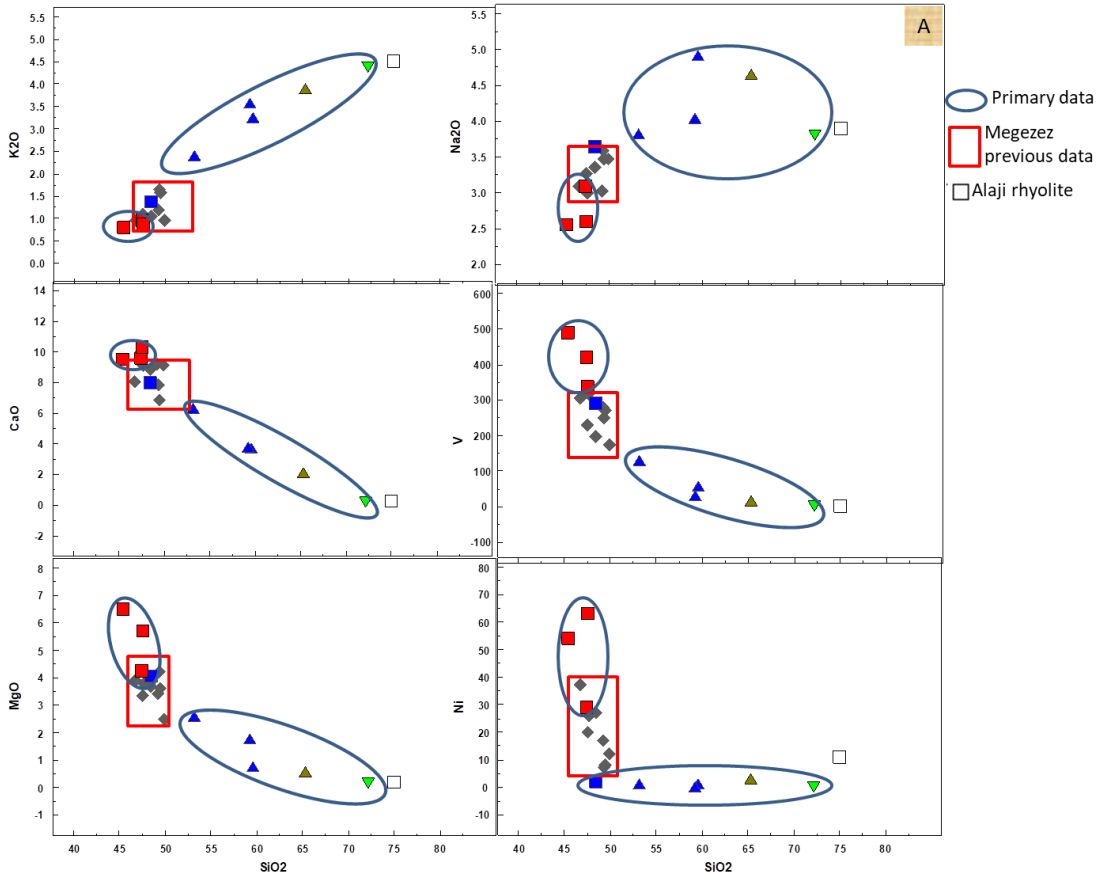

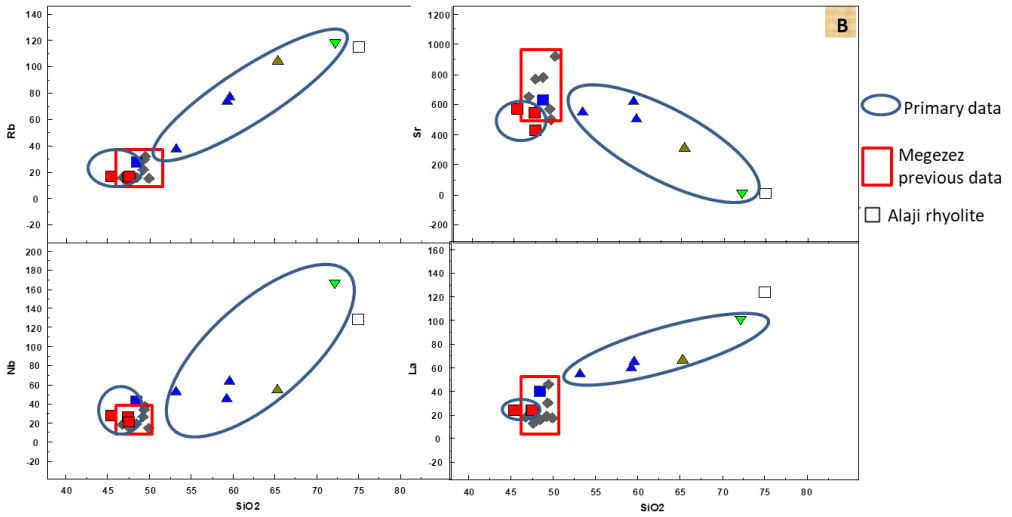

Fig. 5.5. Different Variation diagrams: (A) selected major elements and highly compatible trace elements Vs SiO_2; (B) highly incompatible trace elements Vs SiO2. Geochemical results for Megezez primary and secondary data comparison. Concentrations expressed in ppm for trace, and wt% for major elements.

Spider diagrams for primordial mantle normalized trace elements comparing the analyzed primary data with previous work data of Megezez and Alaji felsic rocks (see Fig. 5.5) show similar signatures in all cases. Gezahegn Yirgu (1997) has argued the similarity in incompatible trace element patterns for plateau and Megezez basalts. Some Megezez basalts exhibit relative enrichment in Ba relative to Rb and Th and relative depletion in Ti. Primary and secondary data from Megezez and Alaji felsic rocks show similar incompatible trace element patterns having strong negative anomaly of Ba, Sr, Ti and positive anomaly of Th, Ta, Nb, Zr (see Fig. 5.5). The role of these negative and positive spikes of various incompatible elements has an implication to fractional crystallization and differently accumulating of rock forming minerals. With the same idea discussed in previous sections (section 5.2); strong negative anomaly displayed in Ba, Sr, and Ti are indicatives of roles of alkali feldspars, plagioclase, and accessory minerals (magnetite), respectively during the evolution/ or genesis of analyzed rocks. The spider diagrams of trace elements presented here together with the characteristic trends observed in major and trace element variation diagrams generally show similar patterns of abundances between Megezez basalts (both primary and secondary data) and rhyolite samples (Megezez and Alaji). This similar characteristic features suggest the direct genetic relationship of acid rocks with basalts through the process of differentiation controlled by fractional crystallization (this study and Gezahegn Yirgu, 1997).

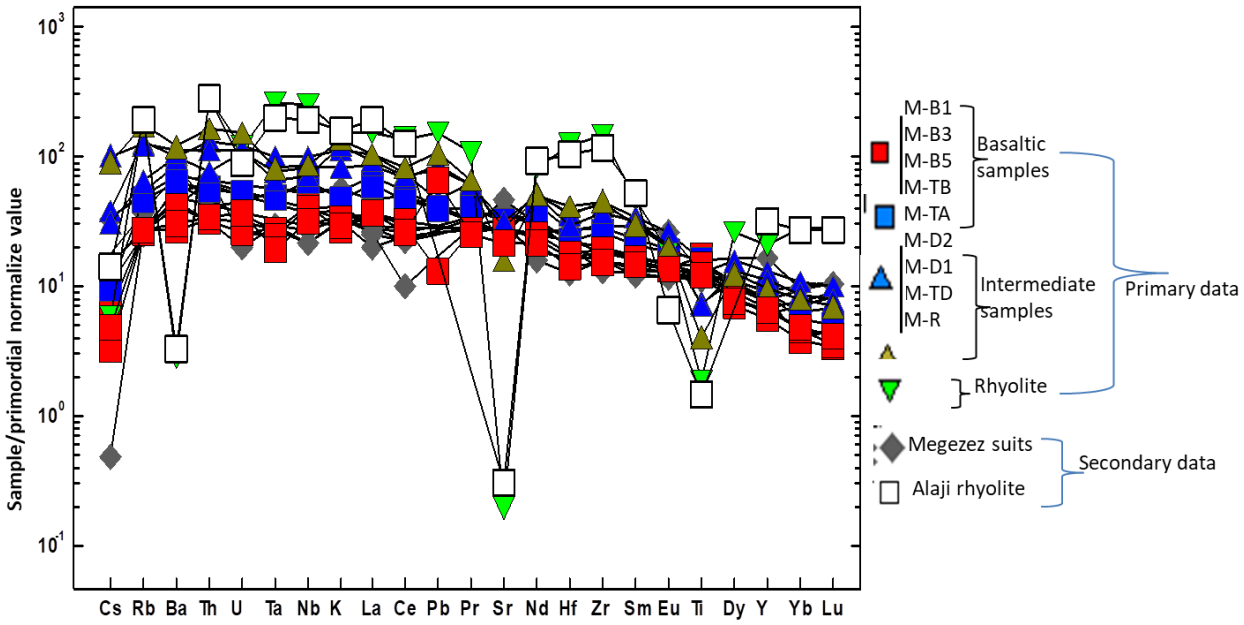

Fig. 5.6. Primordial mantle (Sun and McDonough, 1995) normalized trace element spider diagram for comparison of primary and previous work data in Megezez volcanics.

Fig. 5.7 below shows Rb/Nb as a function of Rb variation plot for geochemical modeling. It was previously used to evaluate the major processes in generating both basalts and evolved volcanic rocks from plateau, Megezez and Alaji silicics (Gezahegn Yirgu, 1997). The primary and secondary basalts of Megezez clustered around the Rb/Nb value of unity; whereas, primary intermediate samples fall in the region of assimilation fractional crystallization (AFC) and rhyolites on fractional crystallization (FC). Because both Rb and Nb are highly incompatible elements the increase in Rb/Nb is due to the dominant effect of AF and some involvement of AFC. The model presented with these elements shows the derivation of intermediate and felsic rocks of Megezez from common basaltic parent magma through Fractional Crystallization (FC) and some Assimilation Fractional Crystallization (AFC) for intermediate samples. This model is important to semi-quantitatively strengthen interpretations of fractional crystallization from various variation and spider plots of major and trace elements discussed in section 5.2 and section 5.3.

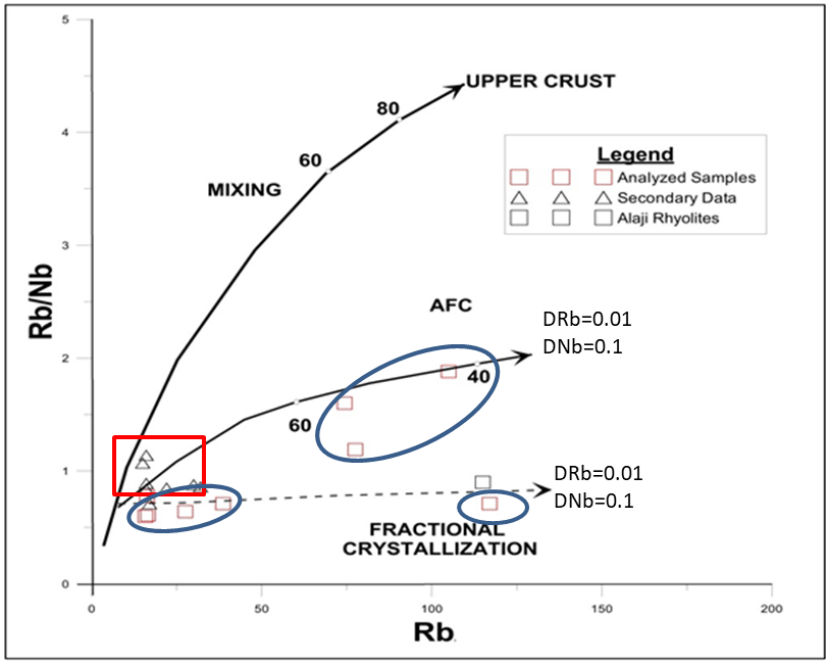

Fig. 5.7. Fractional crystallization (FC) and Assimilation fractional crystallization (AFC) models for the present studied Megezez volcanic rocks of plotted with previously studied Megezez basalts and Alaji rhyolite, according to Taylor and MacLennan (1885) adopted by Gezahegn Yirgu (1997). DRb=0.01 and DNb=0.1 are values of partition coefficient measuring their degree of incompatibility; as Rb is more incompatible than Nb. Numbers along the evolution trends are to indicate the amount of residual liquid which determined from previous study and adopted for comparison with this study.

Table 5.1.Selected incompatible trace elements ratios (Rb/Nb, La/Nb, and La/Yb) for comparison of Megezez shield volcanics (mafic, intermediate and felsic samples) to, north western flood basalt, shield volcanics and Wegel Tena rhyolites.

		Rb/Nb	La/Nb	La/Yb	Data sources
Flood basalts		0.13-2.16	--		Kieffer et al.,(2004)
Wegel Tena rhyolite		0.8-1.3	0.8-2.3		Dereje Ayalew and Gezahegn Yirgu (2003)
Guna volcanics	Rhyolite	0.93-1.31	0.76-1.03		Addise Mekonnen(2006)
	Trachyte	0.40-0.57	0.37-0.84		
	Phonolite	0.31-0.89	0.34-0.70		
Alaji rhyolites		<1	--		Gezahegn Yirgu(1997)
Megezez shield volcanics	Basalts	0.6-0.78	0.88-1.14	11.07-15.91	This study
	Trachyandesite	1.19-1.6	1.02-1.3	15.5	
	Trachydacite	1.88	1.21	19.45	
	Rhyolite	0.71	0.6	8.04	
North western flood and shield volcanics	tholeitic			4.2	Kieffer et al.,(2004)
	Alkaline			9.2	
	Magnesian alkaline				

CHAPTER- SIX

6. Conclusion and Recommendation

6.1. Conclusions

Ethiopian Plateau comprises both flood and shield volcanic provinces; in which shield volcanic products overlying the flood volcanics in the area they cover. North western Ethiopian plateau is characterized by extensive flood and large shield volcanics. Northwestern Ethiopian shield volcanoes include Megezez (the main focus of this study), Simien, Guguftu, Choke, and Guna volcanoes.

This study addresses the scientific gaps on Megezez shield volcanics. In order to achieve the scientific merit it incorporates field observation, geological mapping, petrographic, geochemical, and structural analysis. The major findings from the present study are as follows:

- Megezez shield volcanics exhibit petrographic compositions of wide range in mineral compositions. It comprises highly porphyritic, moderately porphyritic, sparsely porphyritic and aphanitic textures of rocks. Porphyritic basalt has large area coverage relative to the other mappable units; and generally shows abundant phenocrysts of plagioclase, clinopyroxene, and Fe-Ti oxide minerals. All the observed and analyzed volcanic rocks of Megezez shield are lava flow with lack of pyroclastic products.

- Megezez volcanic products characterized as silica oversaturated. CIPW norm calculation results that basalts are hypersthene normative; whereas, rhyolites are quartz normative.

- Megezez shield is not only basaltic-trachytic in composition; rather it shows wide range of compositional variations as mafic-intermediate-and felsic (45.5-72.2 wt% silica content). The volcanic successions have chronological order from oldest to youngest as: Trachyandesite-Trachybasalt – Trachydacite - Rhyolite– Basalt.

- Megezez basalts and intermediate volcanic suits are transitional type; whereas, rhyolites are peralkaline rocks.

- The volcanic rocks of Megezez shield have co-genetic relationships of source region shown by signatures from pairs of highly incompatible trace element and spider diagrams of REE.

  Intermediate and felsic rocks evolved from basaltic parent magma through the major process of fractional crystallization. Assimilation fractional crystallization has some role in modifying

the genesis of intermediate rocks (trachyandesite, trachydacite products). The source of basalts is spinel-peridotite and the remaining intermediate and felsic suites evolved through fractional crystallization process.

- Megezez shield volcanic area exhibits normal faults trending NE-SW strike and SE dip direction; imitating general trends of regional tectonic structures of the border faults of the MER.

6.2. Recommendation

Megezez shield volcanic area requires the following major studies:

- Further investigations by increasing the number of sampling and field techniques to map non-accessible areas
- Geochronologiclly determined stratigraphic sections with thickness of lava flows supported by absolute dating
- Isotope geochemistry requires for quantitative interpretations of magma evolution and genesis of Megezez shield volcanic products
- Studies on mineral chemistry to determine the quantitative and qualitative mineral composition of volcanic rock suits

References

Abbate, E. and Sagri, M. (1980). Volcanites of Ethiopian and Somali Plateaus and major tectonic lines. *Atti Convegni Lincei* **47**:219-227.

Abbate, E., Bruni, P., and Sagri, M.(2015). Geology of Ethiopia: A review and geomorphological perspective. *Springer* 33-59.

Addise Mekonnen (2006). Geology and Geochemistry of Guna Volcanic Massif, North western Ethiopian plateau. Unpublished MSc Thesis, Addis Ababa University, Addis Ababa, Ethiopia, 100 pp.

Barberi F., Ferrara G., Santacroce R., Treuil M., and Varet J. (1975) A transitional basalt-pantellerite sequence of fractional crystallization. *The Boina Centre (Afar Rift, Ethiopia). J. Petrol.* **16**, 22–56

Beccaluva, L., Bianchini, G., Natali, C., and Siena, F. (2009). Continental flood basalts and mantle plumes: a case study of the northern Ethiopian plateau. *Journal of petrology* **50**(7): 1377-1403.

Bekele Abebe, Acocella b, Tesfaye Korme and Dereje Ayalew (2007). Quaternary faulting and volcanism in the Main Ethiopian Rift. *Journal of African Earth Sciences* **48**: 115-124.

Boccaletti, M., Bonini, M., Mazzuoli, R., Bekele Abebe, Piccardi, L., and Tortorici, L. (1998). Quaternary oblique extensional tectonics in the Ethiopian Rift (Horn of Africa). *Tectonophysics* **287**(1): 97-116.

Bonini, M., Corti, G., Innocenti, F., Manetti, P., Mazzarini, F., Tsegaye Abebe, and Pecskay, Z. (2005). Evolution of the Main Ethiopian Rift in the frame of Afar and Kenya rifts propagation. *Tectonics* **24**(1): 1-25.

Chorowicz, J. (2005). The East African rift system. *Journal of African Earth Sciences* **43**: 379-410.

Corti, G. (2009). Continental rift evolution: from rift initiation to incipient break-up in the Main Ethiopian Rift, East Africa. *Earth-Science Reviews* **96**(1): 1-53.

Corti, G., Manetti, P., Mazzarini, F., Bonini, M., and Tsegaye Abebe (2009). The Volcano-tectonic Activity of the Main Ethiopian Rift (East Africa): Insights into the Evolution of Continental Rifting. *Acta vulcanologica* **20**(1/2): 133-144.

Coulie, E. (2001). Chronology 40Ar/39Ar et K/Ar de la dislocation du plateau Ethiopia et de la dechirure continentale dans la Corne de l'Afrique depuis 30 Ma. Ph.D. thesis, Universite de Paris Sud, Orsay.

Davaille, A. and Vatteville, J. (2005). On the transient nature of mantle plume. *Geophysical Research Letters* **32**: 1- 4.

Dereje Ayalew, Barbery, P., Marty, B., Reisberg, L., Gezahegn Yirgu, and Pik, R. (2002). Source, genesis and timing of giant ignimbrite deposits associated with Ethiopian continental flood basalts. *Geochemica et Cosmochimica Acta* **66**(8): 1429-1448.

Dereje Ayalew and Gezahegn Yirgu (2003).Crustal contribution to the genesis of Ethiopian Plateau rhyolitic ignimbrites, basalt and rhyolite geochemical provinciality. *Journal of the Geological society* **160**(1): 47-56.

Dereje Ayalew, Jung, S., Romer, R.L., Kerstend, F., Pfänder, J.A., Garbe-Schönberg, D. (2016). Petrogenesis and origin of modern Ethiopian rift basalts: Constraints from isotope and trace element geochemistry. *Lithos* **258–259**: 1–14

Dereje Ayalew, Jung, S., Romer, R.L., Garbe-Schonberg, D. (2018). Trace element systematics and Nd, Sr, and Pb isotopes of Pliocene flood basalt magmas (Ethiopian Rift): Acase for Afar Plume-Lithosphere interaction. *Chemical geology*, in press.

Ebinger, C., Tesfaye Yemane, Gidey Woldegabriel, Aronson, J., and Walter, R. (1993). Late Eocene– Recent volcanism and faulting in the southern main Ethiopian rift. Journal of the Geological Society 150(1): 99-108.

Ebinger, C.J. and Sleep, N.H.(1998). Cenozoic magmatism throughout East Africa resulting from impact of a single plume. Nature 395: 788-791

Feyissa Dejene Hailemariam, R. Shinjo, H. Kitagawa , Daniel Meshesha , E. Nakamura (2017). Petrologic and geochemical characterization of rift-related magmatism at the northernmost Main Ethiopian Rift: Implications for plume-lithosphere interaction and the evolution of rift mantle sources. *Lithos* **282–283**: 240–261.

Furman, T. (2007). Geochemistry of East African Rift basalts: An overview. *Journal of African Earth Sciences* **48**:147-160.

Gasparon, M., Innocenti, F., Manetti, P., Peccerillo, A., and Tsegaye Abebe. (1993). Genesis of the Pliocene to Recent bimodal mafic-felsic volcanism in the Debre Zeyt area, central

Ethiopia: volcanological and geochemical constraints. *Journal of African Earth Sciences (and the Middle East)* **17**(2), 145-165.

Geological Survey of Ethiopia (GSE, 2009). Geological map of Debre Berhan area. Unpublished report.

George, R. Thermal and tectonic controls on magmatism in the Ethiopian province, thesis, Open University, Milton Keynes, 1997, pp.

Gezahegn Yirgu (1997). Magma – crust interaction during emplacement of Cenozoic volcanism in Ethiopia: geochemical evidence from Sheno-Megezez area, central Ethiopia. *SINET: Ethiopia J. Sc.* **20**(1): 49-72.

Gezahegn Yirgu, Ebinger, C.J., and Maguire, P.K.H. (eds) (2006). The Afar volcanic province with in the East African Rift System. *Geological Society, London, Special Publications* **259**: 327 pp.

Gibson I. L.(1969). The structure and volcanic geology of an axial portion of the main Ethiopia rift. *Tectonophysics* **8**: 561-565.

Gidey Woldegebriel, Aronson, J. L., and Walter, R. C. (1990). Geology, geochronology, and rift basin development in the central sector of the Main Ethiopia Rift. *Geological Society of America Bulletin* **102**(4): 439-458.

Halliday, A.N., Davidson, J.P., Wildreth, W., and Holden, P. (1991). Modeling the petrogenesis of high Rb/Sr silicic magmas. *Chemical Geology* **92**: 107-114.

Hofmann, C., Courtillot, V., Fe´raud, G., Rochette, P., GezahegnYirgu, Endale Ketefo and Pik, R. (1997). Timing of the Ethiopian flood basalt event and implications for plume birth and global change. *Letters to nature*.

https://en.climate-data.org/location/928323/ accessed on 23.02.2018.

Irvine, T. and Baragar, W. (1971). A guide to the chemical classification of the common volcanic rocks. *Canadian journal of earth sciences* **8**(5):523-548.

Kieffer B., Nicholas A., Henriette L., Florenece B., Delphine. B. Arnaud P., Gezahegn Yirgu, Dereje Ayalew, Dominique W., Dougal A.J, Francine K., and Claudine M., (2004). Flood and shield Basalt from Ethiopia magmas from the African super swell. *Journal of petrology* **45**: 793-834.

Kier, D., Ebinger, C. J., Stuart, G.W., Daly, E., and Atalay Ayele (2006). Strain accommodation by magmatism and faulting as rifting proceeds to breakup: Seismicity of the northern Ethiopian rift. *Journal of Geophysical Research* **111**: 1-17.

Le Bas, M. J., Le Maitre, R., Streckeisen, A. and Zanettin, B. (1986). A chemical classification of volcanic rocks based on the total alkali-silica diagram. *Journal of Petrology* **27**(3):745-750.

Maguire, P., Keller, G., Klemperer, S., Mackenzie, G., Keranen, K., Harder, S., Khan, M. (2006). Crustal structure of the northern Main Ethiopian Rift from the EAGLE controlled-source survey; a snapshot of incipient lithospheric break-up. *Geologycal Society, London, Special Publications* **259**(1):269-292.

Marty, B., Pik, R., and Gezahegn Yirgu (1996). Helium isotopic variations in Ethiopian plume lavas: Nature of magmatic sources and limit on lower mantle contribution. Earth and Planetary Science Letters 144: 223-237.

McDonough, W. F. and Sun, S.S. (1995). The composition of the Earth. *Chemical Geology* **120**(3):223-253.

Merla, G., Abbate, E., Canuti, P., Sagri, M. & Tacconi, P. (1979). Geological map of Ethiopia and Somalia and comment with a map of major landforms (scale 1:2,000,000). *Rome: Consiglio Nazionale delle Ricerche* 95.

Minyahl Teferi Desta, Dereje Ayalew, Ishiwatari, A., and Tamura, A. (2014). Ferropicrites from the Lalibela area in the Ethiopian large igneous province. *Journal of Mineralogy and Petrological Sciences* **109**: 191-207.

Mohr, P. (1983). Ethiopian flood basalt province. *Nature* **303**: 577-584.

Mohr, P.(1967). Reviews of the geology of the Semien mountains. *Bulletin of the Geophysical Observatory of Addis Ababa* **10**: 7993.

Mohr, P. and Zanettin, B. (1988). The Ethiopian flood basalt province. In: Macdougall, J.D.(ed), continental flood basalts. *Klwuer Academic Publishers, Dordrecht*, PP 63-110.

Mulugeta Alene, Alan Deino, Beverly Z. Saylor, Luis B. Gibert, Stanley Mertzman, William K. Hart, Yohannes Haile-Selassie (2017). Geochemistry of Woranso–Mille Pliocene basalts from west-central Afar, Ethiopia: Implications for mantle source characteristics and rift evolution. *Lithos* **282-283**: 187-200.

Mulugeta Dugda, Nyblade, A. A., and Julia, J. (2007). Thin lithosphere beneath the Ethiopian Plateau revealed by a joint inversion of Rayleigh wave group velocities and receiver functions. *Journal of Geophysical Research:Solid Earth* (1978–2012), 112.

Peccerillo, A., Barberio, M., Gezahegn Yirgu, Dereje Ayalew, Barbieri, M. and Wu, T. (2003). Relationships between mafic and peralkaline silicic magmatism in continental rift settings: a petrological, geochemical and isotopic study of the Gedemsa volcano, central Ethiopian rift. *Journal of Petrology* **44**(11).

Peccerillo, A., Donati, C., Santo, A., Orlando, A., Gezahegn Yirgu and Dereje Ayalew (2007). Petrogenesis of silicic peralkaline rocks in the Ethiopian rift: geochemical 112 evidence and volcanological implications. *Journal of African Earth Sciences* **48**(2):161-173.

Pik, R., Deniel, C., Coulon, Ch., GezahegnYirgu, Hofmann, C. and Dereje Ayalew (1998). The northwestern Ethiopian plateau flood basalts: classification and spatial distribution of magma types. *Journal of Volcanology and Geothermal Research* **81**: 91-111.

Pik, R., Deniel, C., Coulon, C., GezahegnYirgu, and Marty, B. (1999). Isotopic and trace element signatures of Ethiopian basalts evidence for plume lithosphereic interactions. *Geochimica et Cosmochemica Acta* **63**: 2263 – 2279.

Rogers, N.W., MacDonald, R., Fitton, J.G., George, R., Smith, M. and Barreiro, B. (2000). Two mantle plumes beneath East African rift system: Sr, Nd, and Pb isotope evidence from Kenya rift basalts. *Earth and Planetary Science Letters* **176**: 384-400.

Rogers, N.W., Davies, M.K., Parkinson, I.J., Gezahegn Yirgu (2010). Osmium isotopes and Fe/Mn ratios in Ti-rich picritic basalts from the Ethiopian flood. basalt province: No evidence for core contribution to the Afar plume. *Earth and Planetary Science Letters* **296**: 413–422

Rooney, T., Furman, T., Bastow, I., Dereje Ayalew, and Gezahegn Yirgu (2017). Lithospheric modification during crustal extension in the Main Ethiopian Rift. *Journal of Geophysical Research: Solid Earth* 1978–2012.

SeifeMichael Berhe, Belay Desta, Nicoletti, and Mengesha Teferra, (1987). Geology, Geochronology and Geodynamic Implications of the Cenozoic magmatic province in W and SE Ethiopia. *Journal of the Geological Society, London* **144**: 213-226.

Sun, S, S. and McDonough, W. F. (1989). Chemical and systematic of oceanic basalts: implications for mantle composition and processes. In: Saunders, A. D. and Norry, M. J. (eds) Magmatism in the ocean Basins, Geological Society, London. *Special publications* **42**: 313-347.

Tadiwos Chernet, Hart, W. K., Aronson, J. L., and Walter, R. C. (1998). New age constraints on the timing of volcanism and tectonism in the northern Main Ethiopian Rift–southern Afar transition zone (Ethiopia). *Journal of Volcanology and Geothermal Research* **80**(3-4): 267-280.

Tadiwos Chernet and Hart.W.K.(1999). Petrological, Geochemical and Geocronological Investigation of Volcanism in the Northern Main Ethiopian Rift- Southern Afar transition Region. *Acta Vulcanologica* **11**(1): 21-41.

Tsegaye Abebe, Maria Laura Balestrieri, and Giulio Bigazzi (2010).The Central Main Ethiopian Rift is younger than 8 Ma: confirmation through apatite fission-track thermochronology. *Terra Nova*. 470-476.

Ukstins, I.A., Renneop.R., Wolfenden, E., Baker, J., Dereje Ayalew and Menzies, M. (2002). Matching conjugate volcanic rifted margins.40Ar/ Ar39, K-Ar Chronostratigraphy of pre- and syn rift bimodal flood volcanism in Ethiopia and Yemen. *Earth and planetary Science Letters* **198**: 289-306

Wolfenden, E., Ebinger, C., Gezahegn Yirgu, Deino, A., and Dereje Ayalew (2004). Evolution of the northern Main Ethiopian rift: birth of a triple junction. *Earth and Planetary Science Letters* **224**(1): 213-228.

Zanettin, B. (1992). Evolution of the Ethiopian Volcanic Province. *Memorie Lincee Scienze Fisiche e Naturali* **1:**155---181.

APPENDIX-A : Petrographic analysis results

Sample	Rock type	Average modal proportion (%)		Phenocryst maximum grain size (mm)	Average grain shape, form, texture
M-R	Sparsely porphyritic rhyolite lava flow	Quartz	2%	~1.25	Anhedral
		Alkali feldspar	4.5%	~3	Euhedral-Subhedral, tabular form
		Clinopyroxene	0.5%	~1.1%	Euhedral-Subhedral
		Opaque	1%	~1	Anhedral
		Groundmass	92%	-	Cryptocrystalline
M-RD	Glassy rhyolite dyke	Glass/quartz	~5%	0.12	Subhedral-Anhedral
		Alkali feldspar	~2%	1	Tabular, Subhedral
		Clinopyroxene	~1%	0.4	Euhedral-Subhedral
		Rock fragment	~0.2%	-	-
		Opaque	~0.2%	0.2	anhedral
		Plagioclase	~%3	0.3	Tabular, lathe, euhedral
		Groundmass	~89%	-	Glassy texture
M-TD Sparsely porphyritic trachy dacite		Plagioclase	~6%	1.8	Tabular, euhedral
		Alkali feldspar	~5%	2.5	Euhedral-Subhedral, tabular
		Clinopyroxene	~3.5%	1.4	Euhedral-Subhedral, tabular
		Opaque	~3%	0.7	Anhedral-Subhedral
		Open space	~6%	-	-
		Groundmass	~82.5%	-	Microcrystalline-glassy nature
M-TA	Sparsely porphyritic trachy andesite	Hornblende	~4%	5.5	Euhedral-Subhedral, tabular, rimmed
		Alkali feldspar	~2%	1.5	Tabular, lathe-shape
		Plagioclase	~1%	5	Tabular, euhedral, altered
		Opaque	~1%	1.2	Euhedral-anhedral
		Groundmass	~91%	-	Microcrystalline and trachytic texture
M-D2	Sparsely	Plagioclase	~2.5%	3	Euhedral, tabular, altered

	porphyritic trachy andesite dyke	Clinopyroxene	~1%	1.5	Subhedral, altered
		Alkali feldspar	~3%	4	Subhedral, tabular, difficult to differentiate from plagioclase
		Quartz	~0.5	1.25	Subhedral
		Opaque	~1%	0.6	Anhedral-Subhedral
		Groundmass	~92%	-	Microcrystalline forming trachytic texture
M-TB	Aphaneritic trachy basalt	Generally it is aphaneritic texture lacking significant phenocryst, but few clinopyroxene is visible; other ways it shows microcrystalline ground mass. Groundmass composed of mafic minerals with no possibilities to distinguish each mineral phase			
M-D1	Basaltic trachy andesite	Composed of lathe-shape feldspars and mafic minerals (like pyroxene and opaque). The groundmass is entirely composed of microphenocrysts mineral phases with difficulty to distinguish which form intergranular texture.			

M-B1	Porphyritic basalt	plagioclase	~20%	6.5	Tabular, euhedral to Subhedral, highly zoned and twin
		Alkali feldspar	~2%		Tabular shape identified from plagioclase with it optical properties of no twinning and showing light to light gray extinction colors
		Clinopyroxene	~3%	1	Euhedral to Subhedral, slightly altered, forming sub ophitic and sub pokiolithic texture
		Opaque	~2%	-	Results of pyroxene alteration effect,
		Open spaces	9%	-	-
		Groundmass	~74%		Microcrystalline texture
				Generally three samples M-B4, MW-B, M-B13	Plagioclase is highly zoned, twinned, altered, has euhedral shape and tabular form

M-B4	Porphyritic basalt	Plagioclase	~29%	have average grain size of plagioclase 8-9.5	
		Clinopyroxene	~3.6%	0.23	Subhedral-euhedral, slightly to completely altered
		Alkali feldspar	~1.5%	1.6	Tabular
		Opaque	~3%	0.4	Subhedral
		Groundmass	~63	-	Microcrystalline in which matrix is composed of mafic mineral phases, with no distinction to specify phases
MW-B	Porphyritic basalt	Plagioclase	~31	Generally, samples have similar textural features to which plagioclase shows strong zoning (core-rim feature); polysynthetic twining. Clinopyroxene (0.23mm) show sub ophitic texture, altered to opaque minerals/Fe-Ti oxide minerals (0.4mm). Sample M-B13 is relatively fresh showing less degree of alteration in pyroxene and plagioclase.	
		Clinopyroxene	~3		
		Opaque	~1.5%		
		Alkali feldspar	~0.6%		
		Groundmass	~64%		
M-B13	porphyritic basalt	Plagioclase	~26%		
		Clinopyroxene	~4%		
		Opaque	~2%		
		Alkali feldspar	~1%		
		Groundmass	~67%		
M-B5-1	Porphyritic basalt	Plagioclase	~13%	5 mm	Tabular form, euhedral shape, sieved texture, twining, and zoning.
		Clinopyroxene	~2%	0.6 mm	Subhedral shape with alteration effect.
		Opaque	~3%		Subhedral-euhedral
		Alkali feldspar	~1%	1.75 mm	Subhedral shape, tabular form
		Groundmass	~81%	-	Lathe-shaped, sieved, microcrystalline texture.
		Plagioclase	~11.5%	6 mm	Plagioclase is weakly zoned, form intergrowth texture with altered
		Clinopyroxene	~4%	1 mm	

M-B14	Porphyritic basalt	Opaque	~1%	0.6 mm	clinopyroxene; plagioclase exhibit lathe-shape and tabular form with euhedral shape. Clinopyroxene is rimming opaque minerals as alteration effect is outward developing to form opaque. The groundmass is composed of microcrystalline matrix in which mafic mineral phases are visible with no chance to differentiate.
		Alkali feldspar	~1.5%	2.5 mm	
		Groundmass	~82%	-	
M-B8	Porphyritic basalt	Plagioclase	~9.75%	3.5 mm	Tabular form, lathe-shape, less twinned and zoned
		Clinopyroxene	~8.75%	0.5 mm	Subhedral shape, with high birefringence interference color
		Alkali feldspar	~4%	4.8 mm	Show Carlsbad twin, euhedral, tabular form
		Opaque	~3.5%	1.5 mm	Euhedral-Subhedral, some resulted from alteration of pyroxene
		Groundmass	~74%	-	Matrix composed of lathe-feldspars and microcrystalline mafic mineral phases
M-B5-3	Porphyritic basalt	Plagioclase	~2%	This sample is different from the rest of analyzed volcanic units in the study area. As explained in chapter three, section 3.2.7; it is not mappable rather exposed as plug volcanics in restricted area. Minerals show difficult feature in petrographic microscope to exactly differentiate and characterize. The sample exceptionally composed of few feldspars(plagioclase and alkali feldspar), instead with abundance pyroxene. Phenocryst of pyroxene range in grain size and shape 1.2-4.6 mm and Subhedral shape of crystals. Plagioclase shows simple twining and polysynthetic twin. Void spaces present in the clinopyroxene core. Groundmass composed of entirely mafic mineral phases of microcrystalline	
		Clinopyroxene	~11%		
		Orthopyroxene	~1%		
		Olivine	~4%		
		Opaque	~0.7%		
		Alkali feldspars	~0.3%		
		Open spaces	~1%		
		Groundmass	~81%		

				texture
M-B3-4	porphyritic basalt	Plagioclase	~11%	Generally, constitutes lathe-shaped and tabular plagioclase phenocryst phases with sub ophitic texture, ~3 mm grain size, some clustered in random fashion. Clinopyroxene is slightly altered forming anhedral to Subhedral shape, show inclusion of opaque mineral phases. The groundmass is composed of microcrystalline matrix and some lathe-feldspars.
		Alkali feldspar	~2%	
		Clinopyroxene	~7%	
		Opaque	~1.4%	
		Groundmass	~79%	

APPENDIX-B: Analyzed data for geological structures

Type of structure		Orientation		Rock unit
		Strike	Dip	
Faults	Fault-1	N45^0 E	78^0 SE	Porphyritic basalt
	Fault-2	N54^{0}E	75^0 SE	Porphyritic basalt and trachy dacite flow
	Fault-3	N53^{0}E	70^{0}SE	Porphyritic basalt and trachy dacite flow
	Fault-4	N38^{0}E,	68^{0}SE	Porphyritic basalt
		N57^{0}E		
		N44^{0}E		
	Fault-5	N55^{0}E	65SE	
	Fault-6	N46^{0}E	78^{0}SE	
	Fault-7	N44^{0}E	76^{0}SE	
	Fault-8	N44^{0}E	78^{0}SE	Rhyolite lava flow, Trachy andesite flow and trachy basalt

		Strike	Dip	Joint spacing(cm)	Rock unit
Joints	Joint-1	105^0 SE	75^0 SW	0.3	Trachy andesite flow
	Joint-2	102^{0}SE	73^{0}SW	0.5	
	Joint-3	102^0 SE	65^0 NE	17	
	Joint-4	075^0	80^0 SE	21	
	Joint-5	N35^{0}E	75^0 SE	19	
	Joint-6	E-W	75^0 S	24	Rhyolite lava flow
	Joint-7	N40E	85^0 SE	34	
	Joint-8	104^{0}SE	60^0 NE	27	
	Joint-9	N25^{0}E	10^0 NW	23	
	Joint-10	N15^{0}E	30^0 NW	21	
Flow banding	Banding-1	N30^0 E	N20^0 W	Trachy andesite flow	
	Banding-2	N15^0 E	10^0 NW		
	Banding-3	N25^0 E	15^0 NW		
	Banding-4	N20^0 E	35^0 NW		
	Banding-5	025^0 NE	10^0 NW	Porphyritic basalt	
	Banding-6	280^0	50^0 SW		
	Banding-7	270^0	60^0 SW		

APPENDIX-C: Selected trace element ratio of analyzed samples

Sample	K/Rb	K/Ba	Rb/Sr	Zr/Nb	Nb/Th	Th/La	Nb/Y	Gd/Yb	La/Y	La/Yb	Tb/Yb	Ce/Pb	Rb/Ba
M-TA	347.08	40.09	0.15	6.82	6.28	0.16	1.71	3.48	1.74	23.48	0.49	17.79	0.12
M-B1	397.49	36.64	0.03	7.23	10.54	0.11	1.12	3.47	0.99	14.00	0.49	24.50	0.09
M-TB	410.57	27.61	0.04	6.50	9.64	0.11	1.15	3.50	1.06	15.91	0.49	12.87	0.07
M-R	309.37	1956.58	30.00	9.27	7.33	0.23	1.84	1.21	1.11	8.04	0.23	10.04	6.32
M-B3	493.92	28.69	0.03	7.64	10.44	0.10	0.95	3.12	0.87	11.59	0.44	-	0.06
M-D1	516.19	30.56	0.07	8.67	8.81	0.11	0.97	2.73	1.00	11.54	0.40	8.88	0.06
M-D2	397.25	40.49	0.12	8.37	5.17	0.15	0.98	2.89	1.27	15.80	0.41	9.96	0.10
M-TD	307.57	40.88	0.33	8.52	4.23	0.20	1.38	2.90	1.66	19.45	0.43	8.69	0.13
M-B5	440.72	35.35	0.04	7.78	7.72	0.11	0.72	2.86	0.83	11.07	0.43	4.38	0.08
	Ti	K	P	Ti/K	(La/Sm)N	(La/Yb)N	(Tb/Yb)N	Eu/Eu*	(La/Yb)N	Rb/Nb	Ba/La	La/Nb	Rb/Y
M-TA	8992.50	26898.48	2574.88	0.33	3.31	15.65	2.29	0.87	15.83	1.19	10.14	1.02	17.66
M-B1	20383.00	6558.58	1440.19	3.11	2.31	9.33	2.29	1.03	9.44	0.61	7.52	0.88	7.43
M-TB	19423.80	11290.72	2225.74	1.72	2.84	10.61	2.31	1.02	10.73	0.64	10.41	0.92	10.99
M-R	2218.15	36196.72	87.28	0.06	3.25	5.36	1.09	0.50	5.42	0.71	0.19	0.60	0.21
M-B3	17505.40	7803.88	1483.83	2.24	2.18	7.72	2.07	1.02	7.81	0.60	11.29	0.92	9.78
M-D1	15287.25	19924.80	3535.00	0.77	2.47	7.70	1.86	0.90	7.78	0.71	11.79	1.02	11.75
M-D2	8452.95	29555.12	2138.46	0.29	2.94	10.53	1.92	0.81	10.65	1.60	12.07	1.30	15.37
M-TD	4855.95	32294.78	1091.05	0.15	3.43	12.97	2.02	0.84	13.11	1.88	11.70	1.21	19.46
M-B5	14687.75	7139.72	1134.69	2.06	2.45	7.38	1.99	1.04	7.47	0.78	8.52	1.14	7.06

APPENDIX-D: Secondary geochemical data of Megezez (Termaber formation) and Alaji rhyolite (sample TM-L) from GezahegnYirgu(1997). Analytical methods used are XRF trace element with asterisks) and INAA (other trace elements without asterisks).

	MEZ-8	MEZ-14	MEZ-11	MEZ-16	MEZ-3	MEZ-18	MEZ-2	MEZ-9	TM-L
SiO2	46.76	47.61	47.70	48.47	49.23	49.35	49.55	49.91	75.05
TiO2	2.39	2.86	2.64	2.34	2.55	3.07	3.23	2.26	0.29
Al2O3	18	18.03	17.81	19.29	18.01	15.17	14.99	21.86	10.92
Fe2O3	7.43	4.75	5.18	3.99	5.89	3.79	8.58	1.61	2.19
MnO	0.16	0.16	0.15	0.14	0.16	0.18	0.18	0.12	0.12
MgO	3.91	3.35	3.79	3.65	3.42	4.18	3.58	2.48	0.19
CaO	8.02	9.33	9.11	8.84	9.14	7.86	6.84	9.09	0.21
Na2O	3.08	3.26	2.99	3.35	3.02	3.58	3.46	3.47	3.89
K2O	0.9	1.09	0.93	1.04	1.19	1.64	1.58	0.96	4.51
P2O5	0.45	0.59	0.45	0.55	0.5	0.76	0.65	0.55	0.03
LOI	3.25	2.06	2.75	2.25	1.61	1.89	3.58	0.87	0.97
Mg#	41.24	39.76	41.57	44.16	41.03	42.34	39.52	41.07	9.99
La*	18	18	13	16	19	30	46	17	124
Ce*	38	44	41	38	47	85	90	32	213
V*	304	228	316	197	278	249	268	173	1
Cr*	34	7	14	7	0	3	0	26	0.5
Co*	42	31	41	29	31	31	33	19	2
Ni*	37	20	26	27	17	7	8	12	11
Rb*	16	17	16	16	22	30	32	15	115
Sr*	647	765	560	776	567	499	497	918	6
Y*	33	34	34	29	40	34	70	26	135

Zr*	165	190	172	162	210	301	305	136	1225
Nb*	18	24	14	19	26	34	37	14	128
Ba*	298	363	263	319	490	475	560	395	22
Th*	2.5	4.8	5.5	--	--	--	3.3	--	18
La	18	--	19.2	--	--	--	46.8	--	124
Ce	38	--	41	--	--	--	90	--	213
Nd	20	--	23	--	--	--	54	--	115
Sm	4.9	--	5.3	--	--	--	12	--	21
Eu	1.8	--	2	--	--	--	4	--	1
Tb	0.7	--	0.9	--	--	--	1.9	--	3.5
Yb	1.9	--	1.8	--	--	--	4.3	--	12.1
Lu	0.3	--	0.3	--	--	--	0.7	--	1.8
Cs	0.1	--	0.1	--	--	--	0.7	--	0.3
Th	1	--	1.8	--	--	--	3.3	--	18
U	0.4	--	0.5	--	--	--	0.9	--	1.8
Ta	1.1	--	1.1	--	--	--	2	--	7.3
Hf	3.5	--	4.7	--	--	--	7.6	--	29
Cr	34	--	14	--	--	--	--	--	0
Sc	19	--	23	--	--	--	22	--	5
Co	42	--	42	--	--	--	33	--	0.9